

Aus dem Max-Planck-Institut für Neurobiologie



REGULATION OF SPONTANEOUS CNS AUTOIMMUNITY BY DIETARY SALT

Dissertation

zum Erwerb des Doktorgrades der Naturwissenschaften

an der Medizinischen Fakultät der

Ludwig-Maximilians-Universität München

vorgelegt von

MATHANGI JANAKIRAMAN

aus

INDIA

Jahr

2021

Mit Genehmigung der Medizinischen Fakultät
der Universität München

Betreuer: PD Dr. Gurumoorthy Krishnamoorthy

Zweitgutachter: Prof. Dr. Ludger Klein

Dekan: Prof. Dr. med. Thomas Gudermann

Tag der mündlichen Prüfung: 05.05.2022

Table of Contents

| | |
|--|-----------|
| Summary (English) | 6 |
| Zusammenfassung (Deutsch) | 7 |
| 1. Introduction | 9 |
| 1.1 Multiple Sclerosis | 9 |
| 1.2 Experimental Autoimmune Encephalomyelitis | 10 |
| 1.3 Immunopathogenesis of MS and EAE..... | 11 |
| 1.4 Induced EAE models..... | 12 |
| 1.5 Spontaneous EAE models | 13 |
| 1.6 T and B cells in EAE | 14 |
| 1.7 Other immune cells in EAE..... | 17 |
| 1.8 Blood Brain Barrier (BBB) in EAE..... | 19 |
| 1.9 CNS resident cells in EAE..... | 21 |
| 1.10 The hygiene hypothesis | 23 |
| 1.11 The gut microbiome – an overview | 23 |
| 1.12 Factors affecting microbial dysbiosis..... | 26 |
| 1.13 Diet, microbiota and disease | 29 |
| 1.14 Diet, microbiota and CNS autoimmunity..... | 30 |
| Objectives of the study | 37 |
| 2. Materials and Methods | 38 |
| 2.1 Materials | 38 |
| 2.2 Buffers..... | 39 |
| 2.3 Mice | 42 |
| 2.4 Blood collection | 42 |
| 2.5 Genotyping..... | 42 |
| 2.6 Spontaneous EAE | 43 |
| 2.7 Actively induced EAE..... | 43 |
| 2.8 In vivo depletion and blocking..... | 43 |
| 2.9 Pertussis toxin treatment | 43 |
| 2.10 EAE scoring..... | 44 |
| 2.11 In vivo intestinal barrier permeability assay..... | 44 |
| 2.12 In vivo blood brain barrier permeability assay | 44 |

| | | |
|------------------------|---|-----------|
| 2.13 | Lymphocyte isolation from Lymphoid organs | 44 |
| 2.14 | Isolation of CNS infiltrating leukocytes..... | 45 |
| 2.15 | Isolation of Leukocytes from intestine lamina propria (LP)..... | 45 |
| 2.16 | Isolation of CNS endothelia | 45 |
| 2.17 | Flow cytometry | 45 |
| 2.18 | Antibodies for flow cytometry..... | 46 |
| 2.19 | Fecal bacterial culture and sequencing | 47 |
| 2.20 | Fecal DNA extraction and qPCR | 48 |
| 2.21 | Caecal metabolite extraction..... | 49 |
| 2.22 | Fecal metabolome analysis | 49 |
| 2.23 | Proliferation assay and ex vivo Splenocyte culture | 49 |
| 2.24 | Differentiation assay..... | 50 |
| 2.25 | In vitro B cell culture and i.p. injection | 50 |
| 2.26 | EROD assay..... | 51 |
| 2.27 | ELISA kits and antibodies | 51 |
| 2.28 | MOG – specific Ig ELISA..... | 52 |
| 2.29 | Cytokine ELISA..... | 52 |
| 2.30 | Fecal IgA ELISA | 52 |
| 2.31 | Western Blot | 52 |
| 2.32 | Histology | 53 |
| 2.33 | Luxol fast blue staining | 53 |
| 2.34 | Statistical analysis | 54 |
| 3. Results..... | | 55 |
| 3.1 | HSD is well tolerated by mice..... | 55 |
| 3.2 | Dietary salt protects OSE mice from spontaneous EAE | 56 |
| 3.3 | Actively induced EAE is not affected by HSD | 59 |
| 3.4 | HSD alters specific gut microbial populations | 60 |
| 3.5 | HSD modifies the fecal metabolome | 63 |
| 3.6 | HSD does not affect intestinal barrier integrity | 66 |
| 3.7 | HSD does not alter immune cell functions | 67 |
| 3.8 | HSD alters T cell subsets in the gut | 70 |
| 3.9 | T _{reg} cell depletion has no effect on disease susceptibility | 77 |
| 3.10 | B cell functionality is unaltered under HSD | 78 |

| | | |
|-------------------------|---|------------|
| 3.11 | HSD does not affect Integrins associated with immune cell migration | 80 |
| 3.12 | HSD-fed OSE mice are not protected from active EAE | 80 |
| 3.13 | No effect of HSD on adhesion molecules | 81 |
| 3.14 | HSD alters blood brain barrier permeability in vivo | 82 |
| 3.15 | HSD-mediated disease protection is reversed by Pertussis toxin | 83 |
| 4. Discussion | | 85 |
| 5. References | | 94 |
| Abbreviations | | 110 |
| Acknowledgements | | 112 |
| Resources | | 112 |
| Curriculum vitae | | 113 |
| Publications | | 114 |

SUMMARY (ENGLISH)

Autoimmune inflammatory diseases are on the rise in western societies. Recent research implicates the role of the gut microbiome and diet-associated factors in the development of these diseases. Research is underway to explore the metabolic and immunological aspects that are elemental to our understanding of these diseases. Indeed, a plethora of research in the last decade has focused on the concerted impact of diet and microbiota on several metabolic and autoimmune diseases like obesity, metabolic syndrome, colitis, and multiple sclerosis.

To this end, a lot of attention has been given to salt, an essential component of our diet and a very dominant component in the western diet. For instance, dietary salt has been shown to influence the induction of a pro-inflammatory T_H17 response in the intestine which in turn has been implicated in autoimmunity. However, data on autoimmunity is predominantly obtained in models where the disease is induced through artificial means. For understanding the role of dietary factors like salt, spontaneous disease models would serve as better tools. They are essential to study disease triggering factors and identify if dietary or microbial components contribute to disease pathogenesis.

In this study, the effect of dietary salt on Experimental Autoimmune Encephalomyelitis (EAE) was explored using a spontaneous EAE model. We found that dietary salt protected mice from autoimmune disease development. On subsequent analysis of alterations due to a High Salt Diet (HSD), the alterations in the gut microbiota, particularly the increase in Enterococci and the decrease in Blautia, were prominent. The HSD-mediated disease protection was observed only in spontaneous EAE and not in an actively induced EAE model.

Further analyses showed no difference between control and HSD-fed animals in functional aspects of the immune system, like T and B cell proliferation, antibody production, or antigen presentation. Analyses on the Gut Associated Lymphoid Tissue (GALT) showed that only the T cells in the intestinal GALT were altered in composition, skewing towards higher levels of IL-17+ T cells and alterations in T_{reg} cell subsets. However, induced EAE experiments and depletion experiments showed that these differences did not have any role in protection from EAE. The expression of cell surface integrins that aid in T cell migration to the Central Nervous System (CNS) was also not altered under HSD.

However, the permeability of the Blood Brain Barrier (BBB) in vivo was significantly altered under HSD. The administration of Pertussis toxin - which is known to disrupt the BBB, was capable of reversing HSD-mediated disease protection. Further analyses on the brain endothelia showed increased levels of the tight junction proteins ZO-1 and Claudin-5 due to HSD, indicating enhanced BBB integrity. The present study has shown that HSD protects against spontaneous EAE, not via alterations in the immune system but by altering the BBB. These results suggest a broader and potentially beneficial role of salt in the pathogenesis of CNS autoimmune disease.

ZUSAMMENFASSUNG (DEUTSCH)

Autoimmunerkrankungen erleben momentan einen deutlichen Zuwachs in der westlichen Welt. Aktuelle Forschungsarbeiten deuten auf einen Zusammenhang zwischen dem Mikrobiom des Darms, ernährungsspezifischen Faktoren und der Entstehung dieser Krankheiten hin. Wissenschaftliche Anstrengungen zielen daher darauf ab die für unser Verständnis dieser Krankheiten essentiellen metabolischen und immunologischen Aspekte zu verstehen wobei im letzten Jahrzehnt viel Aufmerksamkeit auf Krankheiten wie Adipositas, dem metabolischen Syndrom, Colitis und multipler Sklerose lag.

Die Rolle von Salz ist insbesondere daher in den Fokus gerückt, da es eine essentielle und auch in hohen Mengen verwendete Komponente der westlichen Ernährung ist. Es wurde beispielsweise gezeigt, dass Speisesalz die Induktion der pro-inflammatorischen T_H17 -Immunantwort beeinflusst, was wiederum mit Autoimmunerkrankungen assoziiert ist. Problematisch ist hierbei aber die Verwendung von Tiermodellen in denen die Krankheiten künstlich induziert werden. Tiermodelle mit spontaner Krankheitsentwicklung wären besser geeignet um die Rolle von Ernährungsfaktoren wie Speisesalz zu verstehen, da sie helfen die eigentlichen Krankheitsauslöser zu identifizieren und beispielsweise zu klären ob Ernährungsfaktoren oder das Mikrobiom als Auslöser wirken.

Diese Studie untersucht den Effekt von Speisesalz auf die Entwicklung von experimenteller autoimmuner Enzephalomyelitis mittels des spontanen EAE-Modells. Nach Feststellung einer Schutzwirkung durch den Salzkonsum vor der Erkrankung wurden Veränderungen durch Salzaufnahme analysiert. Die Mikrobiota-Veränderungen im Darm aufgrund einer salzreichen Diät (HSD), insbesondere die Zunahme von Enterokokken und die Abnahme von *Blautia*, waren prominent. Gleichmaßen bemerkenswert war, dass die HSD nur im spontanen EAE-Modell, nicht aber im induzierten EAE-Modell, protektiv war.

Weitere Experimente zeigten keinen Unterschied zwischen HSD- und Kontrolltieren in funktionellen Aspekten des Immunsystems, wie T- und B-Zellproliferation, Antikörpersekretion oder Antigenpräsentation. Analysen des darmassoziierten lymphatischen Gewebes (GALT) zeigten, dass nur T-Zellen des GALTs einen leicht erhöhten Anteil IL-17+ Zellen und eine veränderte Komposition der T_{Reg} -Zellen hatten. Experimente mit dem induzierten EAE-Modell und mittels Depletion zeigten aber, dass diese keinen Anteil an der Protektivität der HSD vor EAE hatten. Gleichmaßen unverändert blieb die Oberflächenexpression von Integrinen, welche die T-Zell-Migration unterstützen.

Wichtig erschienen aber HSD-induzierte Veränderungen in der Blut-Hirn-Schranke, deren vermutlich dadurch ausgelöste Protektivität durch Gabe von Pertussistoxin, welches die Blut-Hirn-Schranke beeinträchtigt, zunichte gemacht werden konnten. Weitere Analysen der Endothelien des Gehirns zeigten erhöhte Spiegel der Tight-Junction-Proteine ZO-1 und Claudin-5 aufgrund von HSD, was auf eine verbesserte BBB-Integrität hinweist. Zeigt die aktuelle Studie dennoch, dass HSD vor spontaner EAE schützt, und zwar nicht durch

Veränderungen im Immunsystem, sondern durch eben jenen Einfluss auf die Blut-Hirn-Schranke. Diese Ergebnisse legen eine breitere und potenziell vorteilhafte Rolle von Salz bei der Pathogenese von ZNS-Autoimmunerkrankungen nahe.

1. INTRODUCTION

1.1. MULTIPLE SCLEROSIS

Multiple sclerosis (MS) is a demyelinating disease of the central nervous system. MS was first described by the French neurologist Jean Marin Charcot in the year 1868. It is an autoimmune disorder characterized by the infiltration of immune cells into the Central Nervous System (CNS) which then damages the myelin sheath. The inflammation is transient and remyelination occurs but is not long-lasting [1]. It affects females more than males. As of 2020, MS has been estimated to affect over 2.8 million people worldwide, with a higher incidence in the western hemisphere. This number was observed to be nearly 30% higher than in 2013. In recent years, pediatric onset MS has also seen an increase, with more than 30000 diagnosed cases in comparison to 7000 in 2013 [2].

The most common symptoms of MS are motor problems like muscle weakness, difficulty in balance and coordination, spasms, and ataxia. Other common symptoms are visual problems like a partial or complete loss of vision, pain during eye movement and blurry vision, and sensory problems like numbness in limbs, fatigue, and altered sensitivity to touch or vibrations. Several cases also have optic neuritis or brainstem dysfunction [3]. The specific symptoms are determined by the location of the lesions. 85% of the cases start as a clinically isolated syndrome (CIS). CIS refers to the first episode of neurologic symptoms caused by inflammation or demyelination in the CNS which lasts at least 24 hours. Around 80% of the people diagnosed with CIS go on to have MS. A majority of MS patients experience relapsing-remitting MS (RRMS), where they have an initial disease phase after which they undergo a resolution phase (remission) which is followed by relapses characterized by symptoms lasting at least 24 hours. In some cases, patients experience a gradual worsening in the symptoms over time without any recovery. This is termed primary progressive MS (PPMS). In cases with RRMS, relapses usually occur not over 2 times a year. But, because there is never a complete resolution of symptoms after a relapse, the residual damage persists and accumulates over time to result in progressive disease. This is termed secondary progressive MS (SPMS) [3, 4].

Although the causes of MS are not known, several risk factors have been proposed that include both genetic and environmental factors. Specific genes associated with MS include the Human Leukocyte Antigen (HLA), specifically the DR15 and the DQ6 loci. About 20 to 60% of the genetic predisposition is estimated to be due to HLA differences. However, several other genes like CTLA-4 (cytotoxic T-lymphocyte-associated protein 4) and TCR β (T cell receptor β) are also associated with MS [5]. Environmental factors associated with MS can be either infectious or non-infectious. Infections as triggers for MS was originally proposed in 2 hypotheses – the hygiene hypothesis and the prevalence hypothesis [6]. The prevalence hypothesis postulates that MS is caused by a pathogen more prevalent in regions with higher MS incidence. The hygiene hypothesis on the other hand postulates that early life exposure to infectious agents is protective against MS [6]. Among many infectious agents proposed to

have an association with MS, Epstein Barr Virus (EBV) is a consistent risk factor. The risk of MS is 10 times higher among individuals who experienced EBV infection in their childhood. But this does not exclude the potential role of other microbes [7].

The diagnosis of MS involves the recognition of clinical symptoms along with MRI, oligoclonal bands, and raised IgG indices in the Cerebro-Spinal Fluid (CSF). The advent of the McDonald's criteria has considerably simplified the diagnostic process [4, 8]. After diagnosis, several treatment courses are adopted. Interferon- β and Glatiramer acetate are the most common first-line treatments. Natalizumab and Fingolimod are some of the other drugs used in therapy. Symptomatic therapy is also used in the management of pain and other complications due to MS [4, 9, 10].

1.2. EXPERIMENTAL AUTOIMMUNE ENCEPHALOMYELITIS

MS is a complex and heterogeneous disease and specific pathogenesis pathways are difficult to study directly in patients. Hence, animal models have helped explore the pathogenic mechanisms of MS, chiefly our understanding of the specific roles of the various immune cells and CNS resident cells involved in MS pathogenesis. They have also helped understand the role of various environmental factors like the microbiota, dietary practices and lifestyle, the investigation of which in MS patients is arduous. Additionally, animal models serve as testing tools for investigating disease progression and therapeutic strategies [11].

The most studied animal model for MS is Experimental Autoimmune Encephalomyelitis (EAE). This was first described in rabbits which developed CNS inflammation on immunization with human spinal cord tissue [12]. Later, Rivers et al. described demyelination in the spinal cord leading to paralysis in monkeys immunized with rabbit brain extract [13]. Kabat et al. added Complete Freund's Adjuvant (CFA) and Pertussis toxin to CNS extracts to potentiate the immune response [14]. While induction of EAE was tried in many models, mice and rats provided the best models [15, 16]. With the development of genetic manipulation, transgenic mouse models that spontaneously develop EAE have also been established. Mice from several different genetic backgrounds have been used in EAE [12, 17, 18].

Still, there are some caveats with EAE, and questions have been raised as to whether it does represent a good model for MS. EAE may be induced actively by immunization with antigen along with adjuvants, or passively by transfer of immunogenic T cells. The spontaneous models involve EAE development due to T cells having myelin-specific T Cell Receptors (TCR). MS on the other hand develops spontaneously and its antigen specificity is not yet known. Moreover, the time frame of onset of symptoms is very short in EAE compared to MS. The treatments tested on EAE models also start very early in contrast to human MS which is only detected in its late stages. Another limitation is that EAE studies are done on inbred animals. This limits their applicability to humans. While MS susceptibility depends on several environmental factors, EAE studies are performed in controlled Specific Pathogen Free (SPF) environments. This too limits the transferability of EAE to MS. Nevertheless, the EAE models have allowed a better understanding of some relevant features of human MS.

1.3. IMMUNOPATHOGENESIS OF MS AND EAE

The pathogenesis of MS and EAE is immune-mediated. A schematic illustration of the putative pathogenic cascade in MS and EAE is shown in **Fig 1.1**. The CNS has been recognized as an 'immune-privileged' organ. Under normal conditions, the Blood-Brain Barrier (BBB) precludes the entry of immune cells into the CNS. But during MS or EAE, there is a massive immune cell infiltration into the CNS, resulting in inflammation and eventual neurodegeneration. The disease course in MS and EAE can be either relapsing remitting or progressive, leading to chronic paralysis. The disease is initiated by the infiltration of lymphocytes, in particular, T cells. While MS lesions usually also have CD8+ T cells, CD4+ T cells dominate the CNS lesions in EAE and a majority of the lesions are located in the spinal cord [19]. Though the trigger factors for disease initiation have not been identified, both innate and adaptive responses are thought to be involved in their pathogenesis.

On one hand, CNS antigens like Myelin Basic Protein (MBP) are thought to be constitutively presented in the cervical lymph nodes and can potentially trigger T cell activation. Alternatively, molecular mimicry – which is the structural similarity of epitopes from microbial proteins to those of CNS antigens, or activation of the Toll Like Receptors (TLRs) due to microbial triggers can both lead to CD4+ T cell polarization and differentiation [20, 21]. CD4+ T cells get activated by an antigen presented by Antigen Presenting Cells (APCs) such as Dendritic Cells (DCs) in the periphery that shows similarity with CNS antigens. Activated T cells then differentiate in the periphery to T_H1 and T_H17 cells. It was initially thought that the CD4+ T cells were predominantly T_H1 cells producing IFN γ , but recent evidence implicates the IL-17 producing T_H17 cells too as key players [22].

On the other hand, the presentation of CNS antigen by B cells and DCs to CD4+ T cells also leads to T cell differentiation to T_H1 and T_H17 cells. Primed T_H1 and T_H17 cells migrate to the CNS. They release inflammatory cytokines and promote CNS inflammation, demyelination, and axonal loss. CD8+ T cells are also involved in promoting vascular permeability and oligodendrocyte death. The presence of oligoclonal antibodies in the cerebrospinal fluid of MS patients also reinforces the role of B cells [23]. However, while several studies have looked for the antigen specificity of those antibodies, it is as yet undetermined since a definitive antigen has not been identified.

Activated and polarized peripheral T cells upregulate cell surface integrins like VLA-4 ($\alpha_4\beta_1$) and LFA-1 ($\alpha_L\beta_2$), in addition to enhancing the expression of chemokine receptors like CCR6. They then gain the ability to cross the BBB through the interaction of integrins on the T cell surface with Vascular Cell Adhesion Molecule (VCAM-1) and Intercellular Cell Adhesion Molecule (ICAM-1) in the BBB endothelial cells. While endothelial cells normally express VCAM-1 and ICAM-1 in low levels, their expression is upregulated during EAE in response to stimulus from pro-inflammatory cytokines [24]. Once in the CNS, resident APCs present cognate antigen to the autoreactive T cells, which then are reactivated to produce more proinflammatory cytokines and chemokines like IL-21, IL-22, IFN γ , IL-17, GM-CSF (Granulocyte

Monocyte Colony Stimulating Factor), and $TNF\alpha$, attracting other immune cells like B cells and macrophages to the CNS, thus potentiating an inflammatory cascade.

Macrophages and resident microglia get activated and phagocytose myelin. In addition, generation of nitric oxide and reactive oxygen species by the astrocytes also enhance neuronal damage. Antibodies produced by plasma cells cause tissue destruction by activating the complement cascade [25]. While remyelination does happen, the gradually accumulating neuronal damage renders it ineffective, leading to chronic disease progression. This eventually results in the appearance of clinical symptoms.

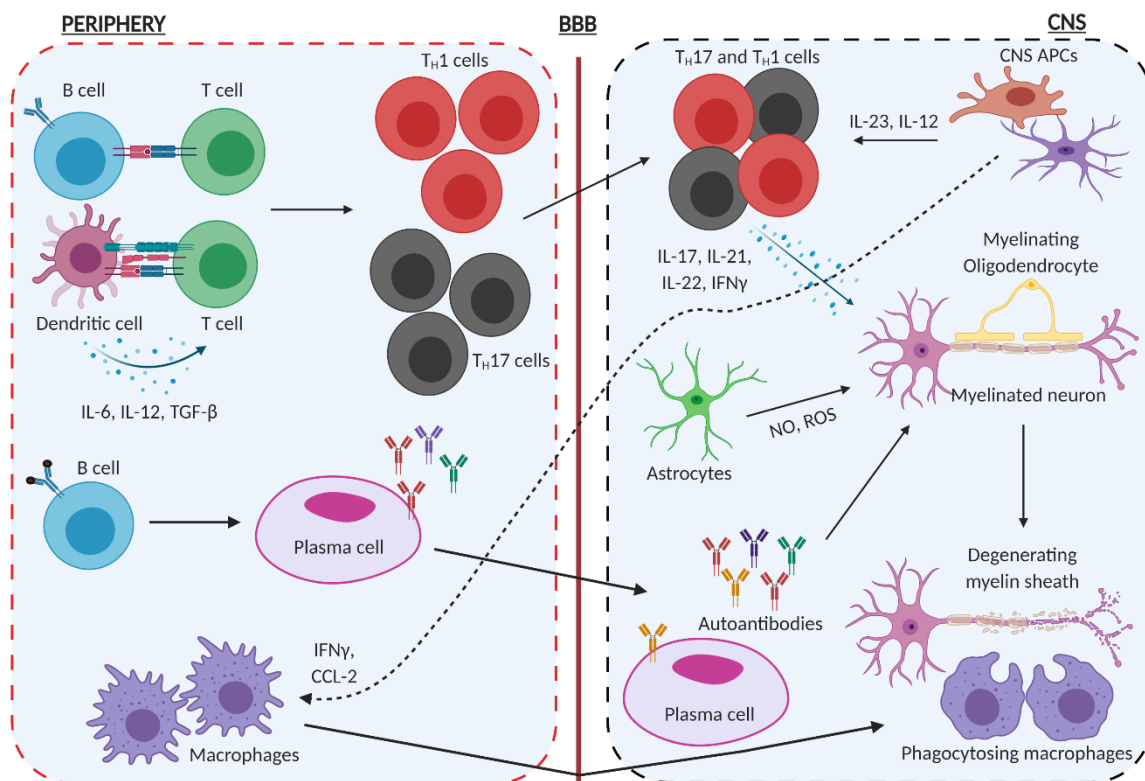


Figure 1.1: Schematic of some key pathological features of EAE and MS. Activated T cells are activated and polarized in the peripheral lymphoid organs. They enter the CNS via the BBB and are reactivated by CNS APCs. In addition, macrophages and plasma cells secreting autoantibodies also enter the CNS. The cytokines produced by the activated T cells, the autoantibodies, and the activated macrophages which are phagocytic, all contribute to demyelination and neurodegeneration. Adapted from [25] and created with BioRender.com.

1.4. INDUCED EAE MODELS

EAE may be induced through either active immunization with protein or peptide, or by transfer of encephalitogenic T cells. The most commonly used antigens to induce EAE are derived from CNS proteins such as Proteolipid Protein (PLP), Myelin Oligodendrocyte Glycoprotein (MOG), or Myelin Basic Protein (MBP) [17-19, 26]. Recent studies have proposed several additional antigens to be involved in EAE. Neurofascin NF155, Transient Axonal

Glycoprotein-1 (TAG-1), Neurofascin NF186, and Neurofilament-M (NFM) are some of the antigens thought to play a role in EAE and MS [27-29].

Active immunization involves the subcutaneous injection of an emulsion of antigen and CFA containing *Mycobacterium tuberculosis* together with an intraperitoneal injection of Pertussis toxin. While CFA contains ligands for TLR2, TLR4, and TLR9 in mineral oil, and enhances the innate immune response, Pertussis toxin facilitates the opening of the BBB which leads to the entry of immune cells into the CNS. An alternative to immunization-based models, adoptive transfer EAE involves the transfer of encephalitogenic T cells into recipient mice. Encephalitogenic T cells are conventionally generated by immunization of donor mice with myelin-derived antigens, isolation of peripheral T cells, and in vitro culture with antigenic stimulus [26]. The transfer model has the advantage of allowing for the polarization of T cells towards any subset of choice before transfer.

Both active and transfer models can develop either chronic or Relapsing-Remitting (RR) EAE depending on the antigenic stimulus and the mouse strain used. Both active immunization with PLP₁₃₉₋₁₅₁ and transfer of PLP-reactive T cells in SJL/J mice result in RR EAE [18]. Likewise, Immunization with MOG₃₅₋₅₅ or transfer of MOG-specific T cells in C57BL/6 mice results in EAE of a chronic nature [12]. Induced EAE models entail a rapid disease course, enabling for shorter periods of study. Studies focusing on the effector phase of disease rather than the trigger can benefit from these models. Therapeutic strategies aimed to target the effector phase can also benefit from them.

1.5. SPONTANEOUS EAE MODELS

The past 20 years have witnessed the development of TCR transgenic mice. T cells from these mice escape Recombination Activation Gene (*RAG*)-mediated recombination of their TCR. More than 90% of the T cells would be specific to a defined antigen or epitope. The first TCR transgenic mice had TCR specific to MBP Ac1-10 on the B10.PL background. They developed EAE when housed in a non-sterile facility, but not in SPF facilities [30]. Subsequently, another transgenic mouse system was developed with specificity to MBP- NAc1-11, which developed spontaneous paralysis on the PL/J background [31]. Following this, the 5B6 and 4E3 mice on the SJL/J background were also developed with specificity to PLP. Bettelli et al. generated MOG₃₅₋₅₅ specific TCR transgenic mice (2D2) in the C57BL/6 background [32]. B cell transgenic mice with a heavy chain knock-in replacing the germline H locus with the variable region gene of the MOG specific monoclonal antibody 8.18C5 (Th mice) were also developed to study EAE [33]. Both 2D2 and Th mice developed more severe EAE than their non-transgenic littermates when active immunization was performed. However, the 2D2 mice showed a propensity to develop spontaneous optic neuritis and spontaneous EAE – albeit at a low incidence, while the Th mice did not spontaneously develop EAE despite having high serum titers of MOG-specific antibodies [32, 33].

Our group has generated 2 spontaneous EAE models. The first is the Opticospinal Encephalomyelitis (OSE) mouse. This is a cross between the 2D2 mice and the Th mice, on the

C57BL/6 background. In this model, T and B cells specific to MOG cooperate to induce chronic EAE in about 50% of the mice [28, 34]. While initially, males show a marginally higher disease incidence than females, eventually the incidence in females also reaches the same incidence levels as in males. The other model is on the SJL/J background and results in a Relapsing-Remitting EAE phenotype (RR/TCR¹⁶⁴⁰ mice). This is a T cell transgenic mouse with TCR specific to MOG₉₂₋₁₀₆. Here, the transgenic T cells recruit endogenous B cells to induce RR EAE, leading to an 80% incidence [35]. Subsequently, the TCR¹⁶⁴⁰ × Th mice have also been developed, and also show a high incidence of RR EAE [35]. In both models, the antigen specificity is to MOG. Hence, the spinal cord and the optic nerve (which express MOG in greater proportion than the brain) are predominantly affected. Both OSE and RR mice have high serum titers of MOG-specific IgG1 and IgG2, as they undergo class switching from IgM. The CNS infiltrates are dominated by Vα3.2+ Vβ11+ CD4+ T cells (2D2 T cells) or Vα8.3+ Vβ4+ CD4+ T cells (TCR¹⁶⁴⁰ T cells) and MOG-specific Th or endogenous B cells. Both these models involve T and B cell cooperation in disease induction without external manipulation and are therefore useful for the elucidation of trigger factors for EAE/MS.

1.6. T AND B CELLS IN EAE

• CD4+ T CELL SUBSETS

Conventionally, EAE is initiated by antigens presented to Major Histocompatibility Complex (MHC) class II restricted CD4+ T cells. CD8+ T cells are in very low frequencies in CNS infiltrating cells. Of the several CD4+ T cell subsets, T_H17 cells and T_H1 cells are known to be the crucial mediators of autoimmunity. FoxP3 expressing regulatory T (T_{reg}) cells are thought to regulate autoimmunity and promote tolerance.

T_H1 cells are differentiated in the presence of IL-12. They express the transcription factor T-bet and produce the cytokines IFNγ, IL-2, and TNF-α [36]. They were originally thought to be the main pathogenic cells in EAE and MS. This was based on the observation that mice deficient in the p40 subunit of IL-12 (IL-12p40^{-/-}) were resistant to EAE [37]. MS patients treated with IFNγ showed exacerbated disease [38]. But IFNγ^{-/-} and STAT-1^{-/-} mice, both of which lack T_H1 cells, develop more severe EAE [39, 40]. Moreover, IL-12p35^{-/-} mice were susceptible to EAE [41]. This led to the notion that other cell types also contribute to EAE.

The discovery of IL-23, a cytokine structurally similar to IL-12 and sharing its p40 subunit helped answer this paradox. IL-23p19^{-/-} mice were resistant to EAE. Hence, IL-23 was identified as being more critical to EAE than IL-12 [41]. The expansion of T_H17 cells was shown to require IL-23 [42]. T_H17 cells require TGF-β and IL-6 for their differentiation. RORγT (Retinoid-related Orphan receptor-γ) controls their differentiation and function [43]. The key role of T_H17 cells in EAE was highlighted by studies showing a reduced severity of EAE due to the neutralization of IL-17 [44, 45]. While there are contradictory data on the role of T_H17 derived cytokines other than IL-17, T_H17 cells have emerged as key players in EAE [41].

Interestingly, it was reported that T_H1 cells can independently induce EAE, but T_H17 cells cannot do so without IFNγ [46]. It was also reported that T_H1 cells access the CNS first and

then recruit T_H17 cells [47]. But a critical role for the recruited host T_H17 cells in EAE development was shown by the observation that IL-17^{-/-} mice showed a lower disease incidence [48]. Moreover, Kroenke et al. demonstrated that T cells modulated by IL-12 and IL-23 can induce EAE in disparate ways, mediated by distinct cell types. IL-12 polarized T cells promote macrophage infiltration, while IL-23 polarized T cells promoted neutrophil infiltration [49]. Recent research has also addressed the plasticity of the T helper cell subsets. T cells producing both IL-17 and IFN γ and expressing both T-bet and ROR γ T are present in CNS infiltrates in EAE [50]. T-bet has been shown to regulate both T_H1 and T_H17 cells in EAE [51]. Therefore, while much of recent research has focused on the relative roles of T_H1 and T_H17 cells, this demarcation is still not resolved.

T_{reg} cells can be both natural and induced (nT_{reg}, iT_{reg}). They express CD25 and FoxP3, which are essential for the regulatory function. They were first identified through their regulatory role in autoimmunity. nT_{reg} cells are positively selected in the thymus and are self-antigen specific. They are thought to play a key role in regulating autoimmunity due to their antigen specificity [41]. iT_{reg} cells are generated in the periphery in the presence of TGF- β , IL-10, and Retinoic acid. Several studies have shown reduced T_{reg} cell functionality in MS patients [52]. T_{reg} cells have been shown to play a protective role in MOG induced EAE [53]. The protective effect is mediated by IL-10. T_{reg} cells from IL-10^{-/-} mice fail to protect from EAE [54]. It has also been shown in a PLP-induced EAE model that the susceptibility of various mouse strains to EAE negatively correlates with the proportion of PLP-specific T_{reg} cells [55].

T_{reg} cells have also been shown to mediate recovery in EAE and their depletion inhibits recovery. The recovery is associated with IL-10 production [56]. Yet, Korn et al reported that T_{reg} cells were incapable of suppressing effector T cells at the peak of disease, even though they were present in the CNS [57]. Recent insight into T_{reg} cell plasticity has also helped better understand their role in EAE. A subset of T_{reg} cells was shown to produce IL-17, which led to the masking of their suppressive effect [58]. These studies indicate that disease progression depends on the shift of balance between the effector and regulatory T cells.

- **CD8+ T CELLS**

While predominant research on EAE has been on CD4+ T cells, lesions in the inflammatory infiltrate in the brain and spinal cord of MS patients have both CD4+ and CD8+ T cells. Several studies have shown that antigen-specific CD8+ T cell lines derived from MS patients show pathogenicity against cells expressing HLA-A2 and neuronal antigens [59, 60]. Further, MHC class I alleles have been associated with a genetic predisposition to MS [61]. Thus, understanding the role of CD8+ T cells in the disease is essential.

The first evidence of a pathogenic role for CD8+ T cells came through the development of a CD8+ T cell mediated EAE model using MBP as the antigen [62]. This came about due to the discovery of CD8+ T cells specific to MBP 79-87 peptide in C3H.*shi* mice (mice having “shiverer” mutation, rendering them deficient in MBP, causing tremors resembling shivering), following which active immunization of WT C3H mice with MBP 79-87 in CFA resulted in CD8+

T cell mediated EAE. Concurrently, Sun et al. showed that MOG 35-55 specific CD8+ T cells induced severe EAE [63]. Subsequently, another study identified MOG 37-46 specific CD8+ T cells as pathogenic effectors in EAE [64]. While these studies used myelin components as antigens, a subsequent report showed that CD8+ T cells specific to Glial Fibrillary Acidic Protein (GFAP - expressed in astrocytes) escape negative selection and can cause CNS autoimmunity [65].

While all of the above studies showed a pathogenic role for CD8+ T cells, some other studies have shown CD8+ T cells to have a role in the initiation of EAE and the potentiation of CD4+ T cell responses. Huber et al. showed that T_H17 cell accumulation in the CNS and subsequent EAE development required Tc17 cells (CD8+ T cells producing IL-17A) [66]. Another study showed that CD8+ T cells specific to MOG 181-189 presented by HLA-A*0201 exacerbated EAE by potentiating CD4+ T cell responses [67].

Spontaneous EAE models have also been developed to study the role of CD8+ T cells. Brisebois et al. showed that mice overexpressing CD86 in the CNS develop EAE characterized chiefly by CD8+ T cell infiltrates and minimal CD4+ T cells and B cells, though the antigen specificity of the response was not determined [68]. Subsequently, the ODC-OVA mice were generated, expressing ovalbumin in the oligodendrocyte cytosol. Here, OT-I CD8+ T cells generated endogenously were shown to have encephalitogenic potential in an IFN γ dependent manner [69]. Later, Wagner et al. also generated the 8.8 mice – a TCR transgenic mouse line with TCR specific to MBP 79-87 presented by MHC class I [70].

CD8+ T cells have also been shown to have a regulatory role in EAE. Studies on CD8^{-/-} mice on the PL/J background showed that the lack of CD8+ T cells resulted in lower mortality, but at the same time a higher rate of relapses, suggesting that CD8+ T cells could act as both effector and regulatory cells [71]. In another study, HLA class I molecules were also shown to have opposing effects in influencing CD8+ T cells during disease. HLA-A3 was associated with enhanced disease and HLA-A*0201 with protection [72]. Several other studies have shown the regulatory role of IFN γ + CD8+ T cells in CD4+ T cell mediated EAE, either by direct cytotoxic action or suppression of effector CD4+ T cell responses [73-75]. Effective therapy with Glatiramer acetate was also shown to require CD8+ T cells [76].

- **B CELLS**

The first evidence of the involvement of B cells in EAE pathogenesis came from studies in rats administered anti-IgM which failed to develop EAE following MBP immunization, but did develop EAE when sera containing anti-MBP was transferred to them [77, 78]. Later, more studies using anti-MOG monoclonal antibodies showed an exacerbation in EAE [79]. Yet all these studies only showed a role for B cells in autoantibody production and augmentation of EAE, not its induction. Subsequent reports showed other roles for B cells in EAE.

Treatment with Rituximab – anti-CD20 – which depletes B cells, was shown to prevent EAE onset by diminishing T cell responses [80]. Also, while B cell transgenic mice do not develop

EAE, OSE mice with both MOG-specific T and B cells spontaneously develop EAE [34]. This suggests the possibility of self-antigen specific B cells acting as APCs to activate autoreactive T cells to initiate disease in addition to producing autoantibodies to augment disease. But RR mice, which are only MOG-TCR transgenic, also developed spontaneous EAE accompanied by autoantibody generation by endogenous B cells. Anti-CD20 was found to protect from disease in this system [35]. Thus, antigen-specific T cells can also expand antigen-specific B cells from the endogenous repertoire which then augment disease.

On the other hand, B cells are also thought to function in a regulatory role in EAE by the production of IL-10 [81]. However, the location and nature of the targets of B cell-derived IL-10 are not yet known. B cells can also produce cytokines that skew T cell polarization towards the anti-inflammatory milieu [82]. Besides, B cells have been shown to regulate T_{reg} cells in an IL-10 independent manner. The emergence of T_{reg} cells in the CNS was found to be delayed in B cell-deficient mice. The expression of B7 by B cells was shown to be important for the emergence of T_{reg} cells in the CNS [83]. Expression of glucocorticoid-induced TNF ligand (GITRL) on B cells was also found to promote T_{reg} cell proliferation [84].

In MS therapy, IFN- β – the most widely prescribed treatment – has been shown to act by increasing the number of regulatory B cells as well as IL-10 secretion by B cells. Interestingly, the IFN- β induced increase in the production of autoantibodies also indicates a role of humoral immunity and autoantibodies in a protective role as opposed to promoting disease [85]. Amidst growing evidence of B cells acting in a regulatory capacity, Tedder and colleagues showed that the timing of B cell depletion influenced the disease course. While depletion before disease induction was found to exacerbate EAE, depletion after disease initiation proved beneficial in resolving the disease [86]. They identified IL-10-producing CD1d^{hi} CD5+ regulatory B cell subset (B10 cells) that protected from EAE initiation but had no role during disease progression.

Aside from these reports, studies on MS patients showed that B cells also mediate cytotoxicity and apoptosis of neurons and oligodendrocytes by secreting non-immunoglobulin factors, independent of Ig and cytokine secretion [87, 88]. This indicates that a lot still needs to be understood about B cell function, specifically the timing of opposing B cell functions and their relative contribution to disease, as well as their roles in addition to antibody secretion and being APCs to harness potential therapeutic strategies.

1.7. OTHER IMMUNE CELLS IN EAE

• MACROPHAGES

During the effector phase in EAE, monocytes infiltrate the CNS, where they differentiate into macrophages, express MHC class II and release pro-inflammatory factors [89]. Infiltrating macrophages accumulate in the node of Ranvier and initiate demyelination without affecting CNS resident microglial populations [90]. Indeed, MS patients have been found to have CCR1+ CCR5+ monocytes in demyelination zones [91]. In addition to releasing chemokines like CXCL-2 which enable the infiltration of neutrophils as well into the CNS, they also produce a host

of pro-inflammatory cytokines like IL-6, IL-1 β , TNF α , and IL-23, which promote T cell polarization [92, 93].

On the other hand, a protective role has also been identified in macrophages. PD-L1/PD-L2+ macrophages have been shown to have an alleviating effect on EAE [94]. The differentiation of monocytes into M2 macrophages has also been shown to have a protective role, and modulation of macrophage phenotype in mice towards M2 resulted in striking improvement in neurological symptoms and survival during EAE [95]. M2 polarized macrophages produce the anti-inflammatory cytokine IL-10 and reduce their production of IL-6, IL-1 β , and IFN γ . This differential polarization of macrophages to regulate CNS autoimmunity is being explored therapeutically. Spermidine has been shown to alleviate EAE by reducing the expression of CD80 and IL-1 β in monocytes and enhancing Arginase-1 expression, thus programming them towards an M2 phenotype [96]. Lenalidomide has also been shown to regulate EAE by polarizing monocytes towards an M2 phenotype [97]. Many other drugs like Forskolin and Bryostatins were also shown to alleviate EAE through the modulation of macrophage phenotype [89]. The role of the different macrophage subtypes and their roles in MS/EAE is becoming increasingly clearer, though more research is still needed for additional therapeutic applications.

- **NEUTROPHILS**

Neutrophils comprise a significant portion of CNS infiltrates in EAE. MS patients have also been shown to have primed neutrophils in their blood, and their neutrophil to lymphocyte ratios were found to be significantly higher [98, 99]. They have been shown to promote EAE through the production of pro-inflammatory cytokines IL-6 and TNF α , in addition to inducing the expression of MHC class II, CD80, and CD86 on local APCs to aid in their maturation. Interestingly, this was shown to be mediated only by CNS derived neutrophils [100]. Neutrophils also have a role in the disruption of the BBB. While an exact mechanism for barrier disruption is not known, it is thought to be due to their secretion of matrix metalloproteases and reactive oxygen species [101]. Their depletion in EAE has been shown to maintain barrier integrity and reduce EAE severity [102, 103]. Yet, therapeutic applications involving neutrophils are made challenging by the dearth of studies on their role in MS patients. This necessitates acquiring a deeper understanding of their role using EAE systems in order to help lead to therapeutic implications.

- **DENDRITIC CELLS (DCs)**

DCs are key players in the presentation of antigen to T cells and the initiation of adaptive immune response. They have been shown to have differential roles in CNS autoimmunity. On one hand, CNS inflammation is associated with the migration of DCs into the CNS, and DCs are the most efficient in presenting antigen to encephalitogenic CD4+ T cells [104]. Also, in EAE resistant MHC class II deficient mice, expression of MHC class II in DCs alone was sufficient to induce EAE [105]. Plasmacytoid DCs have been shown to promote EAE by enhancing T_H17 cell priming [106]. Due to their high expression of chemokine receptors like CCR7, DCs

recruited during CNS inflammation are also thought to migrate from the CNS into the cervical lymph node after interaction with CNS antigens, and then activate peripheral naïve T cells, thus exacerbating CNS autoimmunity [107]. Further, in active EAE, DCs have been shown to accumulate in the CNS after EAE induction, but before the clinical onset of EAE [108].

On the other hand, they have also been associated with regulatory roles. Mice lacking DCs were shown to have enhanced EAE severity, and DCs engineered to present CNS antigens were shown to promote tolerance and protect from EAE through PD-1 mediated induction of T_{reg} cells [109]. Additionally, antigen specific CD8⁺ T cells were shown to mitigate CD4⁺ T cell mediated EAE by modulating cytokine production by DCs. IL-10 produced by DCs was found to be essential for EAE suppression [110]. The synthetic terpenoid CDDO-DFPA is known to be protective against EAE through the modulation of IL-10 and TGFβ production by DCs. Also, DCs exposed to CDDO-DFPA were found to be ineffective in activating T_H17 and T_H1 cells [111]. While several immunomodulatory drugs used in treating MS are known to modulate DC functionality, since they were not designed to specifically target only DCs, the design of DC specific therapy still leaves much to be understood about pathways regulating DC function. In this regard, some advances have been made on characterizing the role of the Aryl hydrocarbon receptor (Ahr) in DC function and this has emerged as a potential target for therapeutic modulation [112], opening up the possibility of using Ahr ligands as therapeutics.

1.8. BLOOD BRAIN BARRIER (BBB) IN EAE

The extravasation of encephalitogenic T cells requires 4 key families of molecules - the integrins, cell adhesion molecules, chemokines, and selectins. **Fig.1.2.** shows a schematic of immune cell transmigration across the BBB during EAE. T cells first get captured onto the BBB due to the interaction of T cell surface integrins that are upregulated upon activation, with cell adhesion molecules on the surface of the BBB endothelia. The key integrins involved in this process are VLA-4 ($\alpha_4\beta_1$) and LFA-1 ($\alpha_L\beta_2$). VLA-4 interacts with VCAM-1, while LFA-1 interacts with ICAM-1 and ICAM-2. ICAM-1 and VCAM-1 are upregulated during EAE [113]. Deletion of the α_4 integrins in T cells was shown to prevent the entry of T_H1 cells, but not T_H17 cells into the CNS [114]. T_H17 cells were found to enter the CNS independently of α_4 but needed LFA-1 [115]. The drugs Natalizumab and Efalizumab administered to MS patients target disruption of the α_4 -VACM-1 and LFA-1-ICAM-1 interactions respectively [116].

After the initial contact of T cells and the BBB cells, the strength of this interaction is enhanced to sustain shear resistance to the blood flow. This is achieved by the interaction of chemokines on the endothelial surface with the chemokine receptors on the T cell surface. The chemokines largely associated with EAE are CCL19, CCL20, CCL21, and CXCL12 [117-119]. These chemokines bind chemokine receptors (belonging to the GPCR family) like CCR6 and CXCR3 on the T cell surface [120, 121]. Pertussis toxin, which is used in active EAE models, can disrupt the BBB-T cell interaction by modifying G proteins and disrupting GPCR signaling [122]. Endothelial P-selectin interaction with PSGL-1 on the T cells also aids in this process. The P-Selectin – PSGL-1 interaction begins the capture process. T cells roll on the endothelial cell

layer forming transient P-Selectin – PSGL-1 interactions until the integrin-Cell Adhesion Molecule (CAM) interaction forms [123].

Once captured, T cells then crawl on the BBB and find a site permissible for diapedesis. Again, integrin-CAM interactions are responsible for the crawling process. Then, diapedesis occurs either through a paracellular route – via endothelial cell-cell junctions, or a transcellular route through the endothelial cell body. The paracellular route is thought to be the major pathway for diapedesis. But recent studies posit that the transcellular route is used equally well [124]. Both routes of diapedesis depend on the endothelial cell surface junction molecules. Paracellular migration is actively mediated by CD31 (PECAM-1 – platelet/endothelial cell adhesion molecule) and JAM (Junctional adhesion molecule) [125]. PECAM-1 and Caveolin are thought to be critical for transcellular migration [126].

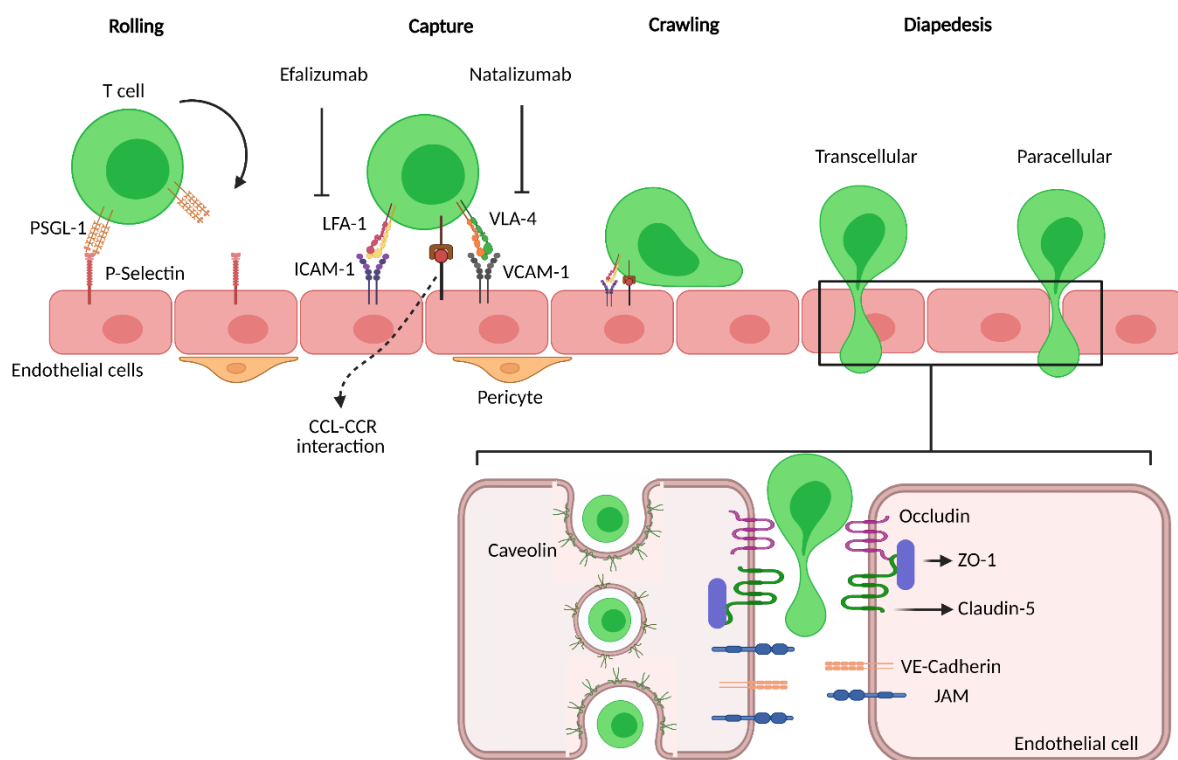


Figure 1.2: Schematic of T cell transmigration across the BBB during EAE. Activated T cells upregulate the expression of PSGL-1, integrins, and chemokine receptors. The key steps in transmigration through the BBB are rolling (through PSGL-1/P-Selectin interaction), capture (integrin-CAM and Chemokine (CCL) – Chemokine receptor (CCR) interaction), crawling, and diapedesis. Diapedesis can be transcellular (bottom left) or paracellular (bottom right). The transcellular process involves caveolin mediated endocytosis. The paracellular process involves junction proteins like ZO-1, Claudin-5, Occludin, and JAM. Adapted from [116, 126, 127] and created with BioRender.com.

The endothelial Tight Junction Proteins (TJPs) are also major determinants of diapedesis. Alterations in the TJP levels are associated with either a ‘tightening’ or ‘loosening’ of the BBB, resulting in the altered permeability of endothelial cells. Indeed, a re-localization of ZO-1, a key TJP, has been shown in induced EAE models [128]. It has also been shown that T_H17 cells

can disrupt the TJPs ZO-1 and Occludin, and promote the transmigration of T cells across the BBB [129]. Pertussis toxin has also been shown to reduce the integrity of the BBB by modulating the TJP localization [130]. The BBB has also been exploited in therapeutic studies in EAE. Resveratrol, a naturally occurring polyphenol, has been shown to protect BBB integrity by ameliorating the loss of TJPs and repressing ICAM-1 and VCAM-1 expressions [131]. BBB modulators have extensive therapeutic potential that can be tapped into with further studies on animal models and eventually in MS patients.

1.9. CNS RESIDENT CELLS IN EAE

• MICROGLIA

Microglial activation is a prominent factor in MS. Pre-active lesions are composed of microglia highly expressing CD68, HLA-DR, TNF, and IL-10, showing both inflammatory and regulatory signatures [132, 133]. Microglia in active MS lesions also produce the TNF family of cytokines, IL-6, IL-12, and IL-23 in addition to chemokines like CCL4, CXCL12, and CCL5. In EAE, single cell RNAseq has identified at least 4 distinct subsets of microglia localized to lesions and highly expressing pro-inflammatory genes like Ly86, CCL5, and CXCL10 [134]. Microglial activation is in part thought to be driven by secretion of IL-17 and IFN γ by infiltrating T cells, and during activation, they upregulate the production of several chemokines like CCL2, CCL3, CCL4, CCL5, and CCL7 [90, 135]. Microglia also produce IL-6 in large quantities and this is thought to contribute to EAE, as its depletion was shown to ameliorate disease. This is hypothesized to be because of the activation of IL-6 receptors on BBB endothelial cells, which eventually leads to BBB disruption [136]. The cholesterol derivative 15-alpha-hydroxicholestene (15-HC) – found in the sera of RRMS patients – was found to activate TLR-2 in microglia and enhance microglial production of nitric oxide (NO), CCL2, and TNF which all contributed to promoting inflammation [137]. Sphingosine-1-phosphate receptor modulating drugs used in MS therapy – fingolimod, ozanimod, laquinimod - have been shown to exert part of their effect by inhibiting the release of pro-inflammatory mediators like NO and TNF by microglia [138]. Many other drugs like the CSF1R inhibitor GW2580, nimodipine (which induces microglial apoptosis), and ER β agonists all have shown benefits in EAE through their action on microglia [139].

However, several other reports also point to a protective role of microglia during EAE. Microglia have been shown to also produce factors that enable reparative functions in the CNS in response to signals in the CNS environment. One such signal is IFN γ from infiltrating T cells, silencing the binding of which in microglia was shown to exacerbate disease [140]. IFN β , one of the most common treatments for RRMS, was shown to be predominantly produced by CNS resident microglia, and IFN β -producing microglia were shown to remove myelin debris more effectively [141]. While the normally produced quantity of IFN β is probably not enough to protect from EAE altogether, the use of polyinosinic–polycytidylic acid – a potent inducer of IFN β – after the advent of EAE symptoms, was observed to mitigate EAE [142]. Rothhammer et al. showed that the production of TGF α by microglia in response to microbial metabolites in an Ahr dependent manner had protective effects in EAE models [143]. Also,

while CSF1R was shown to have detrimental effects in EAE, other reports suggest that the stimulation of CSF1R in microglia has neuroprotective effects [144]. This indicates that we need a better understanding of the breadth of microglial responses in MS/EAE to identify novel therapeutics targeting microglia.

- **ASTROCYTES**

Astrocyte reactivity is known to be a common phenomenon in EAE and MS that begins at disease onset and persists into the chronic phase of the disease. In EAE, astrocyte activation is observed in the CNS even before the appearance of clinical symptoms, preceding cellular infiltration [145]. Astrogliosis can be observed right from the pre-symptomatic stage, and directly correlates with disease severity [146]. Astrocytes were shown to be damaged during EAE, and these damages correlated to increased BBB permeability, suggesting that astrogliosis may influence BBB permeability [147]. Astrocytes have been shown to have differential roles during various stages of EAE. For instance, the selective depletion of proliferating reactive astrocytes which was initiated either prior to EAE induction and continued until acute disease phase, or initiated immediately after onset, resulted in exacerbated EAE, which was attributed to an increased BBB permeability in the absence of astrocytes [148, 149]. But their depletion during the chronic phase of disease was shown to be protective and improved clinical outcomes [148].

Astrocytes produce both pro and anti-inflammatory cytokines and chemokines during different phases of EAE [148]. They are also a major source of ROS and NO and contribute to oxidative damage and resulting cytotoxicity [150]. They contribute to BBB integrity via the expression of aquaporin 4 and dystroglycan, both of which are dysregulated during EAE [151]. The expression of sonic hedgehog in astrocytes has also been shown to promote barrier integrity and downregulate ICAM-1 and CCL2, thereby reducing the migration of immune cells into the CNS [152].

Glycolipids like lactosylceramide (LacCer) have been found to regulate astrocyte activation, promoting a pro-inflammatory phenotype during EAE. LacCer induces the activation of microglia and the production of CCL2 and GM-CSF, which play a role in the recruitment of innate immune cells to the CNS [148]. TGF α and VEGF-B have also been shown to modulate astrocyte activation and the balance between pro and anti-inflammatory phenotypes. TGF α exerts a regulatory effect under normal conditions, suppressing *NF- κ B*, *Nos2*, and *IL1 β* , but during EAE, VEGF-B production by microglia is enhanced, leading to a pro-inflammatory cascade as a result of NF- κ B activation. This was shown to be modulated by microbial metabolites via the Ahr signaling cascade, indicating a potential therapeutic avenue [143].

The Sphingosine-1-phosphate receptor modulating drug fingolimod has also been shown to exert its effect partly via astrocytes, by suppressing TNF, IL-6, CCL2, and CCL20 and upregulating CXCL12 in astrocytes [153]. The astrocyte specific depletion of sphingosine-1-phosphate receptor has been shown to reduce the therapeutic efficiency of the drug in EAE [154]. Moreover, like microglia, astrocytes have also been shown to respond to Type-I

interferon signaling by upregulating Ahr, which in response to dietary and microbial metabolites downregulates inflammatory signaling through the SOCS2-dependent inhibition of NF- κ B [155].

1.10. THE HYGIENE HYPOTHESIS

There has been a growing understanding of the role of immune cells, the BBB, and CNS resident cells, but the trigger factors for MS are not well understood. While genetic and environmental factors are both associated with MS, studies on monozygotic twins discordant for MS have shown that environmental factors would most likely dominate [156, 157]. The hygiene hypothesis was thus proposed to explain how environmental factors affect several diseases including MS.

Over the last few decades, our society has collectively become more and more 'hygienic'. This collective hygiene has resulted in the depletion of several microbial species with which we have co-evolved, from the environment. These changes have been postulated to result in alterations in immunomodulation [158-160]. The term 'Hygiene hypothesis' has been used to refer to this phenomenon. The hygiene hypothesis is supported by robust epidemiological data [161]. Over the years, this hypothesis has been refined to "the old friend's hypothesis" [162] and posits the alterations in our normal gut microbiota as the key reason for the increase in the occurrence of autoimmune diseases.

A key factor in the transition to better collective hygiene is the decline in occurrences of infectious diseases over the last 2 centuries due to vaccination and better therapeutic methods [163]. This is also tied to the extensive usage of antibiotics, particularly in early life [164], leading to gut microbial alterations. Subsequently, the rampancy of smoking, usage of various drugs, and a decline in the propensity towards exercise/physical activity were also found to contribute in minor roles [165]. Widespread change in dietary practices, specifically the shift in preference towards processed food, which in turn leads to gut microbial alterations, has also been postulated as a factor in the increase in occurrence of autoimmune diseases.

1.11. THE GUT MICROBIOME – AN OVERVIEW

Vertebrates are hosts to a diverse ecosystem comprising several microbial species. These serve to diversify both the genetic and metabolome repertoire of the host [166]. The microbiota colonizes several 'hotspots' in the body that are exposed to the environment, the most dominant being the skin, mouth, gut, and vagina. Of these hotspots, the dominant community both in terms of absolute number and species diversity are the microbiota inhabiting the gut [167]. The development of culture-independent analyses has furthered research into the gut microbiome. 16S rRNA sequencing enables the characterization of bacterial species. Additional characterization of the metagenome, transcriptome, proteome, and metabolome enables the expansion of information on various levels of gut microbial physiology [168]. Further, the development of Germ-free (GF) mice and techniques for

microbiota colonization and transplant has helped understand several of the microbiota's functional roles.

- **ACQUISITION OF THE MICROBIOTA**

Mammals acquire their microbiota repertoire from their immediate environment. The first exposure to the microbiome happens during birthing and is dependent on the mode of delivery (vaginal or caesarian) [169]. During the first months, the continuity and duration of breastfeeding influence the intestinal microbiota [170]. Subsequently, throughout early life, this initial microbiome diversifies due to various factors like diet, antibiotic usage, usage of probiotics/supplements, geography, and exposure to different environments shaping the microbiota [171]. In humans, the microbiota predominantly acquires a stable composition between 2 and 3 years of age.

- **ROLE IN DIGESTION AND METABOLISM**

The primary role of the microbiota is in the digestion of dietary components. Dietary polysaccharides like xyloglucans are metabolized by the Bacteroides family [172]. Glycoside hydrolases in *Bacteroides thetaiotaomicron* metabolize dietary fiber [173]. Microbial fermentation of dietary fiber to Short Chain Fatty Acids (SCFAs) has been extensively studied [174]. The microbiota has also been implicated in protein metabolism and the synthesis of several amino acids [175] including biogenic amines [176]. *Escherichia coli* and the Enterococcus genus can metabolize tryptophan derivatives that regulate host defense and colonization resistance from enteric pathogens and can act as neurotransmitters [127, 176, 177]. Also, many essential vitamins including B complex and K are synthesized by gut bacteria [178-180]. Further, the maintenance of a healthy mucin layer in the gut is contingent on the commensal *Akkermansia muciniphila* [181]. Additionally, several of the host's and the microbiota's pathways are interdependent [182].

The microbiota also plays a role in detoxification. For instance, *Clostridia* and *Bifidobacteria* have a host of enzymes enabling the detoxification of sulfur-containing compounds [175, 183]. The gut microbiota is also involved in the metabolism of xenobiotics. The metabolism of Benzodiazepine class drugs like Nitrazepam and clonazepam is one example [184, 185]. Ranitidine, a common drug used to treat peptic ulcers, is metabolized by colonic bacteria [186]. Some other drugs that are known to be metabolized by the microbiota are Digoxin, Metronidazole, L-DOPA, and also the antibiotic Chloramphenicol [187-190].

- **ROLE IN IMMUNE HOMEOSTASIS**

Another key role of the microbiota is to promote immune homeostasis. The immune system develops a tolerance to the microbiota, yet maintaining their ability to clear infections. The microbiota regulates several components of the immune system. Early studies in GF mice showed that the absence of commensal microbiota resulted in profound defects in intestinal lymphoid tissue and GALT architecture. GF mice have significantly reduced numbers of $\alpha\beta$ and $\gamma\delta$ Intra-Epithelial Lymphocytes (IELs) compared to conventionally housed mice. These IELs

rapidly expand upon colonization [191]. Further, macrophages from GF mice cannot efficiently effectuate chemotaxis and phagocytosis [192]. GF mice also have underdeveloped Peyer's patches, mesenteric lymph nodes, and lymphoid follicles, all of which develop normally after the introduction of microbiota [193].

Microbial ligands serve as stimuli for the receptors on DCs and epithelial cells. Different bacteria stimulate different TLRs on the APCs. For instance, the microbial cocktail VSL#3 which comprises gram positive bacteria like *Lactobacillus acidophilus*, *Lactobacillus delbrueckii subsp. bulgaricus*, *Lactobacillus casei*, *Lactobacillus plantarum*, *Bifidobacterium longum*, *Bifidobacterium infantis*, *Bifidobacterium breve*, and *Streptococcus salivarius subsp. Thermophilus*, activates TLR9, while LPS from gram negative bacteria stimulates TLR2 and TLR4 [194]. The differential regulation of TLR activation shapes intestinal barrier integrity - as TLRs regulate the expression of tight junction proteins. It also mediates clearance of pathogens and protection from gut injury [195, 196].

Also, several species in the gut have been associated with the regulation and balance of T cell subsets. *Bacteroides fragilis* can induce T_H1 cell differentiation, the Segmented Filamentous Bacteria (SFB) induce T_H17 differentiation and Clostridia promote T_{reg} cell development. While T_H17 cells can be either pro-inflammatory or anti-inflammatory depending on their microenvironment, commensal-induced T_H17 differentiation generates homeostatic non-inflammatory cells involved in maintaining the intestinal barrier [191]. A recent study also showed that the gut microbiota and microbial metabolites are necessary for the transition of antigen activated CD8+ cells into memory cells [197]. Additionally, the generation of T-follicular helper (Tfh) cells also necessitates the gut microbiota, as evidenced by their impairment in GF mice. Tfh cell differentiation requires the presence of TLR ligands to activate MyD88 signaling. Further, SFBs promote Tfh differentiation in Peyer's patches by limiting access of IL-2 to CD4+ T cells, suppression of IL-2R α , and upregulation of the master regulator Bcl-6 [198]. Tfh cells in turn aid in B cell maturation in the germinal center in Peyer's patches and mesenteric lymph nodes.

The microbiota also influences B cell development in the intestinal lamina propria. The differentiation of regulatory B cells in both the spleen and mesenteric lymph nodes requires the microbiota [199]. Moreover, the gut microbiota drives mucosal IgA production. IgA can be produced in both a T cell dependent and T cell independent fashion. The recognition of microbial flagellin by TLR5 on DCs induces the production of retinoic acid by DCs which promotes the retention of IgA producing plasma cells in the lamina propria. Also, microbial modulation of IgA production depends on PD1 produced by Tfh cells [200]. In turn, IgA acts as a regulator of microbial levels in the gut, thus maintaining a balanced microbial repertoire which in turn regulates T cell differentiation and T cell dependent IgA response in a feedback loop [191, 192]. For instance, altered IgA levels lead to altered levels of *Bifidobacterium* and *Bacteroides*, and an increase in Enterobacteriaceae [200].

1.12. FACTORS AFFECTING MICROBIAL DYSBIOSIS

As they have such diverse roles, the decrease in many microbes from the environment due to collective hygiene [201] impacts our acquired microbial repertoire and results in 'dysbiosis' (microbial maladaptation in the body). Alterations in gut microbial composition lead to a restructuring of several metabolic pathways and alterations in the metabolome profile. The predominant factors influencing the fully established gut microbiota are diet, usage of medication, and host genotype.

- **GENOTYPE**

Many studies have addressed how host genotype influences the microbiota. For instance, a study on monozygotic and dizygotic twin pairs for concordance on leanness and obesity revealed that while the microbiome was shared among family members, the specific bacterial lineages vary even between twin pairs. The study also showed that many bacterial genes were shared between the sampled individuals, indicating that while the organismal diversity may be high, a 'core microbiome' can be identified, defined by shared genes rather than organismal lineages [202]. This also indicates a high degree of redundancy in the microbiome.

In comparison, another study showed that many microbial taxa were influenced in part by host genetics. The study identified several heritable taxa like the Christensenellaceae family and the Methanobacteriaceae. Monozygotic twin pairs showed more correlation in microbial taxa than dizygotic twin pairs. The Bacteroidetes family was found to be non-heritable [203]. Yet another study reported *Bifidobacterium* and *Turicibacter* to be the most heritable taxa. Other genera like *Blautia* and *Akkermansia* were also, to a lesser degree, heritable, and associated with the host genes SIGLEC15 and CD36 [204]. While several reports describe heritable microbial taxa by associating specific microbial taxa to host genes, they all lack a robust effect, even among monozygotic twin pairs. It is hypothesized that the higher correlation in the microbial community among monozygotic twin pairs is not the impact of host genetics alone, but shared diet and lifestyle preferences as well [205]. So, while host genetics does exert an influence on the microbiome, its impacts are overshadowed by the dominant effects due to diet and lifestyle.

- **USAGE OF MEDICATION**

The past 2 decades have witnessed a decrease in the incidence of infectious diseases, primarily due to the widespread usage of antibiotics. While antibiotics help in controlling infections, several studies show that they also affect the resident microbiota in the host. Willman et al. showed reduced gut microbial diversity on treatment with ciprofloxacin and cotrimoxazole. They also showed the emergence of potential pathogens like *Acinetobacter johnsonii* and a rise in the percentage of antibiotic-resistance genes in the gut [206]. Clarithromycin has been shown to reduce the *Bifidobacterium*, *E. coli*, and *Lactobacillus* populations in the short term, while treatment with Amoxicillin has been shown to increase the levels of Enterobacteria, anaerobic Gram-positive Lactobacilli and Bifidobacteria [207]. Some studies have shown that the microbiota return to normal levels 2 to 4 weeks after the

treatment stops, while some studies report the persistence of the changes for up to 6 months after termination of treatment [208-210].

Other commonly used drugs also affect the gut microbiota. Vich Vila et al. showed through a metagenomics screen, that Proton Pump Inhibitors (PPIs), Metformin, and Laxatives were associated the strongest with the microbiome [211]. PPI use has been associated with increased Enterococcaceae and Streptococcaceae and decreased Clostridiales, with an associated increase in genes related to bacterial invasion, predisposing PPI users to *Clostridium difficile* infections [212, 213]. Metformin treatment increased *Escherichia coli* and lowered *Intestinibacter* in T2D patients [214]. While several such associations have been reported, besides the role of drugs, the impact of diet dominates microbial alterations.

- **DIET**

The complex interactions between the microbiota and a multitude of dietary components sustain gut homeostasis. Accordingly, any change in diet would effect perturbations in the microbiota – dietary component interactions, resulting in dysbiosis. The gut microbiota has been shown to exhibit a linear dose response to dietary changes [215]. Diet switch for a short term has been shown to alter the microbiome rapidly, but the effect does not persist. Repeated diet oscillation experiments have shown that the microbiota changes for the most part are dependent on the diet alterations and change rapidly when the diet changes [215]. But for the change in the microbiota to persist longer, the altered diet has to persist for longer durations [216]. This has been thought to reflect past evolutionary selective pressures, due to our antecedents' diet consumption being very volatile. The flexibility of the microbiota community would enable quick shifts in their repertoire in response to diet and hence allow for increased dietary flexibility [217].

An analysis of microbiota from several mammalian species showed that the overall distribution of microbial species does not mirror mammalian phylogeny. On the other hand, the microbiome from herbivores was enriched in enzymes involved in the biosynthesis of amino acids. Microbiome from carnivores was enriched in enzymes involved in amino acid degradation [218]. Likewise, cyclical changes in the microbiota have also been noted to occur due to seasonal dietary variations. For instance, there is a higher abundance of Bacteroidetes in the dry season in Hadza hunter-gatherers when hunting dominates, and a lower abundance of Bacteroidetes in the wet season when honey consumption dominates [219].

Apart from feeding behavior and seasonal dietary variations, another factor influencing dietary variation is urbanization. A rural diet, which is predominantly raw or wild food enriches Bacteroidetes and depletes Firmicutes. Rural diets also result in a more diverse microbiome than westernized diets. But, while urbanization is associated with a loss of microbial diversity, the large variety of food available in urban environments leads to greater inter-individual variability in the gut microbiota [220]. Also, a higher baseline microbial diversity offers greater resilience to diet perturbations [220].

In recent times, there has been a lot of research on the negative effects of ‘Western diet’ [221, 222]. Conventionally, the western diet is characterized by high fat and high salt, as opposed to Mediterranean and Asian diets which do have high salt content, but contain low fat and high fiber levels. Each of these components influence the microbiome distinctly, and their relative quantities in the diet shapes the microbial diversity. For instance, Bier et al. showed that *Erwinia* and *Anaerostipes* were altered due to a HSD. They also observed alterations in SCFA levels corresponding to the microbial alterations [223]. HSD is also known to decrease the relative abundance of the *Lactobacillus* species. Lactobacilli, one of the dominant genera in the gut, are material for the production of butyrate and the metabolism of tryptophan. The HSD – induced microbial alteration hence results in alterations in indole metabolites and butyrate levels in the gut [224, 225].

A high fat diet has been negatively associated with the abundance of *Akkermansia* [226]. In humans, the intake of a diet rich in saturated fatty acids has been correlated with reduced microbiota richness [227, 228]. The high fat diet has also been associated with increased *Alistipes* and *Bacteroides* levels and decreased levels of *Faecalibacterium*. These changes are accompanied by corresponding changes in the SCFAs and indole metabolites [229]. Omega-3 fatty acids have been shown to increase *Bifidobacterium*, *Roseburia*, and *Lactobacillus* [230].

Like fat, the microbiota can be influenced by the protein content in the diet. First, the source of the protein influences the microbiota. White meat protein sources have higher levels of the beneficial genus *Lactobacillus* than red meat [231]. The consumption of a meat-rich diet in the long-term is associated with increased levels of *Bacteroides* [216]. Short-term consumption of a meat-rich diet increases the bile tolerant genera *Alistipes* and *Bilophila* [217]. In contrast, consumption of a plant-protein-rich diet increases the levels of *Lactobacilli* and *Bifidobacteria*, with an associated elevation in the SCFA levels [232].

The effect of dietary fiber on the microbiome depends on the source, types, and amounts of the fiber. For instance, *Bifidobacteria*, which can degrade arabinoxylans in grains like wheat, are in abundance in people consuming a grain-rich diet [233]. A cellulose-rich diet increases the abundance of Enterococcaceae – specifically *Enterococci faecalis* and *Enterococci hirae* [234]. Long-term consumption of complex carbohydrates in humans has been shown to increase the genus *Prevotella* [216]. Colonization by *Bacteroides thetaiotaomicron* is regulated by dietary fructose and glucose levels [235]. On the other hand, deprivation of dietary fiber in mice can lead to the expansion of mucin – degrading bacterial species like *Akkermansia muciniphila* and *Bacillus caccae*, as 80% of the mucin biomass are glycans [236, 237]. This in turn leads to a compromised intestinal barrier.

In addition to these macronutrients, several other components of diet like emulsifiers or sweeteners also impact the gut microbiota [238, 239]. The interaction between diet and microbiota holds promise in the therapeutic approach. Personalized nutrition is an emerging concept that has implications in individual patient care. But further research with more clinical trials is necessary to better understand human-microbial interactions.

1.13. DIET, MICROBIOTA AND DISEASE

Our improved understanding of diet-microbiota interactions over the last 2 decades has facilitated a plethora of research into the relevance of microbiota in several diseases. Diet, both via microbial alterations and independent of microbiota, can have an impact on several diseases. In particular, some nutritional aspects collectively termed the western diet, which includes high fat, excessive salt, and high sugar, have been known to promote metabolic syndrome. Recent research has also revealed their role in autoimmunity.

Both dietary fat and the microbiota have been shown to play a role in the development of obesity [240]. Transplantation of microbiota from obese humans into mice resulted in the development of obesity in those mice. The transplanted microbiome exhibited higher expression of genes involved in cobalamin synthesis, metabolism of several amino acids, and the pentose phosphate pathway. The microbiota could thus influence metabolites that characterize an obese phenotype [241]. Dietary fiber and production of SCFAs by microbiota, on the other hand, promote metabolic benefits like weight loss and control of glucose metabolism in obese mice [242].

Diet and the microbiota have also been implicated in cardiovascular diseases. Haraszthy et al noted the presence of DNA from several bacterial species in atherosclerotic plaques [243]. HSD has been shown to cause hypertension [244]. Some recent studies have also shown an association between microbiota and hypertension. Microbiota from hypertensive rats was shown to induce hypertension in normotensive rats [245]. On the contrary, Mell et al showed that while normotensive and hypertensive rats differ in their microbiota composition, transfer of microbiota from hypertensive rats to normotensive ones doesn't alter Blood Pressure (BP) in the latter. Microbiota transfer from normotensive rats to hypertensive rats resulted in exacerbation of BP. Interestingly, this was only observed when the rats were fed HSD. This reinforces the importance of understanding diet-microbiota interaction to better understand their role in disease [246].

Autoimmune diseases that are known to be prominently influenced by diet are Inflammatory bowel diseases (IBD) [247]. Several studies have shown a positive correlation between intake of saturated fats, polyunsaturated fatty acids, and meat to increased risk of Crohn's disease (CD) and Ulcerative colitis (UC). CD and UC have also been negatively associated with a higher intake of vegetables, fiber, and fruits [248]. Additionally, while the effects of age, geography, and diet lead to inconsistencies in the species-specific characterization of the altered microbiota in IBD patients, there are common features, like an overall reduction in species richness and a reduced abundance of Firmicutes and Bacteroides [249].

Even if species-specific identification is inconsistent, changes in microbial functionality can be used as markers for IBD. Production of hemolysins and cytolethal toxins by *E. coli* in IBD patients and production of Gelatinases by Enterococci that disrupt the intestinal barrier, are indicative of IBD [250]. Yet another functionality, the interaction between the microbiota and the colonic mucosa is also lost in UC patients [251]. The geographic clustering of IBD

incidences in western nations, as well as its association with both the microbiota and a westernized diet necessitate further investigations of the link between diet-microbiota interactions and IBD [252].

Diet and intestinal commensals have also been shown to affect other autoimmune disorders. The SFBs, whose levels are affected by Vitamin A promote autoimmune arthritis via T helper 17 cells (T_H17) [253, 254]. The occurrence and pathogenesis of Systemic Lupus Erythematosus (SLE) are also associated with diet and the microbiota [255]. HSD could impact colitis by altering *Lactobacillus* levels [225]. The severity of colitis was also shown to be differentially affected by fibers and protein from different sources via microbial alterations. For instance, Psyllium, Pectin, and Cellulose reduce the severity of colitis, while methylcellulose increased its severity. A Casein-rich diet resulted in the exacerbation of colitis. A combination of high Casein and Psyllium in diet showed that Psyllium could offset the deleterious effect of Casein [256]. As human diets consist of several components, more such studies on combinatorial influence of these components are necessary.

1.14. DIET, MICROBIOTA AND CNS AUTOIMMUNITY

Diet and microbiota have been shown to have multifaceted effects on MS and EAE by regulating different components associated with immune homeostasis. Their effects can be either interdependent, or independent of one another i.e., Diet can play a role in MS/EAE by modulating the gut microbiota, but also play microbiota independent roles through the modulation of host metabolites or through the direct effect of dietary constituents.

• MICROBIOTA IN MS AND EAE

Early observations in a spontaneous EAE model with MBP-specific T cell transgenic mice by Goverman et al. showed that EAE incidence was higher in conventional dirty facilities compared to clean facilities [30, 257]. A study on the RR mice by our group showed that GF mice were protected from EAE as opposed to mice housed under SPF conditions [257]. Administration of antibiotics was also found to impact EAE severity in active EAE [258].

In view of these observations, there have been several reports that have examined the role of the microbiota in MS patients. One report on MS patients from the USA showed that the patients had increased levels of *Akkermansia* and *Methanobrevibacter*. They also showed that patients on disease modifying treatment had a higher abundance of *Prevotella* and *Sutterella* [259]. Another study observed an increase in *Pseudomonas*, *Blautia*, and *Mycloplana* in MS patients, with a decrease in *Parabacteroides* and *Prevotella* [260]. But whether all these changes affected MS, was not characterized in either study. With a growing understanding of the role of microbiota in maintaining immune homeostasis, many of the ways by which the microbiota affects CNS autoimmunity are being deciphered.

CD4⁺ T cells being crucial for EAE, the gut microbiome is essential for shaping their development and functionality. Since CD4⁺ T cells are activated by antigen presentation by APCs like DCs and B cells, microbial antigens can induce specific differentiation programs in T

cells and can also modulate cytokine production. In this regard, Berer et al. reported that gut microbiota transplant from twin pairs discordant for MS into GF RR mice brought about increased EAE incidence in mice that received microbiota from MS patients as compared to mice that received microbiota from their healthy counterparts. This effect on EAE incidence was shown to be exerted by modulation of IL-10 production by T cells. The dominant difference in the microbiota was the reduction in *Sutterella* species and increase in *Akkermansia* in mice receiving microbiota from MS patients [261].

The intestine contains high frequencies of T_H17 cells under normal conditions and these are key components in EAE. Their differentiation necessitates the microbiota, as shown by their absence in GF mice (Atarashi et al. 2008). This is due to the requirement of ATP derived from the microbiota, which induces CD11c⁺ cells in the gut to produce IL-23 and IL-6. But this response is not driven in equal measure by all gut commensals. The SFBs specifically trigger the development of T_H17 cells [262]. They use microbial adhesion-derived endocytosis to move SFB-derived antigens like Flagellins to the intestinal epithelia and modulate immune homeostasis. Serum amyloid A has also been identified as a key component for the induction of T_H17 cells by SFBs [263].

The commensal microbiota has also been shown to modulate T_{reg} cell frequencies in the gut. A recent study showed a reduction in T_{reg} cell frequencies and an increase in T_H1 cell frequencies due to microbiota derived from MS patients. The species *Parabacteroides distasonis*, which was identified as promoting anti-inflammatory T_{reg} cell responses, was found to be reduced in microbiota derived from MS patients [264]. Also, colonization with the commensal *Bacteroides fragilis* was shown to be protective against EAE. This was observed to be due to Polysaccharide A expressed by the bacterium, which induces the expansion of IL-10 producing T_{reg} cells [265]. Several species of *Clostridium* were also shown to modulate the colonic T_{reg} cell number and function by modulating the levels of TGF- β [266].

The commensal microbiota also impacts the function of APCs in the GALT. DCs and macrophages in the GALT produce CD103 in response to commensal derived antigens, and subsequently interact with naïve T cells. This interaction facilitates the expression of gut homing receptors like CCR9 and $\alpha_4\beta_7$, in addition to promoting the expression of FoxP3 by T cells [267], conferring a regulatory phenotype to the gut homing T cells.

Gut microbiota Modulation of B cells by the gut microbiota has also been implicated in MS and EAE. MS patients were found to have gut-microbiota specific IgA⁺ B cells in the CNS [268]. IgA produced by intestinal B cells is a key mediator of mucosal tolerance and is produced in response to microbial antigens. They can be secreted and remain in soluble form, or bind to cell surface antigens on the microbiota and remain associated with the bacteria. They also serve to control the populations of gut bacterial species to promote diversity and symbiosis. Mucosal IgA has been implicated in a protective role in EAE and MS. MS patients were found to have reduced fecal IgA bound bacteria. In addition, IgA⁺ plasma cells were found to be reduced in the gut during EAE. Moreover, the introduction of gut derived IgA⁺ plasma cells

was found to protect from EAE, and mice having an abundance of IgA⁺ plasma cells were shown to be EAE resistant. Production of IL-10 by the gut IgA⁺ plasma cells was found to be necessary for this protective phenotype [269].

The contribution of the gut microbiota towards the development and maturation of CNS resident cells and the BBB also cannot go unstated. For instance, GF mice were shown to have impaired maturation of resident microglia and underdevelopment of the BBB, both of which were restored by re-introduction of microbiota [270, 271]. This can have an impact on both immune cell entry into the CNS and local antigen presentation in the CNS by the resident APCs.

While GF mice have been the tool of choice for the bulk of research into the microbiota, there are caveats to consider. Mono-colonization does not provide insights into interactions between microbial species or the impact of a consortium of microbes on disease. Also, the gut microbiota has a lot of functional redundancy i.e., species level alterations may not necessarily have a functional impact, because due to the sheer number and diversity of the microbiota, many species share common functional roles. Several of the aforementioned studies on MS patients' cohorts have shown differential alterations in not just one but several microbial species. Their functional impact would be more diverse than the modulation of a single species. Nonetheless, some studies do show that a single microbial species by itself can modulate disease phenotype. The modulation of EAE by *Bacteroides fragilis* is one such example. Another such example is the protection from EAE mediated by *Escherichia coli* Nissle 1917. This bacterium was shown to decrease inflammatory cytokine production by T cells while increasing IL-10 production. It was also shown to repair the intestinal barrier dysfunction caused by EAE induction [272]. Likewise, *Prevotella histicola* was also shown to suppress EAE by modulating the balance between T_H17, T_H1, and T_{reg} cells, and inducing tolerogenic DCs and suppressive IL-10 producing macrophages with low antigen presentation capacity [273]. Thus, while the microbiota cannot entirely be dissected and taken as isolated species, the characterization of individual species can aid in the identification of potential therapeutic species.

- **DIET IN MS AND EAE**

Early evidence for the role of diet in MS/EAE came from studies on guinea pigs that showed lipemia after EAE induction and the subsequent discovery that Vitamin C deprivation in diet led to the prevention of EAE [274]. Subsequently, there have been several reports characterizing individual dietary components and their effect on MS patients.

Some studies have found positive correlations between MS and the intake of meat and dairy fat, and a negative correlation of MS with plant-based fat. Subsequent investigation into Poly-Unsaturated Fatty Acids (PUFA) showed that they do have a role in MS, disease progression involves dysregulation of fatty acid metabolism, and specific supplementation can modify disease progression [275]. A comprehensive large-scale study on more than 2000 MS patients showed that patients with a stable or decreasing disease activity predominantly consumed

more fruits and vegetables and rigorously controlled their fat intake, while patients with increasing disease activity consumed meat-based fat and very less fruits and vegetables [276]. About salt, one study positively correlated the intake of salt to increased disease activity in MS patients [277], while a later study showed no correlation between salt intake and MS [278]. In addition, fasting has also been shown to be beneficial in RRMS patients [279].

In the last decade, multiple studies have characterized roles for specific dietary components in disease through EAE models. With the incidence of MS being higher in western countries, and with data from epidemiological studies implicating the 'westernized diet', the predominant focus has been on dietary fat, fiber, salt, and calorie restriction.

Most animal-based diets are metabolized by the host and microbial pathways predominantly into Long Chain Fatty Acids (LCFAs). They have been implicated in the enhancement of pro-inflammatory T_H17 and T_H1 responses in the gut, eventually leading to EAE. On the other hand, SCFAs, microbial fermentation products of dietary fiber, are beneficial during EAE. They have been shown to promote T_{reg} cell responses and protect against EAE [280]. Docosahexaenoic Acid (DHA), has been shown to prevent maturation of DCs and reduce their antigen presenting capabilities, in addition to modulating T_H subset frequencies in the gut. DHA is also the most abundant SCFA in the CNS and acts on the infiltrating T cells and resident APCs in the CNS to ameliorate EAE [281]. Omega-3 and Omega-6 fatty acids have been shown to ameliorate EAE by inducing the production of TGF- β 1 and Prostaglandin E_2 , both of which had been previously shown to regulate EAE [282]. SCFAs can also influence the development and maturation of microglia. GF mice were shown to have defects in microglial maturation, which was ameliorated by supplementing SCFAs with diet [283]. LCFAs have been reported to consistently decrease SCFA levels, by altering the gut microbiome. The levels of *Bacteroides* and *Prevotella* are decreased due to an increase in LCFAs, and as a result, the metabolism of fiber to SCFAs is impaired [280]. On the other hand, plant-based non-fermentable fibers like cellulose have been shown to alter the gut microbiota and increase levels of eicosanoic acid and palmitic acid. These FAs have been found to have a protective effect on EAE [234].

Another group of molecules that have been shown to have a profound impact on EAE are tryptophan metabolites. The Aryl hydrocarbon receptor (Ahr) binds indole compounds generated by the host and microbial metabolism of dietary tryptophan. Ahr has been of particular interest due to the fact that while most of its ligands share structural similarities to tryptophan and indole, different ligands binding to Ahr elicit different phenotypic responses [284]. Ahr ligands have been implicated in the differential regulation of the T_H17/T_{reg} balance [285]. CD103+ DCs in the gut were shown to induce a tolerogenic phenotype by the expression of indoleamine 2,3-dioxygenase, which metabolizes tryptophan to generate kynurenine. Kynurenine interacts with Ahr to induce T_{reg} cell differentiation in the gut [286, 287]. Dietary tryptophan was shown to ameliorate CNS inflammation during EAE via an IFN- γ mediated pathway which induces Ahr expression in astrocytes. Dietary tryptophan binding to Ahr on astrocytes leads to a decrease in expression of CCL-2 and Nos2, leading to reduced chemotactic activity and regulation of macrophage and microglia recruitment [288].

Tryptophan metabolites produced by the commensal flora have also been shown to control microglial activation and TGF α and VEGF-B production, and act via the Ahr to modulate astrocyte mediated damage during EAE [143].

Sodium chloride in the diet was also reported to have an impact on EAE. HSD was shown to promote T_H17 differentiation via the salt sensing kinase SGK-1 [289]. Several reports have shown that sodium chloride drives EAE through the induction of pro-inflammatory T_H17 cells [290-292]. Sodium chloride has also been shown to alter the levels of Lactobacillus species, which are found to be protective against EAE due to their production of tryptophan metabolites like Indole Acetic Acid (IAA) [290]. The effect of sodium chloride on EAE is thought to be both through the modulation of the microbiota and its direct effect on T_H17 differentiation. An increase in gut T_H17 differentiation due to sodium chloride was shown to impact nitric oxide synthase in the CNS endothelial cells, thereby affecting vascular permeability [293]. This could have implications in EAE, by disrupting BBB permeability and enabling better access to the CNS for infiltrating immune cells.

Vitamins A and D are some other dietary factors known to have an impact on EAE. Vitamin A is metabolized specifically by intestinal DCs into Retinoic Acid (RA), which is a crucial factor for the reciprocal regulation in the differentiation of T_H17 and T_{reg} cells [294]. Apart from commensal microbial antigens, RA is also essential for the DCs to be able to imprint CCR9 and $\alpha_4\beta_7$ in naïve T cells for gut homing [295]. The Vitamin D derivative 1,25-dihydroxyvitamin D3 has been shown to prevent EAE [296]. This is via the IL-10 signaling cascade [297]. Other effects of Vitamin D include the modulation of DCs to enhance regulatory T cell activation, inhibition of T_H1 cells and B cell responses [298].

Furthermore, both dietary tryptophan and fiber have been known to impact intestinal barrier permeability via the microbial metabolism of fiber to SCFAs and tryptophan to indole derivatives. Indole derivatives alter the intestinal barrier permeability due to both a direct effect of the junction protein expression by endothelial cells and indirectly via the TLR signaling cascade. SCFAs also directly modulate the junction proteins to enhance barrier integrity [299]. Vitamins D and A too have been shown to enhance intestinal barrier integrity by directly modulating the levels of ZO-1, Claudin-5, and E-cadherin [300]. Several food additives like emulsifiers, organic solvents and nanoparticles that are increasingly being used in the food industry have deleterious effects on the intestinal barrier, by actin disbandment in the intestinal epithelia and re-localization of the junction proteins. The increased use of these additives has been positively associated with an increase in both the incidence and severity of MS [301]. **Fig.1.3** illustrates the afore-described roles of the diet and commensal microbiota in CNS autoimmunity.

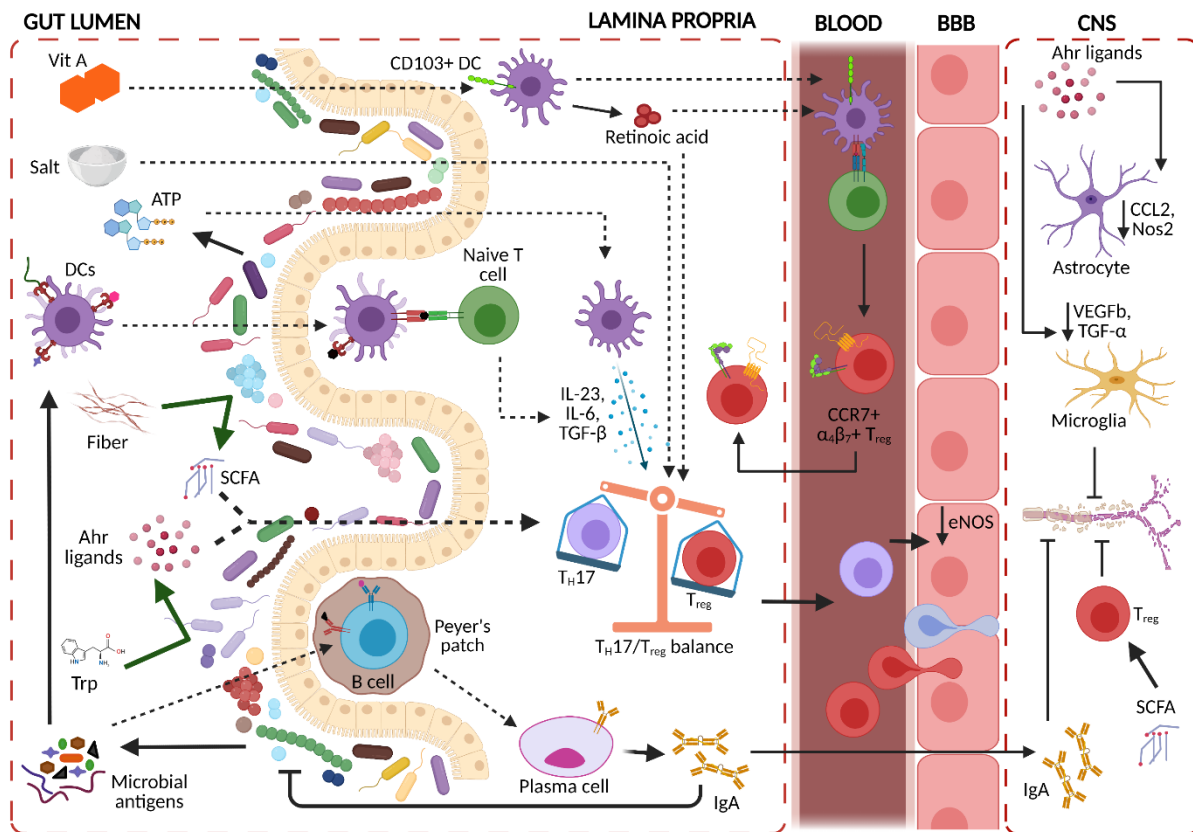


Figure 1.3: Schematic of the role of diet and the microbiota during EAE. Microbial antigens stimulate DCs, which stimulate naïve T cell differentiation into various subsets depending on the antigenic stimulus. Microbial antigens were shown to activate B cells in the Peyer's patch, which produce IgA. IgA reciprocally regulates microbial population. Microbiota metabolize dietary fiber and tryptophan (trp) into SCFA and Ahr ligands respectively, which regulate T_{reg}/T_H17 balance. Vitamin A is metabolized by DCs to retinoic acid, which promotes T_{reg} cell differentiation and gut homing. Retinoic acid, dietary salt, and microbiota derived ATP all differentially regulate T_{reg}/T_H17 balance. Ahr ligands reach the CNS and mediate anti-inflammatory phenotype in CNS resident cells. SCFAs reach the CNS and enhance T_{reg} cell functionality. Together, all of these factors act to regulate CNS autoimmunity. Created with BioRender.com.

In addition to dietary components, another aspect of diet that affects EAE/MS is caloric intake. Caloric restriction is beneficial in EAE. An EAE study employing a Fasting-Mimicking diet (FMD) reported reduced EAE severity in all mice consuming FMD, and a complete reversal in 20% of the mice consuming FMD. This was due to the higher levels of corticosterone and T_{reg} cells under FMD. Another study on intermittent fasting showed an increase in microbial diversity and richness of Lactobacillaceae and Prevotellaceae, which then promoted T_{reg} cell differentiation and reduced T_{eff} differentiation [302]. Yet another study showed an increase in adiponectin and corticosterone, with reduced levels of IL-6 and leptin after chronic caloric restriction. This was shown to promote amelioration of inflammation and demyelination without suppression of immune function [303].

While nearly all of the aforementioned research on diet's role in EAE is on induced EAE models, this has its caveats. Whether diet, independently, or via the microbiota can exert effects that trigger disease cannot be discerned. Also, under strongly induced inflammatory

conditions, many components whose contributions may be subtle and necessary, but not overt and dominant may not be discerned. As our diet consists of a multitude of components, dietary components cannot entirely be segregated as isolated units. But understanding the roles of the individual components is necessary to be able to manipulate diet for therapeutic applications. To this end, induced EAE models enable quicker results and serve as good tools. But it is now necessary to understand the role of those components whose role in induced EAE has been documented, in spontaneous EAE systems, for the results to serve better transferable to humans.

OBJECTIVES OF THE STUDY

Several studies have used induced EAE models to demonstrate the role of a High Salt Diet in exacerbating CNS autoimmunity [225, 290, 304-306]. While this model helps understand the role of dietary components during disease progression, it does not help understand the role of dietary components in the early triggering phases of the autoimmune disease, because the disease induction in this model is largely artificial and uses strong adjuvants. While quite some progress has been made in understanding the pathogenesis of MS using induced EAE models, the “trigger factors” for MS remain poorly understood. That said, association studies have linked the incidence of MS to dietary habits [247, 276], though the role of dietary salt in MS is unclear.

The primary objective of the present study is to study the role of dietary salt in spontaneous EAE, using the OSE mice [34] as a model system. Specifically, the study addressed the following issues:

1. Long term tolerability of the HSD regimen in mice
2. The effect of HSD on spontaneous EAE development
3. The effect of HSD on actively induced EAE
4. HSD-induced alterations in various physiological parameters
5. Impact of HSD on the immune system
6. The effect of HSD on the BBB
7. Validation of the observed functional changes in vivo

2. MATERIALS AND METHODS

2.1. Materials

| Material | Sourced from | Catalog number |
|---|-------------------|-----------------|
| Absolute qPCR master mix | Thermo Scientific | AB-1138/B |
| Bile esculin agar | Sigma Aldrich | 48300 |
| Brain heart infusion (BHI) broth | Sigma Aldrich | 53286 |
| Bovine serum Albumin (BSA) | Roth | 9048-46-8 |
| Brefeldin A | Sigma Aldrich | B7651 |
| Collagenase VII | Sigma Aldrich | 11088866001 |
| Cell strainers (40 and 100µm) | Corning | 431750/431752 |
| CD4 Isolation cocktail | Biolegend | 480006 |
| Clarity western ECL substrate | Bio-Rad | 1705061 |
| Dulbecco's modified eagle's medium (DMEM) | Thermo Scientific | 61965059 |
| Dispase-II neutral protease | Sigma Aldrich | 4942078001 |
| DNase I | Sigma Aldrich | DN25 |
| 7-Ethoxy resorufin | Sigma Aldrich | E3763 |
| Fluorescamine | Sigma Aldrich | 4761400-5523-00 |
| Fluorescein isothiocyanate – Dextran 4kDa | Sigma Aldrich | FD4 |
| Fetal bovine serum (FBS) | Sigma Aldrich | F7524 |
| L-Glutamine | Life tech | 25030024 |
| Hank's Balanced Salt Solution (HBSS) | Thermo Scientific | 14170120 |
| HEPES | Sigma Aldrich | H0887 |
| Heparin sodium salt | Sigma Aldrich | H3149 |
| Iscove Modified Dulbecco Media (IMDM) | Thermo Scientific | 12440053 |
| Ionomycin | Sigma Aldrich | I0634 |
| Incomplete Freund's adjuvant (IFA) | Difco | 263910 |
| Lysing matrix D tubes | Thermo Scientific | 11422420 |
| Mycobacterium Tuberculosis H37 RA (MTB) | Difco | 231141 |
| MEM non-essential amino acids | Sigma Aldrich | M6895 |
| MgCl ₂ | Thermo Scientific | AB0359 |
| dNTPs | Thermo Scientific | R0194 |
| Nitrocellulose membrane | Bio-Rad | 1620112 |
| β-mercaptoethanol | Sigma Aldrich | 63689 |
| Phenol/Chloroform/isoamyl alcohol | Roth | A156.2 |
| Phorbol 12- Myristate 13 acetate (PMA) | Sigma Aldrich | P8139 |
| Penicillin/Streptomycin | Sigma Aldrich | P0781 |
| Percoll | Thermo Scientific | 17-0891-01 |
| Proteinase K | Thermo Scientific | 10407583 |
| Pertussis toxin | Sigma Aldrich | P2980 |

| | | |
|---|---------------------|--------------|
| Phusion High fidelity DNA polymerase | New England Biolabs | M0530 |
| Phusion HF/GC buffer | New England Biolabs | B0518 |
| Protease and phosphatase inhibitor | Thermo Scientific | 78442 |
| PowerUp SYBR Green Master Mix | Thermo Scientific | A25742 |
| Pan B cell isolation cocktail | Biolegend | 480051 |
| Roswell Park Memorial Institute (RPMI) 1640 | Sigma Aldrich | R0883 |
| Resorufin | Sigma Aldrich | R3257 |
| RIPA Buffer | Serva | 39244 |
| SDS containing sample buffer | Sigma Aldrich | S3401 |
| Serum gel tubes | Sarstedt | SAR411378005 |
| Streptavidin beads | Biolegend | 480016 |
| Streptavidin-HRP | Biolegend | 405210 |
| Transcription Factor Staining Buffer Set | eBioscience | 00-5523-00 |
| TMB Substrate solution | Biozol | BLD-421501 |
| Triton-X-100 | Roth | 9002-93-1 |
| Tween-20 | Sigma Aldrich | P1379 |

2.2. Buffers

| Buffer | Components | Concentration |
|--|--|--|
| Phosphate Buffered Saline (PBS) - pH 7.4 | NaCl Na ₂ HPO ₄ KH ₂ PO ₄ KCl | 137mM 10mM 1.8mM 2.7mM |
| Complete RPMI (RPMIc) | Heat inactivated FBS Penicillin/Streptomycin L-Glutamine MEM non-essential amino acids Sodium Pyruvate β-mercaptoethanol RPMI 1640 | 10% v/v 1% v/v 1% v/v 100μM 1mM 0.04% v/v Made up to required volume |
| Complete IMDM (IMDMc) | Heat inactivated FBS Penicillin/Streptomycin L-Glutamine MEM non-essential amino acids Sodium Pyruvate β-mercaptoethanol IMDM | 10% v/v 1% v/v 1% v/v 100μM 1mM 0.04% v/v Made up to required volume |
| RPMI-10 buffer | RPMI 1640 | Required volume |

| | | |
|--------------------------|---|--|
| | Heat inactivated FBS HEPES | 5% v/v 15mM |
| Complete DMEM (DMEMc) | Heat inactivated FBS Penicillin/Streptomycin MEM non-essential amino acids Sodium Pyruvate β -mercaptoethanol DMEM | 10% v/v 1% v/v 100 μ M 1mM 0.04% v/v Made up to required volume |
| HBSS/HEPES buffer | HBSS HEPES | Required volume 15mM |
| HBSS/EDTA buffer | HBSS Heat inactivated FBS EDTA HEPES | Required volume 5% v/v 5mM 15mM |
| SIP Percoll | Percoll 1.5M NaCl | 9 parts v/v 1-part v/v |
| Percoll d-1.08 | SIP Percoll PBS | 10ml 5.7ml |
| 22%, 40% and 80% Percoll | 100% Percoll RPMI 1640 | 22%, 40% or 80% v/v Made up to required volume |
| CNS Wash buffer | HBSS Heat inactivated FBS Glucose | Required volume 10% v/v 0.1% v/v |
| 100% Percoll | Percoll 20X PBS H ₂ O | 9 parts v/v 0.5-part v/v 0.5-part v/v |
| Erythrocyte lysis buffer | NH ₄ Cl H ₂ O | 0.83% w/v Required volume |
| FACS buffer | Bovine serum albumin (BSA) Sodium azide PBS | 1% w/v 0.1% w/v Made up to required volume |
| MACS buffer | Heat inactivated FBS EDTA PBS | 2% v/v 1mM Made up to required volume |
| ABTS substrate solution | Citric acid ABTS H ₂ O H ₂ O ₂ | 10.5g 150mg 500ml 0.1% v/v added fresh during assay |

| | | |
|--|--|---|
| 10X TBS | Tris base NaCl H ₂ O | 24.2g 80g Made up to 1L, pH adjusted to 7.6 |
| 1X TBS-T | 10X TBS Tween 20 H ₂ O | 100ml 1ml Made up to 1L |
| ELISA Blocking buffers | FBS (buffer 1) or BSA (Buffer 2) PBS | 5% v/v Made up to required volume |
| Bile esculin agar (Boiled, not autoclaved) | Bile esculin agar media H ₂ O | 64.5g 1l |
| BHI broth (autoclaved) | BHI media H ₂ O | 37g 1l |
| Running buffer – western blot | Tris base Glycine SDS H ₂ O | 3.03g 14.4g 1g Made up to 1L |
| Blocking buffer – western blot | Non-fat dry milk powder TBS-T | 5% v/v Made up to required volume |
| Transfer buffer – western blot | Tris base Glycine Methanol H ₂ O | 2.9g 14.5g 100ml Made up to 1L |
| Phosphate Buffer, pH 8 | Na ₂ HPO ₄ NaH ₂ PO ₄ H ₂ O | 37.7mM 12.3mM Made up to required volume |
| 2X EROD Solution | 7-Ethoxy resorufin Phosphate Buffer | 4μM Made up to required volume |
| Fluorescamine Solution | Fluorescamine Acetonitrile | 300μg/ml Required Volume |
| ACK buffer | NH ₄ Cl KHCO ₃ EDTA | 150mM 1mM 0.1mM |
| Heparin solution | Heparin sodium salt PBS | 200 units 1ml |
| Tail lysis buffer | Tris-HCl pH 8.5 NaCl EDTA Tween-20 Proteinase K | 100mM 200mM 5mM 1% v/v 1mg/ml |

2.3. Mice

All animals used in the study were bred at the animal facilities of the Max Planck Institute of Biochemistry, Martinsried. Mating pairs were fed rodent control chow diet and unless otherwise specified, offspring mice were raised on chow diet, then weaned onto chow diet, C1000 diet, or High salt diet (HSD) containing 4% NaCl. The diets were given ad libitum. They were given autoclaved drinking water ad libitum. The diets were formulated by Altromin and γ -irradiated. In diet switched mice, body weight measurements were done once every week from the day of diet switch until 4 weeks after diet switch. All animal procedures were in accordance with the guidelines of the Committee on Animals of the Max Planck Institute of Biochemistry and with approval from the Regierung von Oberbayern (Munich, Germany). The mouse lines used in the study are as follows:

- Wild Type C57BL/6 (WT) mice
- 2D2 mice
TCR transgenic mouse on the C57BL/6 background; The mouse has CD4+ T cells expressing TCR specific to MOG35-55 in the context of I-A^b; The TCR is composed of V α 3.2 and V β 11 [32]. The mouse lacks CD8+ T cells.
- Th (IgH^{MOG}) mice
BCR knock-in mouse on the C57BL/6 background; A rearranged heavy chain from the MOG specific antibody 8.18C5 is expressed by the BCR in this mouse. The VDJ region of 8.18C5 was inserted into the natural locus of the V region in the heavy chain [33].
- 2D2 x Th (OSE) mice
2D2 and Th mice were crossed to get the double transgenic OSE mice on the C57BL/6 background; They have both TCR and BCR specific to MOG, lack CD8+ T cells, and about 51% spontaneously develop EAE.

2.4. Blood collection

Unless otherwise specified, all sera collections were done after 3-4 weeks of feeding. Blood was collected by retro orbital bleeding into Serum gel tubes and allowed to stand at RT for 1 h. They were then centrifuged (10000rpm, 5 min, 4°C) to collect serum. Blood was collected by retro orbital bleeding into tubes with 100 μ l of Heparin (200U/mL in PBS) for genotyping.

2.5. Genotyping

Transgenic mice were genotyped by tail biopsy. Tails were digested overnight in tail lysis buffer, followed by phenol-chloroform extraction of DNA and centrifugation (13000rpm, 10min, RT). The upper fraction containing DNA was collected. DNA cleanup was done by centrifugation with 100% Ethanol (13000rpm, 10min, 4°C), and subsequently 70% Ethanol (13000rpm, 5min, 4°C). DNA was resuspended in Tris-HCl (pH 7.4). PCR with transgene specific primers was performed.

Verification of genotyping was done by FACS analysis on PBMCs. Blood was collected in Heparin, and incubated at RT for 5min with 1ml ACK buffer. Samples were then centrifuged (1600rpm, 5min, 4°C). The pelleted cells were incubated with 1ml ACK buffer for 5min. Samples were centrifuged again (1600rpm, 5min, 4°C). FACS staining was done on the pelleted PBMCs.

2.6. Spontaneous EAE

Entire litters of OSE mice were assigned at random to either C1000 or HSD or other treatment groups. Unless otherwise specified, OSE mice were scored for disease twice a week until 12 weeks of age. Diets or other treatments were also maintained at least until 12 weeks of age unless specified otherwise.

2.7. Actively induced EAE

EAE was induced by injecting mice subcutaneously with 200µl of emulsion containing 100µg MOG 35-55 peptide (MEVGWYRSPFSRVVHLYRNGK) and CFA. CFA was prepared by adding 5mg of MTB to 1ml IFA. Additionally, mice received 400ng Pertussis toxin in PBS intraperitoneally (i.p.) on days 0 and 2 after immunization. For low dose EAE experiments, the CFA was diluted 1:10 in IFA and the Pertussis toxin amount remained the same. EAE was monitored until day 30 after induction. Body weight measurements were done before EAE induction and every 3 days after induction until day 30.

2.8. In vivo depletion and blocking (CD25 and IL10)

| Antibody | Clone | Isotype | Catalog Number | Sourced from |
|-----------------|------------|----------|----------------|--------------|
| CD25 | PC61 | Rat IgG1 | | Self-made |
| IL-10 | JES5-2A5.7 | Rat IgG1 | BE0049 | Bioxcell |
| Isotype control | Polyclonal | Rat IgG1 | BE0088 | Bioxcell |

For both CD25 depletion and IL10 blocking experiments, OSE Mice were weaned onto HSD, and antibody injections started 1.5 weeks later. 250µg of anti-CD25 or 250µg of anti-IL-10 was injected into mice i.p. once per week for 4 weeks. Rat IgG1 at the same concentration served as the control for both treatments. EAE was monitored until 12 weeks of age for anti-IL-10 treatment and until 16 weeks for anti-CD25 treatment. Mice were maintained on HSD throughout the duration of the experiment.

2.9. Pertussis toxin treatment

OSE mice were weaned onto HSD and after 1-1.5 weeks of feeding, 400ng of Pertussis toxin in PBS was injected to mice i.p. once per week for 4 weeks – Days 0, 7, 14, 21. EAE was monitored daily and further injection was stopped in mice that got sick. EAE was monitored until day 28. Mice were maintained on HSD throughout the duration of the experiment.

2.10. EAE Scoring

| Score | Clinical signs |
|-------|---|
| 0 | No disease |
| 0.5 | Tone loss in tail |
| 1 | Paralyzed tail |
| 1.5 | Paralyzed tail, ataxia |
| 2 | Partial hind limb weakness, ataxia |
| 2.5 | One hind limb paralyzed or weak |
| 3 | Both Hind limbs paralyzed, less locomotion |
| 3.5 | Hind limbs paralysis, locomotion restricted |
| 4 | Complete hind limb paralysis up to the hips |
| 5 | Moribund |

2.11. In vivo intestinal barrier permeability assay

WT mice fed C1000 or HSD for 3-4 weeks were withdrawn from food and water for 4 h, after which FITC-dextran 4kDa was orally gavaged to the mice at a concentration of 10mg in 400 μ l of PBS per mouse. Mice were further kept withdrawn from food and water for 4 h after which blood was collected and centrifuged (10000rpm, 5 min) to collect serum. The fluorescence of FITC in the serum was measured in 96 well black half area plates at an excitation of 485nm and emission of 515nm. FITC-dextran 4kDa serially diluted 2-fold from a top concentration of 10 μ g/ml in PBS (20 serial dilutions in total) was used as standard.

2.12. In vivo blood brain barrier permeability assay

WT mice fed C1000 or HSD for 3-4 weeks were injected with FITC-dextran 4kDa i.v. through their tail vein. 2mg of FITC-dextran in 200 μ l of PBS was injected per mouse. The tracer was allowed to circulate for 20min, after which the mice were sacrificed. Blood was collected after which mice were trans-cardially perfused with 200U Heparin in 30ml of PBS, followed by 30ml of PBS. The brain and spinal cord were collected and weighed. A Dounce homogenizer was used to homogenize tissue in PBS. The homogenates were centrifuged (13000rpm, 15min, 4°C). The supernatants were collected and centrifuged again (13000rpm, 15min, 4°C) to completely remove all debris. The resulting supernatant was used for measuring the fluorescence of FITC in 96 well black half area plates at an excitation of 485nm and emission of 515nm. FITC-dextran 4kDa serially diluted 2-fold from a top concentration of 10 μ g/ml in PBS (20 serial dilutions in total) was used as standard. The FITC levels in the brain and spinal cord were normalized to serum FITC levels to account for possible errors in initial injection volumes.

2.13. Lymphocyte isolation from Lymphoid organs

Single cell suspensions were prepared from spleen, mesenteric, cervical or inguinal lymph nodes (mLN, cLN, iLN) by mechanical disruption via forcing through 40 μ m cell strainers. Cells

were collected in RPMIc. Spleen cells were further washed in RPMIc (300g, 10min, 4°C), then resuspended in Erythrocyte lysis buffer and incubated for 3min at RT. The lysis buffer was then neutralized with RPMIc and the cells washed and collected.

2.14. Isolation of CNS infiltrating leukocytes

Mice were anaesthetized and trans-cardially perfused with PBS. Brain and Spinal cord were collected. Brain and Spinal cord were mechanically disrupted via forcing through 100 µm cell strainers. After washing the cells in RPMIc (300g, 10min, 4°C), the pellet was resuspended in 5ml RPMIc and mixed with 2.16ml SIP Percoll. It was overlaid on Percoll d-1.08 and centrifuged (1200g, 20min, RT, brakes set to 4). The interface cells were collected, washed, and resuspended in RPMIc.

2.15. Isolation of Leukocytes from intestine lamina propria (LP)

Small intestine and colon were collected in ice-cold HBSS/HEPES buffer. After careful removal of Peyer's Patches, fatty tissue, and fecal content, the intestine was opened longitudinally and cut into small pieces. The intestinal fragments were washed three times for 15 min each, in Erlenmeyer flasks with magnetic stirring (300 rpm) in 25ml of HBSS/EDTA. Next, intestinal pieces were washed for 5 min in RPMI-10, followed by enzymatic digestion for 1 h (37°C, 550 rpm stirring speed) with 100 U/ml Collagenase VII in 12.5ml of RPMI-10. Digested tissue was forced through 100 µm cell strainers and washed twice in HBSS/EDTA. The pellet was resuspended in 5ml of 40% Percoll, overlaid on 2.5ml of 80% Percoll and centrifuged (2000g, 20 min, RT, brakes set to 4). Cells at the interface were collected, washed, and resuspended in RPMIc for culture or in FACS buffer for staining.

2.16. Isolation of CNS endothelia

Brain and spinal cord were collected in ice-cold 1X HBSS. The collected tissue was minced into small pieces with a scalpel and collected in ice cold CNS wash buffer. The pieces were washed once, then digested with 0.9U/ml Collagenase VII and 1U/ml Dispase II in a 1% FBS solution in PBS. Digestion was performed at 37°C for 1 h with rotation. Then, the tissue was centrifuged (300g, 10min, 4°C). Single cell suspension was formed by triturating the pellet in DNase solution (1µg/ml DNase in 1%FBS in PBS) with a 23G needle. Triturated cell suspension was overlaid on 22% Percoll and centrifuged (560g, 10min, RT, brakes set to 3). Myelin and debris layer in the supernatant were removed completely by pipetting. The rest of the supernatant was discarded by inversion. The resulting cell pellet was washed in CNS wash buffer and resuspended in 0.5% BSA in PBS for staining.

2.17. Flow cytometry

In samples where cytokine expression was not analyzed, isolated or cultured cells were directly resuspended in FACs buffer and the staining procedure was performed. In samples analyzed for cytokine expression, cells were activated with 50 ng/ml PMA and 500 ng/ml ionomycin in the presence of 5 µg/ml brefeldin A for 4 h at 37°C before beginning FACS

staining. For detection of cell surface markers, cells were transferred to a 96-well V bottom plate and washed twice with FACS buffer. Then 50µl of antibody mix (prepared in FACS buffer) was added to the cells and resuspended. Antibodies were added to the mix at concentrations between 1:100 and 1:400. Viability dye e780 was used at 1:1000 concentration. Cells were incubated on ice in the dark for 20min. Cells were then washed twice in FACS buffer and either resuspended in FACS buffer for acquisition or used for intracellular staining. If cells were to be sorted, FACS buffer was replaced by 1% BSA in PBS. When biotinylated antibodies were used, the antibody mix contained biotinylated antibodies, and an additional staining step with 50µl of antibody mix containing streptavidin tagged fluorophores was done.

For intracellular staining, surface-stained cells were fixed and permeabilized by incubation with 100µl of Fixation/Permeabilization Buffer in the dark for 30min at RT. After washing twice in Permeabilization Buffer, 50µl of antibody mix (prepared in Permeabilization buffer) was added to the cells and resuspended. Antibodies were added to the mix at concentrations between 1:100 and 1:200. Cells were incubated on ice in the dark for 45min. Finally, cells were washed twice in Permeabilization Buffer and resuspended in 200µl FACS buffer. Stained samples were acquired on FACS Canto (BD Biosciences) or FACS Fortessa (BD Biosciences). For sorting, FACS Aria III (BD Biosciences) was used. Analysis was performed using FlowJo (TreeStar) software.

2.18. Antibodies for Flow cytometry

| Antibody | Clone | Isotype | Source |
|----------|--------------|----------------------|-------------|
| CD4 | RM4-5 | Rat IgG2a, κ | Biologend |
| CD45 | 30-F11 | Rat IgG2b, κ | Biologend |
| B220 | RA3-6B2 | Rat IgG2a, κ | Biologend |
| CD19 | 1D3 | Rat IgG2a, κ | Pharmingen |
| CD11b | M1/70 | Rat IgG2b, κ | Biologend |
| Ly6G | 1A8 | Rat IgG2a, κ | Biologend |
| Ly6C | AL-21 | Rat IgM, κ | Pharmingen |
| IFNγ | XMG1.2 | Rat IgG1, κ | Biologend |
| IL-17A | TC11-18H10.1 | Rat IgG1, κ | Biologend |
| FoxP3 | FJK-16s | Rat IgG2a, κ | eBioscience |
| CD103 | 2E7 | Armenian Hamster IgG | Biologend |
| Helios | 22F6 | Armenian Hamster IgG | Biologend |
| Ki67 | B56 | Mouse IgG1, κ | Pharmingen |
| RORγT | B2D | Rat IgG1, κ | eBioscience |
| KLRG-1 | 2F1 | Syrian Hamster IgG | Biologend |
| ICAM-1 | YN1/1.7.4 | Rat IgG2b, κ | Biologend |
| ICAM-2 | 3C4(mIC2/4) | Rat (LEW) IgG2a, κ | Pharmingen |
| PD1 | J43 | Rat IgG2b, κ | eBioscience |
| PD-L1 | MIH5 | Rat IgG2a, λ | eBioscience |

| | | | |
|-----------------------------------|---------|------------------------|-------------|
| GL7 | GL7 | Rat IgM, κ | Biolegend |
| Ceacam-1 | CC1 | Mouse IgG1, κ | Biolegend |
| CD31 | MEC13.3 | Rat IgG2a, κ | Biolegend |
| CD69 | H1.2F3 | Armenian Hamster IgG1 | Biolegend |
| CD25 | PC61 | Rat (Outbred OFA) IgG1 | Pharmingen |
| CD11a | M17/4 | Rat IgG2a, κ | Pharmingen |
| CD18 | M18/2 | Rat IgG2a, κ | Biolegend |
| Vα3.2 | RR3-16 | Rat IgG2b, κ | Pharmingen |
| Vβ11 | RR3-15 | Rat IgG2b, κ | Pharmingen |
| Integrin α4 | PS/2 | Rat IgG2b, κ | Self-made |
| Integrin β1 | Ha2/5 | Rat IgM, κ | Pharmingen |
| Cell proliferation dye e450 (CPD) | | | eBioscience |
| Viability dye e780 (L/D) | | | eBioscience |

The Fluorophores used are as follows: FITC, PE, PerCP-Cy5.5, PeCy7, APC, APC-Cy7, BV421, eFluor450, eFluor780, BV605, PE-CF594, BV711, BV784, or APC-R700; All antibodies were used either directly in conjugation with the Fluorophores or used in conjugation with biotin and then Streptavidin tagged to any of the aforementioned fluorophores was added.

2.19. Fecal bacterial culture and sequencing

Fecal pellets were weighed and added to Lysing matrix tubes. 1ml PBS was added and the tubes were kept on ice for 1 h. Next, the samples were homogenized twice using TissueLyzer (Qiagen), at 25hz for 10 seconds each time. Samples were then centrifuged (50g, 15min, 4°C). Supernatants were collected and centrifuged again (8000g, 5min, 4°C). Supernatants were collected and frozen to be used for ELISA and the microbial pellets resuspended in 500µl PBS. These were then serially diluted. 1:100 and 1:1000 dilutions were plated in Bile-Esculin agar by spread plate method. Number of dark brown and black colonies were counted after 16 h. CFU was computed by normalizing the number of colonies to the weight of the fecal pellets.

Selected dark colonies were cultured in BHI broth and after they reached an OD of 0.7-0.8, the culture tubes were centrifuged (8000g, 15min, 4°C). Pellets were washed in PBS once and resuspended in 1ml TE buffer (Qiagen). They were transferred to 1.5ml centrifuge tubes and glass beads were added to the tubes. Samples were homogenized using TissueLyzer at 25hz for 7 min, incubated at 95°C for 5 min, and then homogenized again using TissueLyzer at 25hz for 7 min. They were then centrifuged (13000rpm, 1min, 4°C). The genomic DNA containing supernatant was used for PCR with the following conditions:

| Component | Description | Volume (µL) |
|---------------------|------------------------|-------------|
| Primer 27F (10mM) | AGAGTTTGATCMTGGCTCAG | 2.5 |
| Primer 1492R (10mM) | TACGGYTACCTTGTTACGACTT | 2.5 |
| dNTPs (10mM each) | | 2.5 |

| | | |
|--------------------------|------------------------------|------|
| MgCl ₂ (25mM) | | 7.5 |
| Buffer | HF/GC | 12.5 |
| Enzyme | Phusion High fid. polymerase | 0.5 |
| Water | | 92 |
| DNA Template | | 5 |

| Step | Cycles | Temperature | Time |
|----------------------|--------|-------------|-------|
| Initial Denaturation | 1 | 98°C | 30sec |
| Denaturation | 35 | 98°C | 10sec |
| Annealing | | 57°C | 30sec |
| Extension | | 72°C | 1min |
| Final extension | 1 | 72°C | 7min |

After PCR, the samples were run on an agarose gel for verification and purified using the Qiagen PCR purification kit according to the manufacturer's instructions. Purified DNA was sequenced using both 27F and 1492R in separate reactions. From the sequences thus generated, a contiguous sequence was assembled and nucleotide BLAST was used to determine the microbial species.

2.20. Fecal DNA extraction and qPCR

Fecal pellets were thawed to RT. Then glass beads were added along with 500µl of ASL buffer (Qiagen stool DNA kit, 51504). Pellets were homogenized using TissueLyzer at 25hz for 7 min. They were incubated at 95°C for 5 min and then homogenized again using TissueLyzer at 25hz for 7 min. They were then centrifuged (13000rpm, 1min, 4°C). The supernatant was collected and kept for subsequent steps. The pellet was mixed with 20mg/ml of Lysozyme (Sigma Aldrich) in 700µl of ASL buffer and incubated at 37°C for 30min. It was then homogenized using TissueLyzer at 25hz for 7 min, incubated at 95°C for 5 min, then homogenized again using TissueLyzer at 25hz for 7 min and then centrifuged (13000rpm, 1min, 4°C). The supernatant was collected and pooled with the previously collected one. Subsequent steps were done with Qiagen stool DNA kit according to the manufacturer's instructions.

For qPCR, isolated DNA was diluted to 2ng/µl. qPCR was performed with Absolute qPCR master mix using SYBR green probe. Separate PCR reactions were performed using 16s rRNA Universal primers (Reaction 1) and Enterococci specific 16s rRNA primers (Reaction 2). The Enterococci 16s rRNA gene encoded in a linearized plasmid was used as DNA standard for both PCRs. Total fecal bacterial levels were computed using the standard curve obtained from Reaction 1 and Enterococci levels were computed using the standard curve obtained from Reaction 2. Enterococci levels were then normalized to total bacterial levels.

| Gene | Label | Sequence |
|--------------------------|----------|--------------------------|
| 16s rRNA Enterococci sp. | Primer 2 | CCCTTATTGTTAGTTGCCATCATT |
| | Primer 1 | ACTCGTTGTACTIONTCCCATTGT |
| 16s rRNA Universal | Primer 2 | ACTCCTACGGGAGGCAGCAGT |
| | Primer 1 | ATTACCGCGGCTGCTGGC |

For microbiota sequencing, DNA was diluted to 1ng/μL. 16S rRNA genes were amplified using the Phusion® High-Fidelity PCR Master Mix with the I6S V4 specific primer 515F-806R. PCR products were run on a 2% agarose gel for detection. Samples with a bright main strip between 400bp-450bp were chosen for further experiments. PCR products were mixed at equal density ratios and purified with the Qiagen Gel Extraction Kit. Libraries were generated with NEBNext® UltraTM DNA Library Prep Kit and sequenced by the Illumina platform. Paired-end reads were merged using FLASH and chimeric sequences were removed using the UCHIME algorithm. Sequence analysis was performed using Uparse. Sequences having ≥97% similarity were assigned to the same OTU. Representative sequences for each OTU were screened for further annotation. The SILVA rRNA database was used for species annotation at each taxonomic rank. Phylogenetic relationship between OTUs was obtained using MUSCLE (Version 3.8.31). OTU abundance information was normalized using a standard sequence number corresponding to the sample with the least sequences. Diversity analyses were performed using QIIME.

2.21. Caecal metabolite extraction

Caecal contents were weighed and resuspended in either water (for aqueous components) or methanol (for organic components) to a concentration of 1ml/g. The samples were vigorously vortexed for 1min and then incubated at RT for 5min. They were then centrifuged (5000g, 5min) and the supernatants were collected and stored at -20°C until further use.

2.22. Fecal metabolome analysis

Fecal pellets were resuspended in 50% methanol for extraction of metabolites, and the extracted metabolites were characterized by LC/MS (HILIC and qTOF) in both positive and negative ionization modes. Annotations were done based on the MS1 and MS2 spectra. MS1 intensities of identified metabolites were compared and those that showed differences between groups with FDR <0.01 were considered significant changes.

2.23. Proliferation assay and ex vivo splenocyte culture

Single cell suspensions of splenocytes were washed once with PBS and then resuspended in a solution of 1:250 diluted CPD e450 in PBS. Cells were then incubated for 10 min at RT after which RPMIc was added and incubated on ice for 5 min. Cells were pelleted by centrifugation (300g, 10min, 4°C) and plated in 96 well U-bottom plates (2*10⁵ cells/well). The cells were treated with recombinant MOG (MOG 1-125 Recombinant protein – self-made), MOG 35-55

peptide, or anti-CD3. Recombinant MOG and MOG 35-55 were used in a 1:5 dilution series starting with a top concentration of 20µg/ml. Anti-CD3 was used in a 1:4 dilution series starting from 2µg/ml. Ovalbumin protein was used as the negative control at a concentration of 20µg/ml. Cells were incubated at 37°C for 60 h after which they were FACS stained and acquired.

For ex vivo culture, single cell suspensions of splenocytes were plated in 96 well plates (2*10⁵ cells/well). Cells were treated with recombinant MOG (20µg/ml) or anti-CD3 (2µg/ml) and incubated at 37°C for 60 h after which culture supernatants were collected and frozen at -20°C until use.

2.24. Differentiation assay

| Antibody | Clone | Isotype | Catalog number | Sourced from |
|--------------|----------|-----------------------|----------------|--------------|
| CD3 | 145-2C11 | Armenian Hamster IgG1 | BE0001-1 | BioXCell |
| CD28 | 37.51 | Syrian hamster IgG2 | BE0015-1 | BioXCell |
| IFN γ | XMG1.2 | Rat IgG1, κ | BE0055 | BioXCell |
| IL-4 | 11B11 | rat IgG1 | BE0045 | BioXCell |

Single cell suspensions of splenocytes were washed once with PBS and then resuspended in 0.5% BSA in PBS. Cells were then incubated with of CD4 isolation cocktail (75µl per 100 million cells) for 10 min at RT after which Streptavidin beads (75µl per 100 million cells) were added. Cells were placed in a magnet for 2min and the supernatant was collected. Cells were pelleted by centrifugation (300g, 10min, 4°C) and stained with CD4, CD62-L, and CD25 antibodies. Stained cells were washed and resuspended in 0.5% BSA in PBS. CD4⁺ CD62-L⁺ CD25⁻ naïve T cells were sorted and plated in 96 well flat bottom plates (2*10⁵ cells/well in IMDMc) pre-coated with anti-CD3 (2µg/ml) and anti-CD28 (2µg/ml). The pre-coating was done for 3 h at 37°C. IL-6 (30ng/ml), TGF- β (3ng/ml), anti-IFN γ (10µg/ml) and anti-IL-4 (10µg/ml) were added to the cells for T_H17 differentiation. TGF- β (3ng/ml), anti-IFN γ (10µg/ml) and anti-IL-4 (10µg/ml) were added to the cells for T_{reg} differentiation. NaCl was added at 40mM concentration. Caecal metabolite extracts were added at 1% concentration. Cells were incubated at 37°C for 60 h after which they were FACS stained and acquired.

2.25. In vitro B cell culture and i.p. injection

40LB feeder cells (3T3 fibroblasts expressing CD40L and BAFF) were cultured in RPMIc until confluence in 10cm cell culture dishes after which they were irradiated. B cells were purified from OSE mice spleens using the Pan B cell isolation kit and plated (5*10⁵ cells/dish) on the irradiated feeder cells, and the culture was supplemented with 2ng/ml of IL-4. After 3 days of culture, the supernatant was collected. The plates were treated with prewarmed MACS buffer and incubated for 5min at 37°C, then the detached cells were collected and pooled with the culture supernatant. Cells were pelleted by centrifugation (350g, 5min, RT), resuspended in

RPMIc, and replated in new 10cm dishes coated with irradiated feeder cells. 4ng/ml of IL-4 and 2ng/ml of IL-21 were added to the culture. After 3 more days of culture, cells were collected as before, washed once in PBS and counted. They were then resuspended in PBS (1×10^7 cells/ml) and injected i.p. to HSD-fed OSE mice (150 μ l – 15 million cells per mouse). OSE mice were then monitored for 30 days for EAE development. HSD-fed mice receiving no injection were used as controls.

2.26. EROD Assay

HepG2 cells were cultured in DMEMc at 37°C with 10% CO₂ and 95% humidity. After they attained 80% confluence, they were seeded into 96 well black plates at 25000 cells/well in 200 μ l volume and left to adhere overnight. Then, media was completely removed and cells were then treated with 40mM NaCl or 1% (v/v) caecal metabolite extracts in 200 μ l of DMEMc. After 24 h of exposure, the media was removed and the wells were rinsed with PBS. 50 μ l of phosphate buffer was added to the wells, following which 50 μ l of 2X EROD solution was added and the cells incubated at 37°C for 30min. The reaction was stopped by the addition of 75 μ l Fluorescamine solution. Resorufin at a top concentration of 1pmol/ μ l in phosphate buffer – 2-fold dilution series – was used as a standard. In addition, BSA at a top concentration of 1mg/ml in phosphate buffer – 2-fold dilution series – was treated with 75 μ l Fluorescamine solution and used as a protein standard. Fluorescence of resorufin was measured at an excitation of 535nm and emission of 590nm and that of Fluorescamine at 390nm and 485nm respectively. Resorufin levels were normalized to total protein (quantified by fluorescence of Fluorescamine in BSA standards).

2.27. ELISA kits and Antibodies

| Product | Source | Catalog number |
|--------------------------------------|---------------------|----------------|
| Mouse IgE ELISA MAX Standard | BioLegend | 432404 |
| ELISA Ready-SET-Go!™ for Mouse IgG | eBioscience | 15560877 |
| Mouse IL-10 ELISA MAX Standard | Biolegend | 431411 |
| Mouse albumin ELISA quantitation kit | Bethyl Laboratories | E99-134 |
| Mouse Leptin ELISA kit | ENZO life sciences | ADI-900-019A |

| Antibody | Clone | Isotype | Catalog Number | Sourced from |
|------------------------|--------------|------------------------------|----------------|--------------|
| IgG1 ^a | 10.9 | Mouse IgG2a, k | 553500 | Pharmingen |
| IgG2a ^a | 8.3 | Mouse IgG2a ^b , k | 553502 | Pharmingen |
| IgM ^a | DS-1 | Mouse IgG1, k | 553515 | Pharmingen |
| IL-17 (coating) | eBio17CK15A5 | Rat IgG2a, k | 14-7175 | eBioscience |
| IFN γ (coating) | AN-18 | Rat IgG1, k | 551309 | Pharmingen |
| IL-17 (primary) | eBio17B7 | Rat IgG2a, k | 13-7177 | eBioscience |
| IFN γ (primary) | R4-6A2 | Rat IgG1, k | 551506 | Pharmingen |

| | | | | |
|----------------|---------|---------------------|--------|------------|
| IgA (coating) | C10-3 | Rat IgG1, k | 556969 | Pharmingen |
| IgA (Standard) | M18-254 | Mouse BALB/c IgA, k | 553476 | Pharmingen |
| IgA (primary) | C10-1 | Rat IgG1, k | 556978 | Pharmingen |

2.28. MOG – specific Ig ELISA

For MOG-specific Ig measurement, 96 well plates were coated overnight at 4°C with 20µg/ml of recombinant MOG in 100µl PBS. After washing with ELISA wash buffer and blocking with 200µl 10% FBS blocking buffer for 1 h, Serum was added at different dilutions (1:10000, 1:100000) to a final volume of 100µl and incubated for 2 h. The plates were washed, then biotin labelled primary antibodies for IgG1^a, IgG2a^a or IgM^a, were added at 1µg/ml concentration to a final volume of 100µl and incubated for 1 hr. After a subsequent wash, Streptavidin-HRP (1:1000, final volume 100µl) was added and the plates were incubated for 1 h. Finally, 100µl TMB substrate solution was added and after the color change, the reaction was stopped with 100µl of 1N H₂SO₄. Plates were read at 450nm. There were no standards used and OD measurements of both groups were compared directly.

2.29. Cytokine ELISA

For IL-17 and IFN γ ELISA, 96 well plates were coated overnight at 4°C with 1µg/ml of antibodies to IL-17 or IFN γ in 100µl PBS. Plates were then washed with ELISA wash buffer and blocked with 200µl 10% FBS blocking buffer for 1 h. Standards for IL-17 and IFN γ (2ng/ml top, 2 fold dilution series) and culture supernatants (1:10 dilution) were added to a final volume of 100µl and incubated for 2 h. Plates were then washed, and then biotin labelled primary antibodies for IL-17 or IFN γ were added at 1µg/ml concentration to final volume 100µl and incubated for 1 h. Plates were washed and streptavidin-HRP (1:1000, final volume 100µl) was added. After 1 h, ABTS was added and the plates were measured 20min later at 405nm.

2.30. Fecal IgA ELISA

For fecal IgA measurement, 96 well plates were coated overnight at 4°C with 1µg/ml of anti-IgA in 100µl PBS. Plates were then washed with ELISA wash buffer and blocked with 200µl 10% FBS blocking buffer for 1 h. IgA standard at 2ng/ml – 2-fold dilution series, and fecal supernatants (diluted 1:10) were added to a final volume of 100µl and incubated for 2 h. Subsequently, plates were washed and then incubated with 100µl of 1µg/ml biotin labelled primary antibody for 1 h. Plates were washed and Streptavidin-HRP (1:1000, final volume 100µl) was added. Lastly, 100µl TMB substrate solution was added and after the color change, the reaction was stopped with 100µl of 1N H₂SO₄. Plates were read at 450nm.

2.31. Western blot

Brain endothelial cells were processed as described in **2.16**. Cells were subsequently FACS stained for CD31, and CD31+ cells were sorted. Sorted cells were washed twice with PBS, then lysed by boiling for 5min at 95°C with 1:1 v/v of RIPA buffer containing protease and phosphatase inhibitor, and SDS-containing sample buffer. Total proteins were separated on a

4–15% gradient SDS-polyacrylamide gel. Proteins were then transferred onto a nitrocellulose membrane via wet-transfer (complete immersion of both the gel and membrane in transfer buffer for 2 h, 4°C). After blocking for 2 h with blocking buffer, immunoblots were incubated overnight with primary antibodies at a concentration of 1:1000 in blocking buffer. Blots were washed in TBS-T (3 times, 5min each), then further incubated with secondary antibody for 1 h. Blots were subsequently visualized using the chemiluminescent substrate on a Chemidoc MP imaging system (Bio-Rad). The densitometric analysis of each protein signal was obtained using the Molecular Imager Chemidoc (Bio-Rad) and normalized to the expression of β -actin.

| Antibody | Clone | Isotype | Catalog number | Sourced from |
|------------------------------------|------------|-----------------------|----------------|-------------------|
| ZO-1 (primary) | polyclonal | Rabbit IgG | 61-7300 | Thermo Scientific |
| Claudin-5 (primary) | polyclonal | Rabbit IgG | 341600 | Thermo Scientific |
| β -actin - HRP | 2F1-1 | Mouse IgG2b, κ | 640807 | Biolegend |
| Rabbit IgG (H+L) – HRP (secondary) | polyclonal | Goat IgG | R-05072-500 | Advansta |

2.32. Histology

Mice were perfused with PBS, followed by perfusion with 4% PFA in PBS. Spinal cords were preserved in 4% PFA in PBS for at least 24 h. Following that, they were dehydrated by immersing them first in 90% Ethanol for 1 hour, followed by 100% Ethanol 2 times for 1 hour each time, and then 3 times in Xylene for 15 min each time, and lastly in Paraffin bath, overnight at 65°C. They were subsequently embedded in Paraffin. Embedded tissue was sectioned into 5 μ m thick sections using the HM 355 microtome (Thermo scientific), floated onto clean glass slides, and left to dry and attach at RT overnight. Dried slides were stored at RT until staining.

2.33. Luxol fast blue staining

| Reagent | Components | Concentration |
|----------------------------|---|-------------------------|
| Luxol fast blue solution | Luxol fast blue 10% acetic acid 96% Ethanol | 1g 5ml 1000ml |
| 10% Acetic acid solution | Acetic acid H ₂ O | 10g Make up to 100ml |
| Lithium carbonate solution | Li ₂ CO ₃ H ₂ O | 0.1g 100ml |
| Periodic acid solution | Periodic acid H ₂ O | 1g 100ml |

| | | |
|------------------|--|--------|
| Sulfite solution | HCl | 0.5ml |
| | K ₂ S ₂ O ₈ | 0.2g |
| | H ₂ O | 49.5ml |

Slides having spinal cord sections were deparaffinized as follows:

- Xylene, for 10 min, 2 times
- 99% Ethanol, for 2 min, 2 times
- 96% Ethanol, for 2 min, 2 times

Slides were incubated overnight in Luxol fast blue solution at 56°C, after which they were rinsed in 96% ethanol and then in water. They were then immersed in Lithium carbonate solution until differentiation in the staining was visually observed (1.5 to 2 min) after which they were immediately transferred to 70% Ethanol. They were then immersed in water for 5min, followed by immersion in Periodic acid solution for 10min. They were washed in water for 5min, then immersed in Schiff's reagent for 20min. This was followed by washing the slides 3 times in Sulphite solution, 2min each time. After washing the slides in water for 10min, slides were dehydrated as follows:

- 70% Ethanol, for 2 min, 2 times
- 96% Ethanol, for 2 min, 2 times
- 99% Ethanol, for 2 min, 2 times
- Xylene, for 10 min, 2 times

Dehydrated slides were mounted in Entellan (Merck) and coverslip was added. Slides were dried and imaged with a brightfield microscope (Leica, Thermo Scientific) at 10X magnification. Images were processed with SPOT image capture software.

2.34. Statistical Analysis

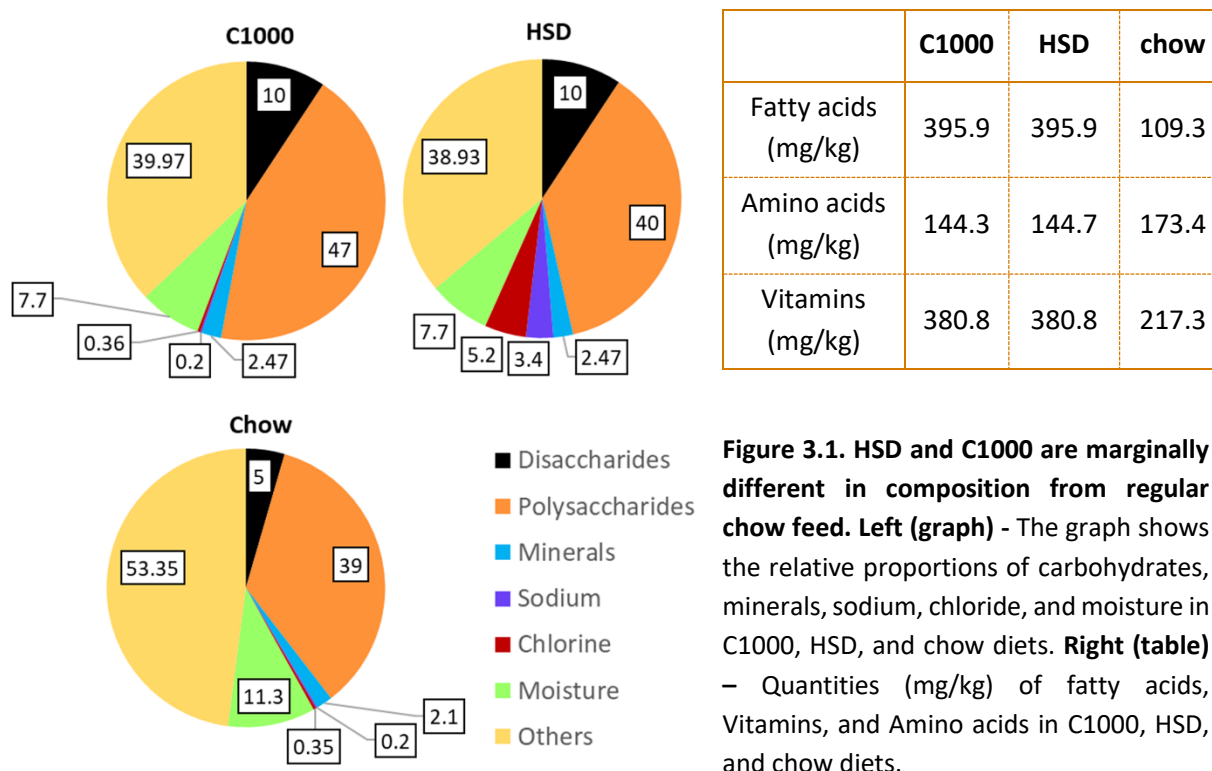
GraphPad Prism 8 (GraphPad Software, Inc.) was used for all statistical analyses. P values < 0.05 were considered significant. All plots show mean ± s.e.m.

3. RESULTS

Growing concerns over lifestyle and autoimmune diseases in the western hemisphere have resulted in this body of research being directed towards dietary components dominating the ‘Western diet’, including NaCl. Mounting evidence for a key role of dietary components like NaCl in autoimmunity necessitates a better understanding of their role using model systems and diet regimens as less artificial as possible to serve for easier extrapolation of results to the human context. Bearing this in mind, this study used the spontaneous EAE (OSE) model, and 4% NaCl supplemented food with normal drinking water as the diet regimen.

3.1. HSD IS WELL TOLERATED BY MICE:

While several studies have investigated HSD in the context of diseases including EAE, the diet regimens used vary marginally across studies regarding the quantum of salt given to the mice, the mode of ingestion i.e., through food or water, and the duration of feeding [225, 290, 293]. Further, their intestinal microbiota composition, which influences nutrient requirements, varies across different facilities. These factors influence the diet’s tolerability in mice. It is thus not valid to presume the suitability of the HSD regimen used in this study based upon prior studies. In this study, we used a purified diet (C1000) as the control diet instead of a regular chow diet. Apart from being supplemented with 4% NaCl, the HSD was compositionally identical to C1000.



Moreover, the chow diet is prepared from crude components obtained from wheat and soy, whereas C1000 and HSD are purified diets prepared using cellulose as the fiber source. Also, C1000 and HSD are identical in composition except for NaCl, but marginally different in

composition from the chow diet (**Fig 3.1**). The fatty acid, amino acid, and vitamin quantities in the purified diets are all different from chow, as is the moisture content. Hence, spontaneous EAE incidence was investigated after diet switch to chow, C1000, and HSD to affirm that incidence under C1000 and chow does not differ significantly and any observed effect would be attributable to dietary salt and can be extrapolated to humans. Diet switched mice were maintained on their respective diets for a minimum of 3-4 weeks after the switch. The tolerability of this regimen in our mouse lines was first addressed.

To begin with, WT mice raised on regular chow feed were switched to C1000 or HSD. To probe for a difference in diet intake between mice fed C1000 and HSD, bodyweight change was monitored up to 4 weeks after diet switch. Bodyweight changes under both C1000 and HSD were similar throughout the observed duration (**Fig.3.2. a**). In addition, the levels of the hormone leptin were measured. Leptin mediates hunger and regulates feeding and energy homeostasis. Its levels are altered correlative to alterations in diet intake and we hypothesized that leptin levels would be altered if HSD-fed mice had moderately altered diet intake which is perhaps not perceptible through body weight measurements. Leptin levels in C1000 and HSD-fed mice, quantified by ELISA in WT mice sera 4 weeks after diet switch, also showed no difference (**Fig.3.2. b**). Thus, we concluded that with this diet regimen, there were no significant differences in food intake and that our HSD regimen was well tolerated by WT mice. Subsequently, this was affirmed in OSE mice as well. OSE mice raised on a regular chow diet were weaned onto C1000 or HSD. Bodyweight change monitored for 4 weeks after diet switch was found to be similar under both diets (**Fig.3.2. c**), indicating that there were no substantial changes in diet intake in HSD-fed mice and that HSD was well tolerated.

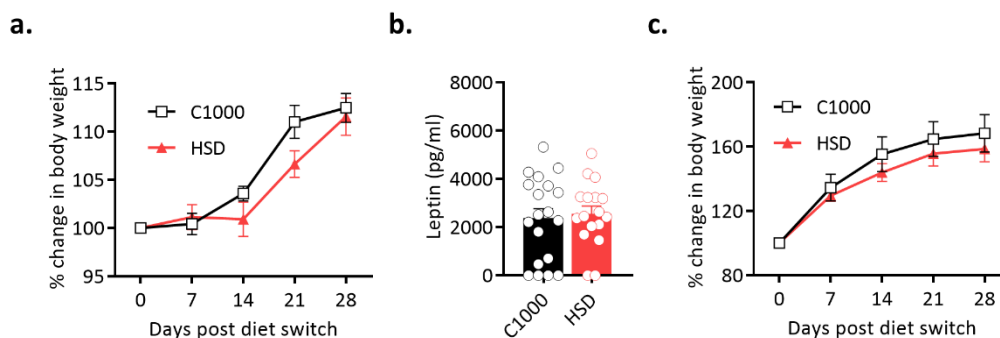


Figure 3.2. HSD is well tolerated by mice. **a.** Body weight change in WT mice after diet switch (C1000 n=7, HSD n=7). **b.** Leptin levels in WT mice 4 weeks after diet switch (C1000 n=19, HSD n=17). Data from sera collected across 3 litters of mice is shown. Each circle represents an individual mouse. **c.** Bodyweight change in OSE mice after diet switch (C1000 n=3, HSD n=3). All data represented as mean \pm s.e.m.

3.2. DIETARY SALT PROTECTS OSE MICE FROM SPONTANEOUS EAE:

Once OSE mice were found to tolerate HSD well, the effect of HSD on spontaneous EAE was investigated. As reported previously, about 50% of OSE mice maintained on a chow diet under SPF conditions develop EAE [34]. Interestingly, our group observed that OSE mice raised on HSD from birth were completely protected from spontaneous EAE as opposed to their chow

fed counterparts (data not shown). However, our rationale was that switching to HSD in early adult life would be more relevant than an HSD regimen from birth if our results are to be applied in the context of MS in humans.

OSE mice raised on a regular chow diet were weaned onto chow, C1000, or HSD, and EAE was monitored until 12 weeks of age. Indeed, while disease incidence under chow and C1000 diets did not differ significantly, Disease incidence under HSD (~20%) was significantly lower than under chow (~50%) or C1000 (~45%) (**Fig.3.3. a, b**). These results suggest that contrary to the published studies, HSD had a protective effect on spontaneous EAE. Yet, in those few mice that developed EAE under HSD, the maximal clinical scores were not significantly different from chow or C1000 fed mice (**Fig.3.3. c**). Additionally, Luxol fast blue staining to visualize myelin was performed on spinal cord sections from both healthy and sick mice, and significant demyelination was seen in sick mice under both C1000 and HSD, as evidenced by the absence of blue coloration - in comparison to their healthy counterparts (**Fig.3.3. d**). These results indicate that while HSD reduces the incidence of spontaneous EAE, it does not mitigate disease severity in those mice that do develop EAE.

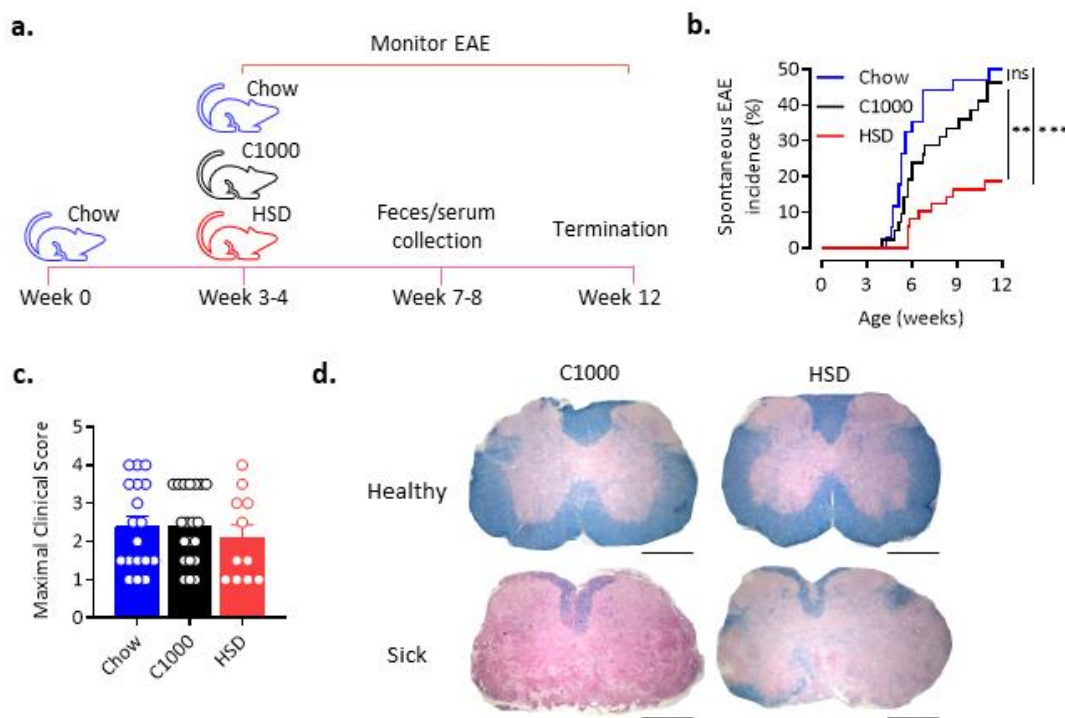


Figure 3.3. Dietary salt protects OSE mice from spontaneous EAE. **a.** Experimental plan for diet switch experiments in OSE mice. Mice were weaned onto the respective diets at 3-4 weeks of age and monitored for EAE until 12 weeks of age. Sample collection was done 3-4 weeks after the diet switch. **b.** Spontaneous EAE Incidence in OSE mice after diet switch. (C1000 n=42, HSD n=49, chow n=34) **P=0.0054, ***P=0.0004 (Gehan-Breslow-Wilcoxon test). **c.** The maximal clinical score attained by OSE mice that got the neurological disease under chow, C1000, or HSD. Each circle represents an individual mouse. (**b, c**) Data from observation across >5 litters of mice are pooled. **d.** Representative images of spinal cord sections from both healthy and sick OSE mice fed C1000 or HSD, stained with luxol fast blue. All data represented as mean \pm s.e.m.

Since CNS infiltrating immune cells are the key players impacting EAE incidence and severity, it was essential to characterize the immune cell populations in both the periphery and the CNS of mice developing EAE. FACS analysis was performed on lymph nodes, brain, and spinal cord of mice that developed EAE under both C1000 and HSD. The predominant proportion of infiltrating cells contain B cells, neutrophils, and the IFN γ + and IL-17+ CD4+ T cells. Proportions of CD4+ T cells, B cells, and neutrophils were first analyzed and they showed no difference (**Fig.3.4. a-c**). Next, frequencies of the major CD4+ cell subsets infiltrating the CNS during EAE - IFN γ +, IL-17+, and IFN γ + IL-17+ CD4+ T cells were also analyzed and showed no difference (**Fig.3.4. d-f**). This further reinforced that HSD does not impact disease severity in those mice that develop EAE.

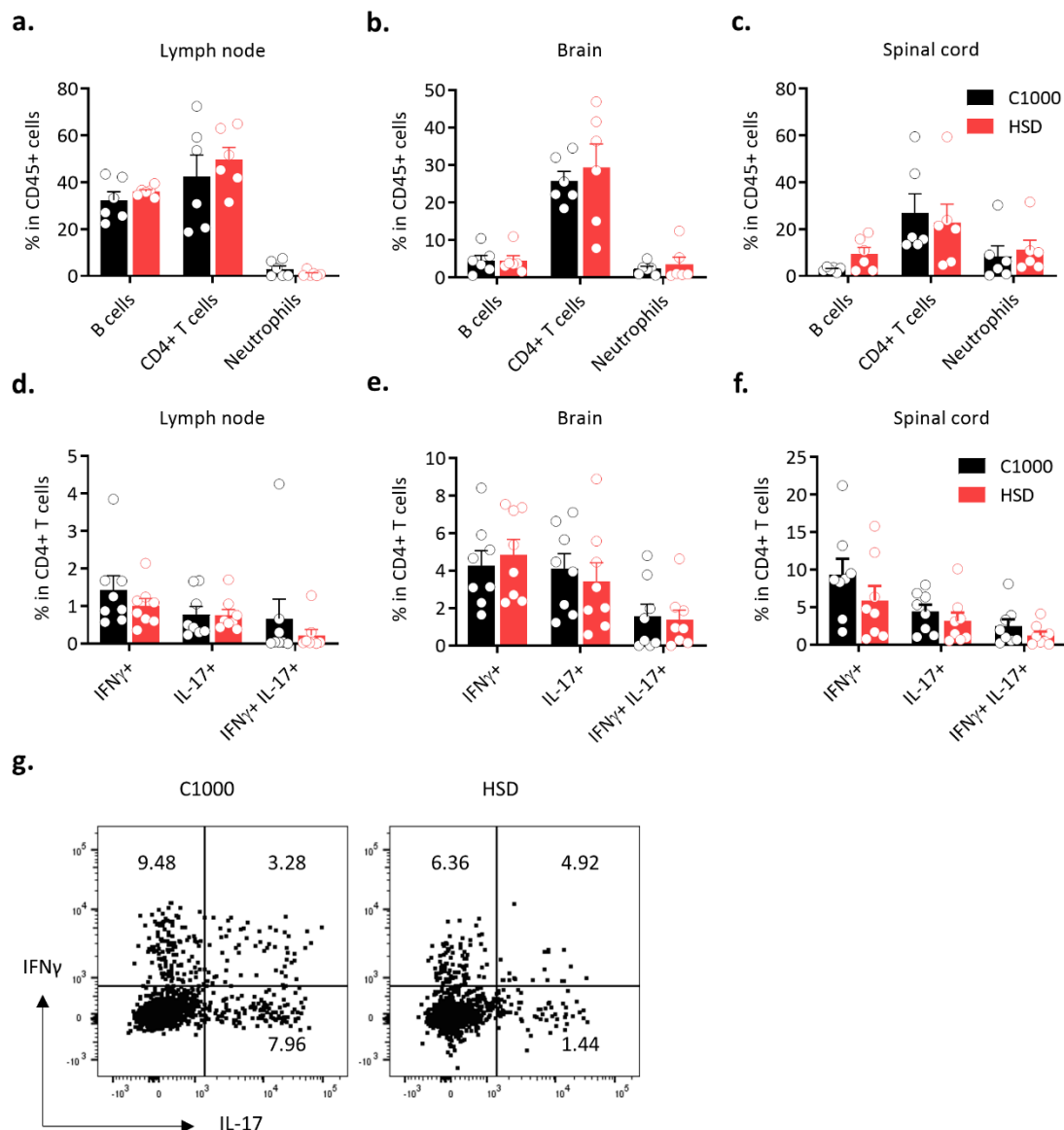


Figure 3.4. Peripheral and CNS Infiltrating immune cell populations in OSE mice with neurological disease. a-c. The frequencies of immune cells in the cervical lymph node (a), brain (b), and spinal cord (c). Frequencies were calculated as a percentage of CD45+ cells. Data from 2 separate experiments are pooled (C1000 n=6, HSD n=6). Each circle represents an individual mouse. d-f. Frequencies of cytokine producing

CD4+ T cells in the cervical lymph node (**d**), brain (**e**), and spinal cord (**f**). Data from 2 separate experiments are pooled (C1000 n=8, HSD n=8). Each circle represents an individual mouse. **g**. Representative FACS plots of cytokine staining, gated on CD4+ cells. All data represented as mean \pm s.e.m.

3.3. ACTIVELY INDUCED EAE IS NOT AFFECTED BY HSD:

Next, we investigated whether the observed disease protection due to HSD is extended to induced EAE as well. Multiple past studies have shown that HSD does not protect from, but rather exacerbates actively induced EAE in WT mice [290, 291]. Unlike these reports, the present study employed a different diet regimen having 4% NaCl supplementation only in food pellets and not in drinking water, and had observed disease protection in spontaneous EAE. Hence, an independent investigation was done on actively induced EAE.

6 to 8 weeks old WT mice were switched to C1000 or HSD and after 3-4 weeks, EAE was induced using CFA containing 500 μ g MTB and 100 μ g MOG 35-55. Unlike in spontaneous EAE, disease incidence was not lower under HSD and more than 80% of the mice developed EAE under both C1000 and HSD (**Fig.3.5. a**). Also, contrary to the aforementioned reports, disease severity was similar in both diets (**Fig.3.5. b**). Moreover, an analysis of CNS infiltrates in sick mice did not show any differences between C1000 and HSD-fed mice (**Fig.3.5. g**).

However, in this experimental setup, the C1000 fed mice already developed severe EAE as evidenced by the high mean clinical score (**Fig.3.5. b**). In order to observe any exacerbation in EAE severity under HSD like in the prior reports, it was necessary to achieve EAE with lower severity in control animals. To this end, mice fed chow diet were immunized using a 10-fold lower MTB dosage in CFA (50 μ g) and either 100 μ g or 50 μ g MOG 35-55. Irrespective of the MOG concentration, the reduced CFA dosage resulted in lower disease severity (**Fig.3.5. d**). But, disease incidence under 50 μ g MOG (~60%) was much lower than under 100 μ g MOG (>90%) (**Fig.3.5. c**). As we had achieved a lower disease severity with 50 μ g MTB in CFA coupled with 100 μ g MOG without affecting incidence, this was chosen as the subsequent experimental setup. With this setup, EAE was induced in WT mice fed C1000 or HSD for 3-4 weeks and it was observed that neither EAE incidence nor severity was altered under HSD (**Fig.3.5. e, f**). From this, it is evident that HSD neither protects nor exacerbates actively induced EAE.

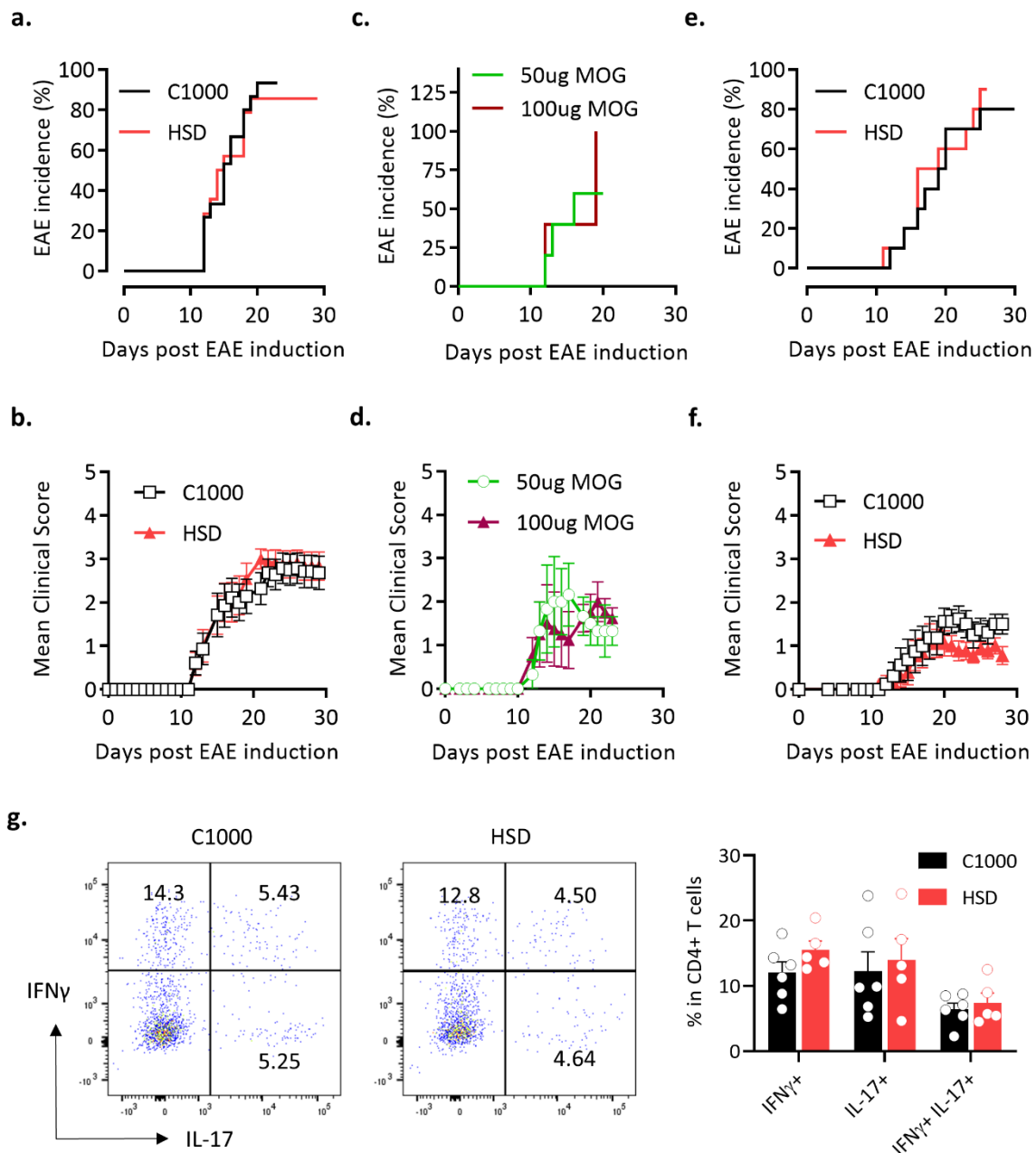


Figure 3.5. HSD does not protect from active EAE in WT mice. **a, b.** Disease incidence (**a**) and Mean clinical score (**b**) after active EAE induction with 100 μ g MOG 35-55 in CFA containing 500 μ g MTB (C1000 n=14, HSD n=14). **c, d.** Disease incidence (**c**) and Mean clinical score (**d**) after active EAE induction with either 100 μ g or 50 μ g MOG 35-55 in CFA containing 50 μ g MTB (C1000 n=5, HSD n=5). **e, f.** Disease incidence (**e**) and Mean clinical score (**f**) after active EAE induction with 100 μ g MOG 35-55 in CFA containing 50 μ g MTB (C1000 n=10, HSD n=10). For plotting mean clinical scores (**b, d, f**), only mice that developed EAE were taken into consideration. **g.** Representative FACS plots of cytokine staining, gated on CD4+ cells (left) and frequencies of cytokine producing CD4+ T cells in the spinal cord of mice that developed EAE (from panel **b**) (C1000 n=6, HSD n=5). Each circle represents an individual mouse. All data represented as mean \pm s.e.m.

3.4. HSD ALTERS SPECIFIC GUT MICROBIAL POPULATIONS

We investigated whether the intestinal microbiota, whose composition and function are hugely dependent on a diet is altered in HSD-fed mice. Previous data from our lab, obtained

from sequencing the 16s rRNA gene from fecal DNA of OSE mice fed chow or HSD from birth, showed increased levels of *Enterococci* in HSD-fed animals (data not published). First, robust validation of this finding was essential before examining its relevance to EAE. So, initially, fecal microbial DNA from OSE mice weaned onto chow or HSD and maintained for 3-4 weeks on the respective diets, was subject to qPCR analysis for *Enterococci* using primers specific to its 16s rRNA gene. The levels of *Enterococci* were significantly higher under HSD. This verified what was observed through 16s rRNA sequencing (Fig.3.6. a).

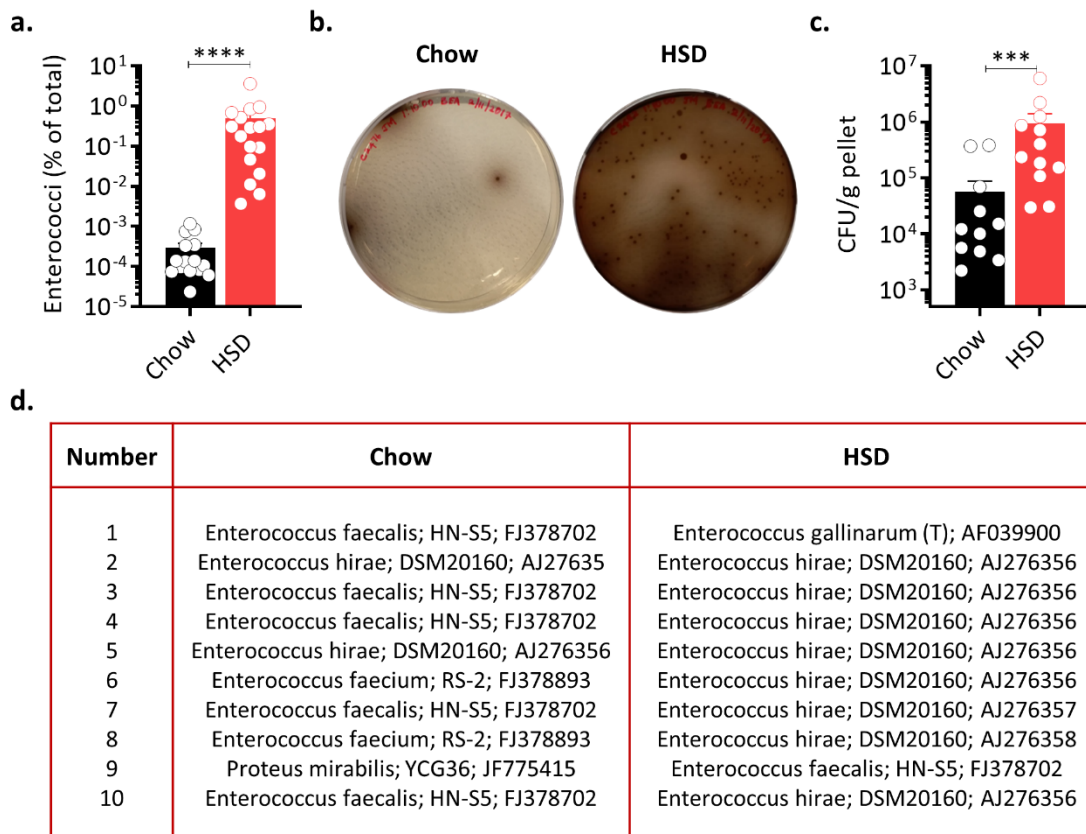


Figure 3.6. HSD increases *Enterococci* levels in the gut. a-d. OSE mice were weaned onto chow or HSD and feces collected 3-4 weeks after diet switch; **a.** 16s rRNA qPCR analysis of fecal DNA with *Enterococci* specific primers represented as % of total microbiota (chow n=15, HSD n=17). ****P<0.0001 (Mann Whitney’s U test). Each circle represents an individual mouse. **b.** Representative Bile-Esculin agar plates spread with 1:1000 dilution of fecal microbiota resuspended in PBS; Dark colonies were counted for CFU computation and isolation/sequencing (c and d). **c.** CFU when cultured in Bile-Esculin agar, normalized to pellet weight (chow n=11, HSD n=12). Each circle represents an individual mouse. *** P<0.001 (Mann Whitney’s U test). **d.** Species distribution of *Enterococci*, obtained from sequencing colonies from the Bile-Esculin agar plates. Dark colonies were selected at random, each from a different plate. Each of the colonies sequenced is from fecal pellets of 10 individual mice from each diet condition. All data represented as mean ± s.e.m.

Next, fecal microbiota from OSE mice weaned onto and maintained on chow or HSD for 3-4 weeks were plated on Bile-Esculin agar (selective medium for *Enterococci*) and their CFU computed. CFU counts indicated a significantly higher frequency of *Enterococci* under HSD, also evidenced by the black coloration in the Bile-Esculin agar around each colony (Fig.3.6. b, c). Isolation, culture, and sequencing of specific colonies from the plates showed *Enterococci*

hirae to be dominant under HSD. Conversely, colonies that were sequenced from the chow diet showed the presence of other *Enterococci* species (Fig.3.6. d).

As elucidated earlier, the overall composition of C1000 and chow diets are marginally different. Hence, it was essential to make a subsequent comparison of the microbiome from HSD-fed mice to that of C1000 to affirm that the observed alterations in *Enterococci* are due to dietary salt. To this end, caecal microbial DNA from C1000 and HSD-fed mice were analyzed by 16s rRNA sequencing. The overall microbial diversity was similar in both C1000 and HSD, as inferred from their similar Shannon diversity index (Fig.3.7. a). Principal component analysis to visualize the inter-group (C1000 vs HSD) variation showed that the microbial profiles were in 2 distinct groups based on diet (Fig.3.7. b).

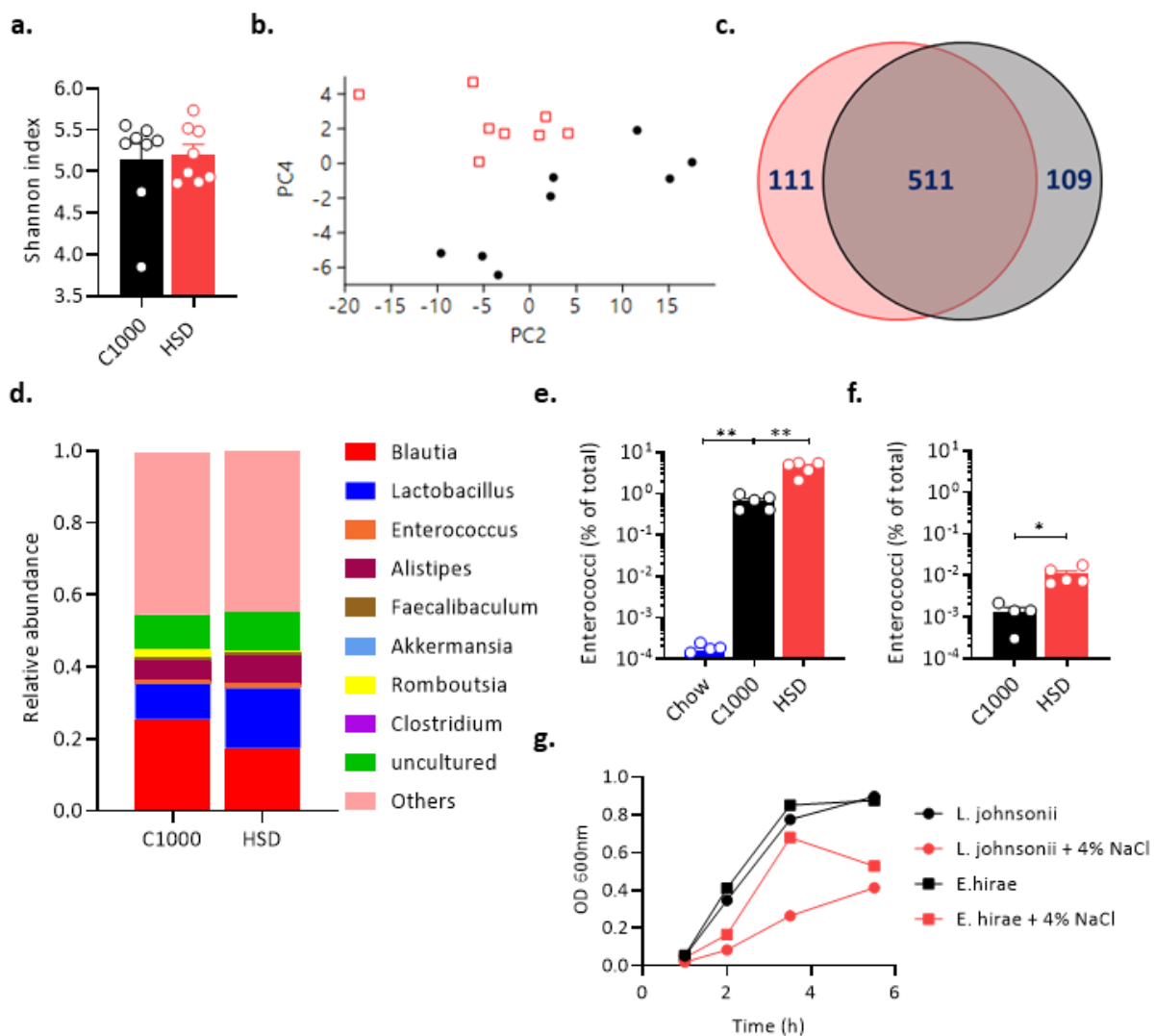


Figure 3.7. HSD increases the relative abundance of Enterococci in the gut. a-d. OSE mice were weaned onto C1000 (n=8) or HSD (n=8) and caecal content was collected 3-4 weeks after diet switch; DNA was extracted and the 16s rRNA gene sequenced; **a.** Shannon diversity index of caecal microbiota from C1000 and HSD-fed mice. Each circle represents caecal content from an individual mouse. **b.** Principal component analysis on caecal microbiota from C1000 and HSD-fed mice. Each symbol corresponds to an individual mouse. **c.** Venn diagram indicating the prevalence of identified microbial species (number of species

indicated in blue) under C1000 and HSD. The black circle represents C1000 and the red circle represents HSD. **d.** Relative abundance (expressed as a fraction of total) of 8 most differentially abundant genera, under C1000 and HSD. **e.** 16s rRNA qPCR analysis of fecal DNA with Enterococci specific primers represented as % of total microbiota (chow n=5, C1000 n=5, HSD n=5). chow vs C1000 **P=0.0079 (Mann Whitney's U test), HSD vs C1000 **P=0.0079 (Mann Whitney's U test). Each circle represents an individual mouse. **f.** 16s rRNA qPCR analysis of fecal DNA with Enterococci specific primers represented as % of total microbiota (C1000 n=4, HSD n=5). *P=0.015 (Mann Whitney's U test). Each circle represents an individual mouse. **g.** OD at 600nm at various time points for the culture of *E. hirae* and *L. johnsonii* in BHI broth with and without 4% NaCl. All data represented as mean \pm s.e.m.

On further characterization, the prevalence of 111 species was shown to be increased under HSD, and that of 109 species under C1000 (**Fig.3.7. c**). Quantification of relative abundances at the genus level identified the most differentially prevalent genera. *Blautia* was reduced under HSD, with a relative abundance of 0.17 as opposed to 0.25 in C1000. *Lactobacillus* was more prevalent under HSD with a relative abundance of 0.16 compared to 0.09 under C1000. *Enterococcus* was also more prevalent under HSD with a relative abundance of 0.013 as opposed to 0.007 under C1000. In addition, *Akkermansia*, *Romboutsia*, and *Alistipes* also differed in their relative abundance under C1000 and HSD (**Fig.3.7. d**). Among these genera, having previously established a significant increase in *Enterococci* under HSD in comparison to chow, qPCR analysis was performed on fecal microbial DNA of WT mice fed chow, C1000 or HSD - 3-4 weeks after diet switch - to characterize *Enterococci* levels. It was seen that while *Enterococci* level under C1000 was already significantly higher than under chow, there was still a significant increase in *Enterococci* under HSD in comparison to C1000 (**Fig.3.7. e**).

These findings were next corroborated in OSE mice fed C1000 or HSD for 3-4 weeks. *Enterococci* levels, determined by qPCR analysis on fecal microbial DNA, were significantly higher under HSD than under C1000 (**Fig.3.7. f**). Subsequently, *E. hirae* was cultured in BHI broth in the presence of NaCl to validate its salt tolerance in comparison to *L. johnsonii* which is known to be sensitive to salt. Indeed, *E. hirae* was observed to be able to grow well with NaCl in the media (**Fig.3.7. g**). In summary, while HSD does not significantly alter overall gut microbial diversity, it alters the relative abundance of many genera including *Enterococci*.

3.5. HSD MODIFIES THE FECAL METABOLOME

Alterations to the microbiota can result in an altered gut metabolome, which thus became our subsequent focus. Accordingly, the fecal metabolite profile from OSE mice fed chow or HSD was first characterized via LC/MS.

The fecal metabolome showed significant alterations under HSD. Principal component analysis showed a clear separation of the chow and HSD samples, indicating a significantly altered metabolome profile (**Fig.3.8. a**). A heatmap with MS¹ intensities of all the identified metabolites under chow and HSD showed that several metabolites were differentially abundant under chow and HSD (**Fig.3.8. b**). Subsequently, 20 metabolites that were the most significantly altered under both the positive and negative ionization modes were identified.

The fold change in their MS¹ intensities under HSD relative to chow was computed, to quantitatively identify their increase or decrease under HSD (Fig.3.8. c).

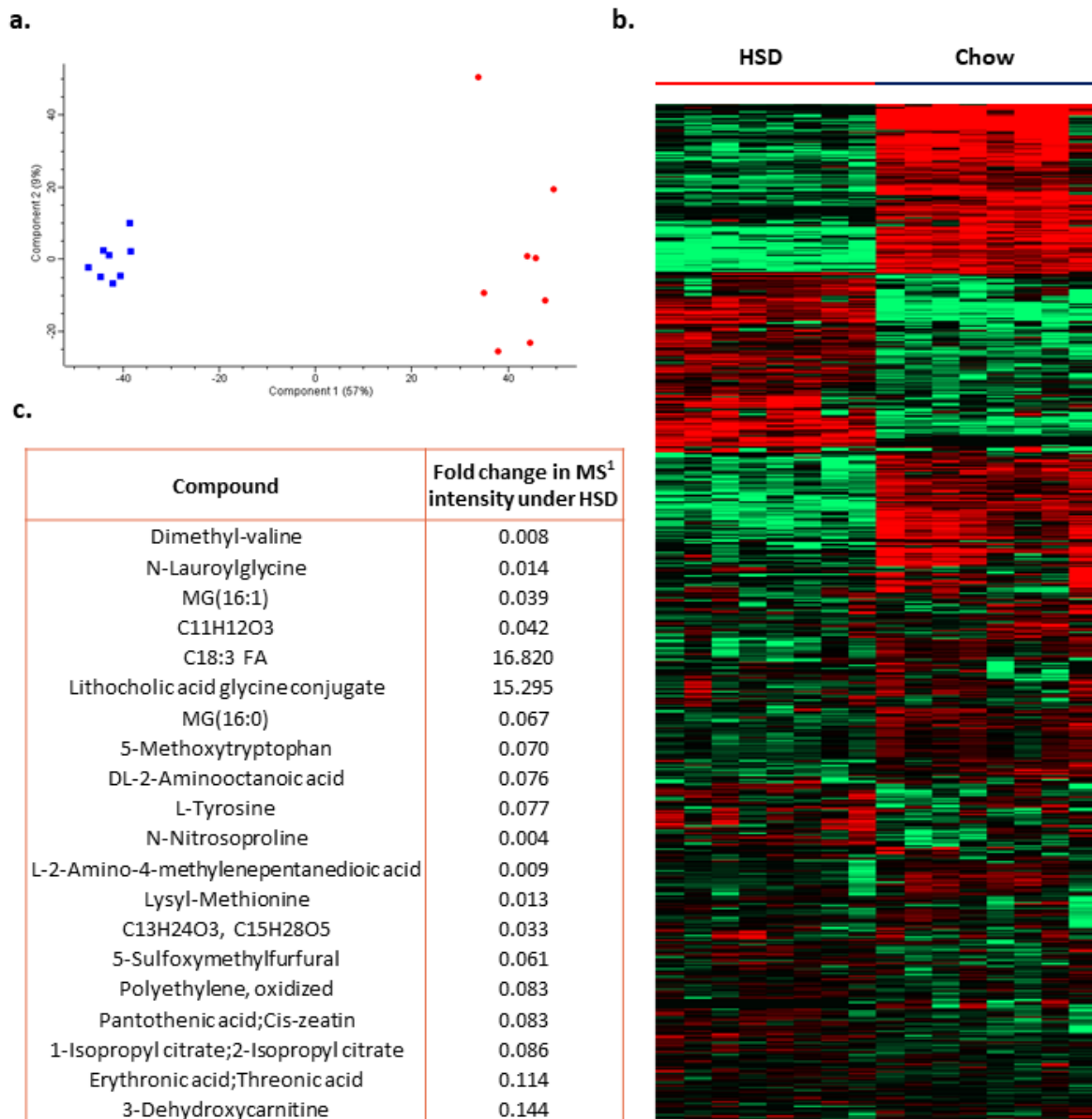


Figure 3.8. HSD alters the fecal metabolome. a-d. OSE mice were weaned onto C1000 (n=8) or HSD (n=8) and feces collected 3-4 weeks after diet switch; Metabolites were extracted in methanol and analyzed by LC/MS; **a.** Principal component analysis on fecal metabolome from chow (blue) and HSD (red) fed mice. Each symbol corresponds to an individual mouse. **b.** Heatmap representing relative intensities of all identified metabolites under chow and HSD. **c.** The 20 most significantly altered metabolites and the fold change in their MS¹ intensities under HSD, relative to chow. To identify the top candidates, metabolites showing significant changes with FDR of 0.01 (t test) in either positive or negative ionization mode, were chosen; $\log_{10}(\text{Intensity under HSD}/\text{Intensity under chow})$ was computed and the chosen metabolites ranked according to the obtained ratio. The top 10 compounds under each ionization mode were then identified and listed along with their fold change in intensity (Intensity under HSD/Intensity under chow).

Having observed an altered metabolome, it was of interest to compare C1000 and HSD next, to validate that increased dietary salt resulted in these alterations. Still, it was more imperative to assess the potential functional relevance of the altered metabolome. We reasoned that upon characterization of potential functional alterations, a metabolomic screen comparing C1000 and HSD could be done subsequently and can reveal significantly altered metabolites that may be associated with any observed functional changes.

In this regard, the potential to activate the Aryl hydrocarbon receptor (Ahr) was explored. Indeed, HSD has been previously shown to alter the levels of Ahr ligands in the intestinal metabolome and many Ahr ligands have been shown to affect EAE [143, 290]. While the xenobiotic ligands of Ahr have diverse structural moieties, endogenous dietary and microbial metabolites that can activate Ahr are predominantly tryptophan derivatives [307]. As we had observed in **Fig.3.8. c**, the >10-fold change in 5-Methoxytryptophan also suggested the possibility of differential Ahr activation under HSD.

The differential activation of Ahr was investigated with an EROD assay – which measures Cyp1a1 activity as a proxy measure of Ahr activation. (**Fig.3.9. a**) explains the principle behind the assay with a schematic. HepG2 liver cells were cultured in the presence of NaCl or FICZ (6-Formylindolo [3,2-b] carbazole – a high affinity Ahr ligand used as positive control) and EROD assay was performed after 24 h. NaCl did not differentially alter Ahr activation (**Fig.3.9. b, c**).

Subsequently, the assay was repeated with caecal extracts from C1000 and HSD-fed mice. While the metabolome analysis had used chow diet as control and didn't compare C1000 with HSD, it was reasoned that if functional alterations were seen, metabolomics analysis comparing C1000 and HSD could then be done and metabolites that had influenced the functional alterations could be identified. Yet, caecal extracts from HSD-fed mice did not differentially alter Ahr activation (**Fig.3.9. d, e**). In summary, HSD results in an altered metabolite profile in the gut which does not affect Ahr activity, but other potential functional pathways were not investigated here.

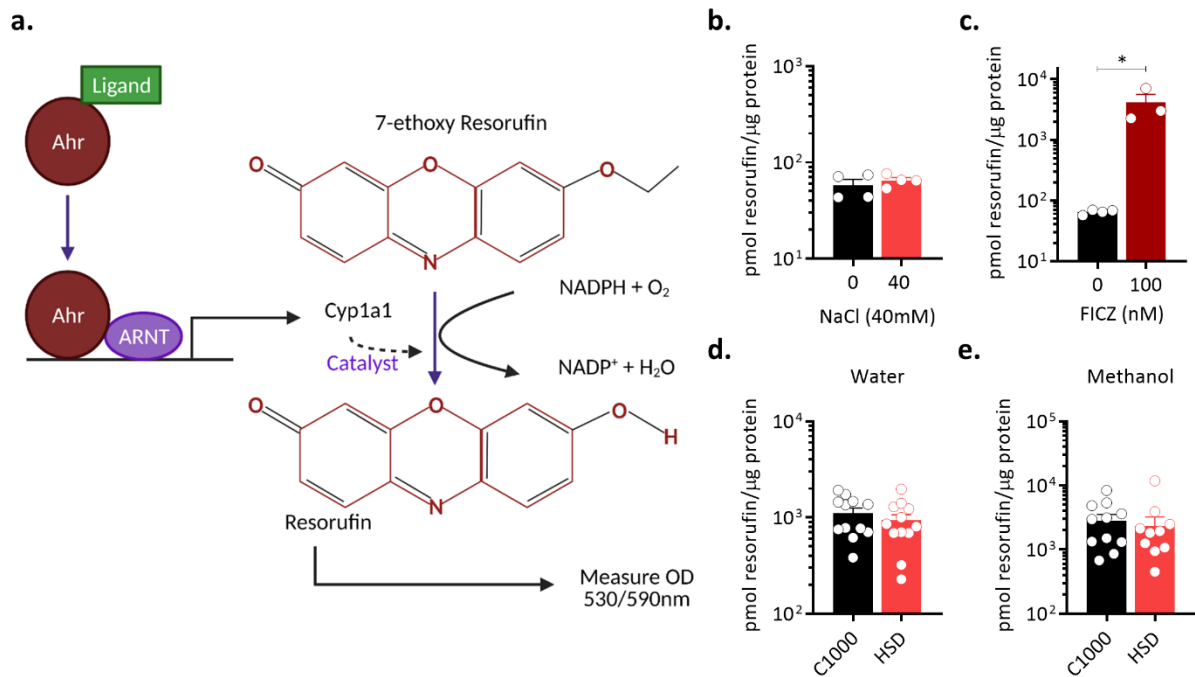


Figure 3.9. HSD-modified metabolites do not differentially activate Ahr. **a.** Schematic of the EROD assay. Ahr activation leads to Cyp1a1 expression. Cyp1a1 catalyzes the conversion of 7-ethoxyresorufin to resorufin, whose fluorescence can be quantified at 530nm/590nm. **b-e.** Resorufin levels (as proxy for Ahr activation) normalized to total protein, in HepG2 cells on treatment with NaCl (n=4) (**b**), the positive control ligand FICZ (n=3-4) (**c**) caecal water extracts from C1000 (n=11) or HSD (n=13) fed mice (**d**), or caecal methanol extracts from C1000 (n=11) or HSD (n=10) fed mice (**e**). One representative experiment out of 2 experiments performed is shown. Each circle represents one technical replicate (**b, c**) and one mouse (**d, e**). All data represented as mean \pm s.e.m.

3.6. HSD DOES NOT AFFECT INTESTINAL BARRIER INTEGRITY

Besides the metabolome, diet-mediated microbial alterations are also conventionally associated with changes in intestinal barrier permeability. These alterations can potentially affect the diffusion of dietary and microbial metabolites or the movement of gut immune cells to the other organs. Thus, it was essential to probe if the increase in *Enterococci* under our HSD regimen resulted in altered intestinal barrier permeability. To this end, the permeability of the intestinal barrier to orally administered FITC dextran was quantified by fluorescence in WT mice kept on C1000 or HSD. Fluorescence levels of FITC in the serum were similar in both C1000 and HSD-fed mice (**Fig.3.10. a**), indicating that intestinal barrier integrity was not altered.

To affirm this finding, fecal albumin levels in WT and OSE mice kept on C1000 or HSD were measured by ELISA. As alterations in the intestinal barrier integrity lead to a differential release of albumin to the interstitial space and subsequently to feces, this is also used as a measure of barrier permeability. Interestingly, fecal albumin levels quantified in both WT and OSE mice showed no difference (**Fig.3.10. b**). The next focus was on intestinal IgA - the production of which is influenced by the microbial species colonizing the gut. Altered IgA levels can influence immune homeostasis as well as contribute to neuroinflammation [268,

308]. To ascertain this, fecal IgA levels in WT and OSE mice kept on C1000 or HSD were quantified by ELISA and found to be similar under both diets (**Fig.3.10. c**).

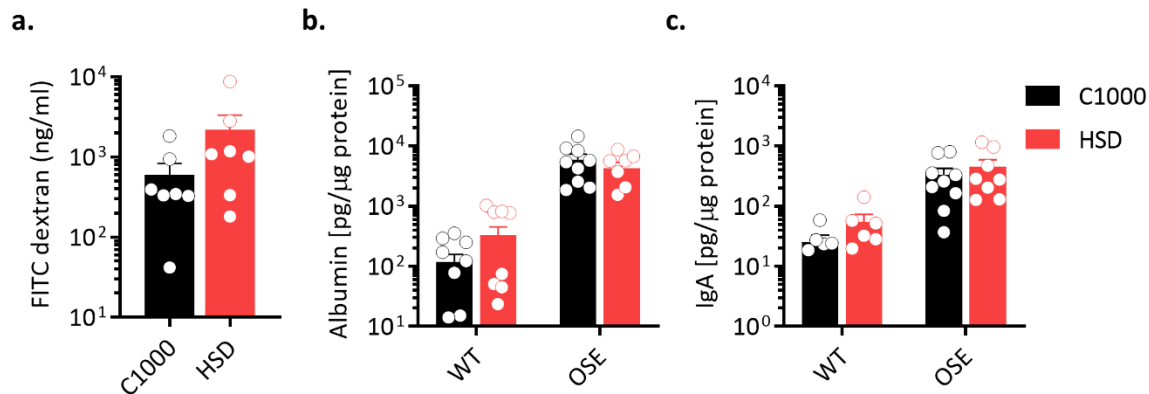
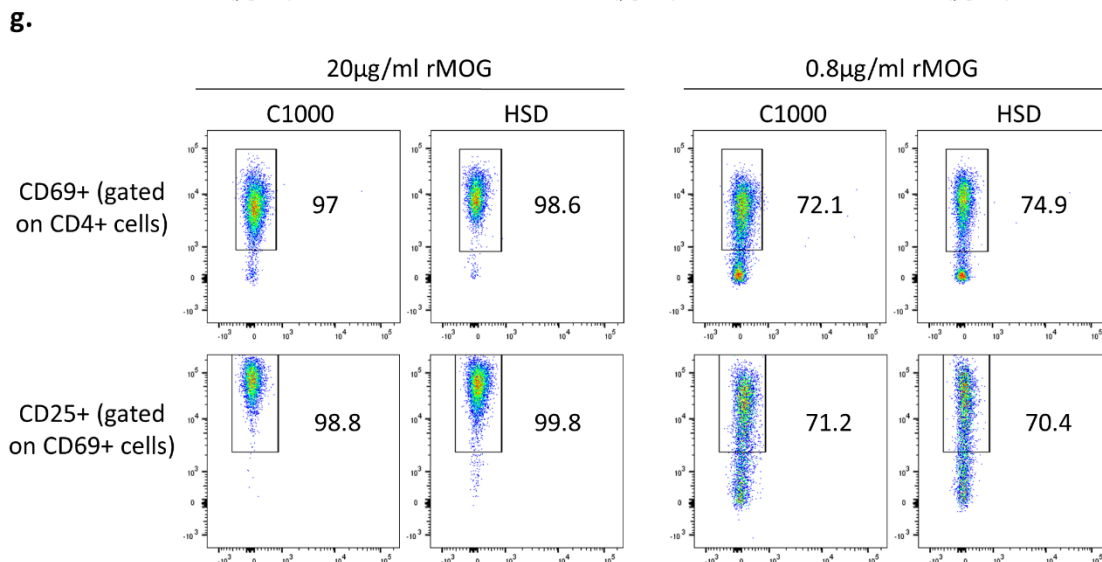
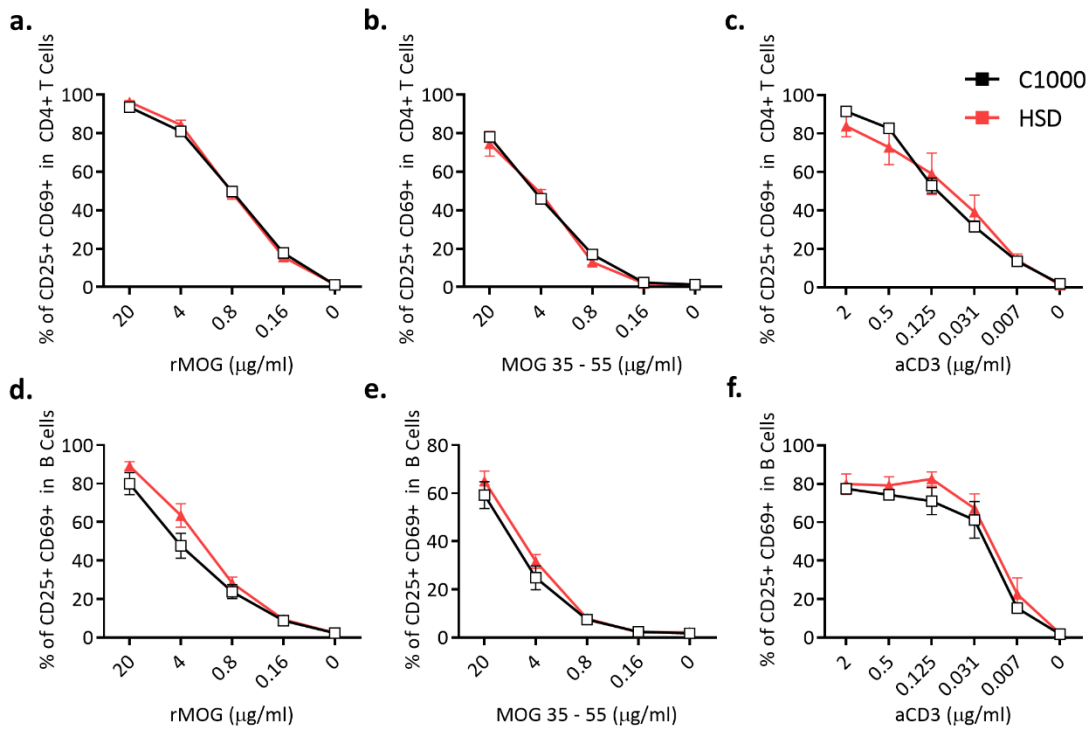


Figure 3.10. HSD does not affect gut barrier integrity. **a.** FITC-Dextran levels in the sera of WT mice fed C1000 and HSD. WT mice (C1000 n=7, HSD n=7) were weaned onto C1000, or HSD and Sera were collected 3-4 weeks after diet switch. Each circle represents an individual mouse. **b.** Fecal albumin levels in WT and OSE mice fed C1000 and HSD, quantified by ELISA and normalized to total protein levels. WT (C1000 n=8, HSD n=8) and OSE (C1000 n=9, HSD n=7) mice were weaned onto C1000 or HSD, and Feces were collected 3-4 weeks after diet switch. Each circle represents an individual mouse. **c.** Fecal IgA levels in WT and OSE mice fed C1000 and HSD, quantified by ELISA and normalized to total protein levels. WT (C1000 n=5, HSD n=6) and OSE (C1000 n=9, HSD n=7) mice were weaned onto C1000 or HSD, and Feces were collected 3-4 weeks after diet switch. Each circle represents an individual mouse. All data represented as mean \pm s.e.m.

In summary, HSD altered the microbiome with an increase in the abundance of *Enterococci* in the gut without any accompanying change in intestinal barrier integrity or IgA levels. But to mediate protection from EAE, NaCl - either directly or through microbial/metabolic alterations, would have to act by affecting one or more factors involved in EAE - immune cells, BBB, or CNS resident cells. The subsequent focus was thus on characterizing alterations in these factors, beginning with the primary players – immune cells.

3.7. HSD DOES NOT ALTER IMMUNE CELL FUNCTIONS

In the OSE model, CD4+ T cells and B cells are the key immune cells involved in the disease process. Antigen recognition and presentation by the B cells are crucial for the activation and expansion of MOG-specific T cells. The proliferation of MOG-specific T and B cells is hence a key process that can potentially affect disease outcomes. To this end, activation and proliferation of T and B cells were studied. eFlour450 labeled cells from the spleen of C1000 and HSD-fed OSE mice were cultured with different concentrations of MOG 35-55, recombinant MOG or anti-CD3, and FACS analysis was done after 60 h to assess activation and proliferation. First, the frequencies of CD4+ T cells and B cells expressing the activation markers CD69 and CD25 were measured. The proportions of CD69+ CD25+ cells from both C1000 and HSD-fed mice were comparable under all antigenic stimuli (**Fig.3.11. a-g**).



Frequency calculation (a-f): % of CD69+ cells (top row) * % of CD25+ cells in CD69+ cells (bottom row)

Figure 3.11. HSD does not impact the expression of activation markers in CD4+ T cells and B cells. a-c. Frequencies of CD25+ CD69+ T cells on treatment with recombinant MOG (a), MOG 35-55 (b) and anti-CD3 (c). **d-f.** Frequencies of CD25+ CD69+ B cells on treatment with recombinant MOG (d), MOG 35-55 (e) and anti-CD3 (f). **a-f.** One representative experiment out of 3 experiments performed is shown (C1000 n=2, HSD n=3). **g.** Representative plots of CD69 (top) and CD25 (bottom) staining with recombinant MOG stimulus. All data represented as mean \pm s.e.m.

Next, proliferation was assessed by quantifying the fluorescence intensity of eFlour450 (which decreases with increased cell proliferation). The proliferation of both CD4+ T cells and B cells from mice fed C1000 or HSD did not differ, irrespective of the antigenic stimulus (Fig.3.12. a-g). These results indicated that the antigen presenting capability of the B cells, which is essential for T cell activation, is not diminished under HSD. The activation of T and B cells

under antigenic stimulus is also unaffected under HSD. Further, T cells and B cells proliferate equally well under both C1000 and HSD.

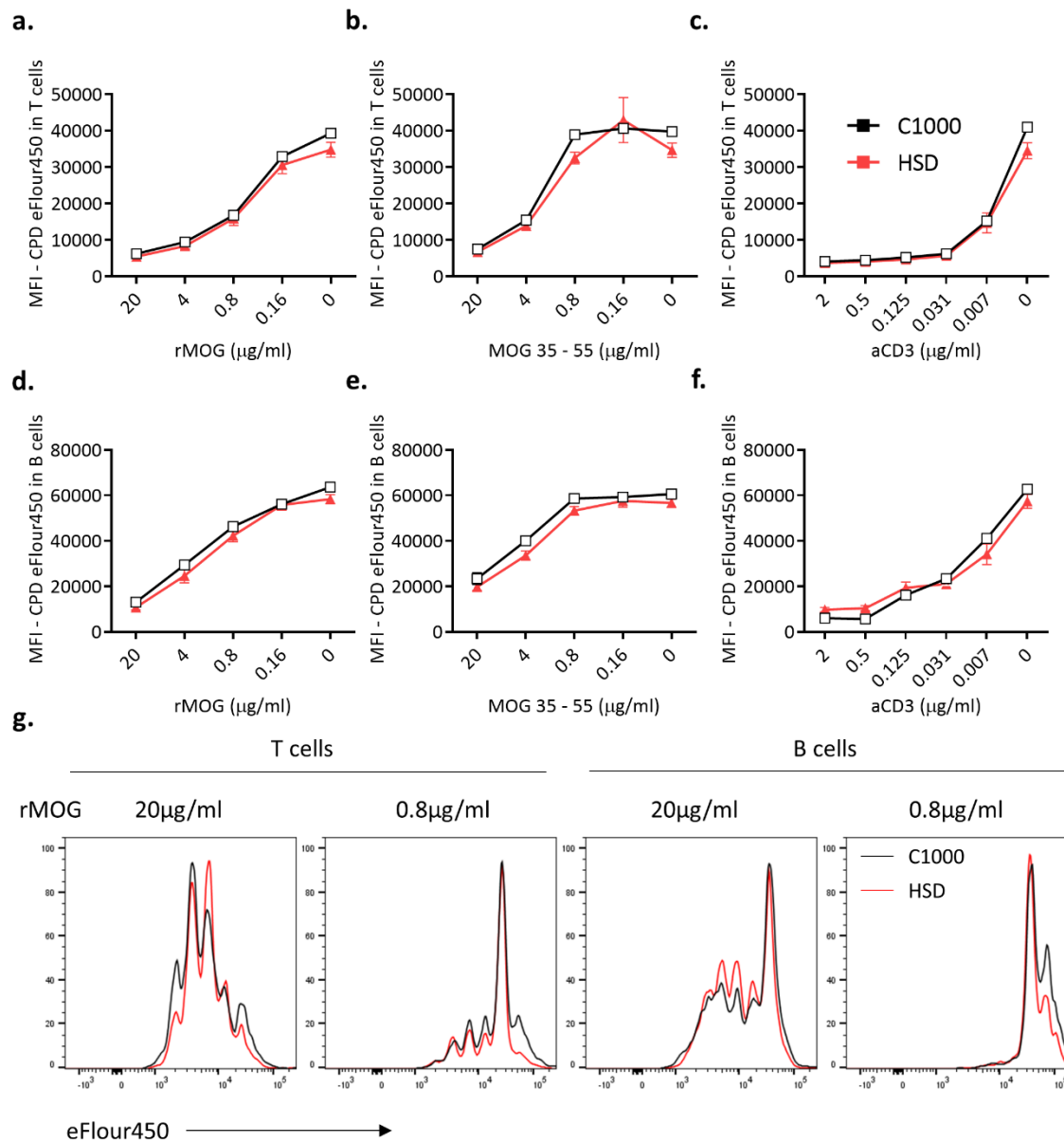


Figure 3.12. HSD has no impact on CD4+ T cell and B cell proliferation. eFluor450 labelled Splenocytes were cultured in vitro with antigenic stimulus. **a-c.** Mean fluorescence intensity of Cell proliferation dye (CPD) eFluor450 in T cells in the presence of recombinant MOG (**a**), MOG 35-55 (**b**), and anti-CD3 (**c**). **d-f.** Mean fluorescence intensity of Cell proliferation dye (CPD) eFluor450 in B cells in the presence of recombinant MOG (**d**), MOG 35-55 (**e**), and anti-CD3 (**f**). **a-f.** One representative experiment out of 3 experiments performed is shown (C1000 n=2, HSD n=3). **g.** Representative plots of proliferation with recombinant MOG stimulus. All data represented as mean \pm s.e.m.

Despite activation or frequencies of proliferating cells not showing differences, it was necessary to assess their cytokine production to determine potential functional differences. The key cytokines that contribute to a pro-inflammatory phenotype in EAE are IFN γ and IL-17. On the other hand, IL-10 is known to contribute to a regulatory phenotype. The levels of

all of the 3 cytokines upon immune cell activation were thus quantified. To this end, splenocytes from OSE mice fed C1000 and HSD were cultured with recombinant MOG or anti-CD3, and the IFN γ and IL10 levels after 60 h of culture were quantified by ELISA and found to be comparable (**Fig.3.13. a, b**). IL-17 was not detectable under recombinant MOG stimulus but was quantified under the anti-CD3 stimulus and there was no difference in its levels either (**Fig.3.13. c**). Thus, cytokine production by activated T and B cells is also not altered under HSD irrespective of the antigenic stimulus.

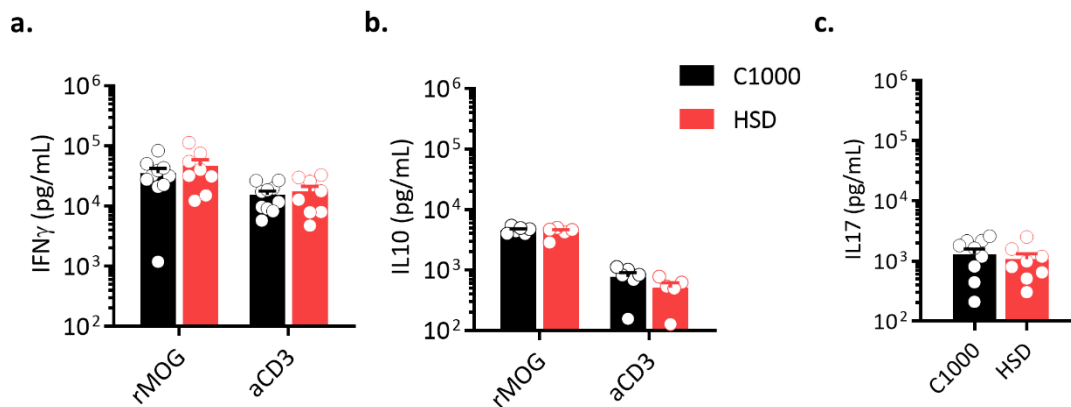


Figure 3.13. Cytokine levels in splenocytes under antigenic stimulus are unaltered. **a.** Levels of IFN γ on treatment with recombinant MOG or anti-CD3 (C1000 n=10, HSD n=8). Each circle represents an individual mouse. **b.** Levels of IL10 on treatment with recombinant MOG or anti-CD3 (C1000 n=5, HSD n=6). Each circle represents an individual mouse. **c.** Levels of IL-17 on treatment with anti-CD3 (C1000 n=10, HSD n=8). Each circle represents an individual mouse.

3.8. HSD ALTERS T CELL SUBSETS IN THE GUT

Another factor influencing EAE is the proportion of various immune cells, notably T cell subsets in the gut and periphery. Indeed, dietary changes have been shown to alter the proportions of various immune cell subsets in the GALT. Specifically, several studies have associated HSD with an increase in IL-17+ CD4+ T cell levels in the small intestine [291-293]. Consequently, the frequencies of CD4+ T cells, B cells, neutrophils, and monocytes were first quantified in the spleen, small intestinal lamina propria (SILP), and colonic lamina propria (CLP) of WT mice 3-4 weeks after switch to C1000 or HSD. FACS analysis showed no difference in the frequencies of any of these populations (**Fig.3.14. a-d**).

Further analyses were done to characterize coreceptors involved in the regulation of T and B cell function. One such protein is Ceacam1, which is known to be important for B cell survival and proliferation in addition to mediating B cell aggregation in the CNS during EAE [309, 310]. Also, the co-inhibitory receptor PD1 is known to regulate effector T cell function during autoimmunity [311]. Differences in the Ceacam1+ B cells and PD1+ CD4+ T cell populations could hence be functionally relevant to protection from EAE under HSD. Thus, the frequencies of Ceacam1+ B cells and PD1+ T cells were analyzed by FACS, but found to be unaltered under HSD (**Fig.3.14. e, f**).

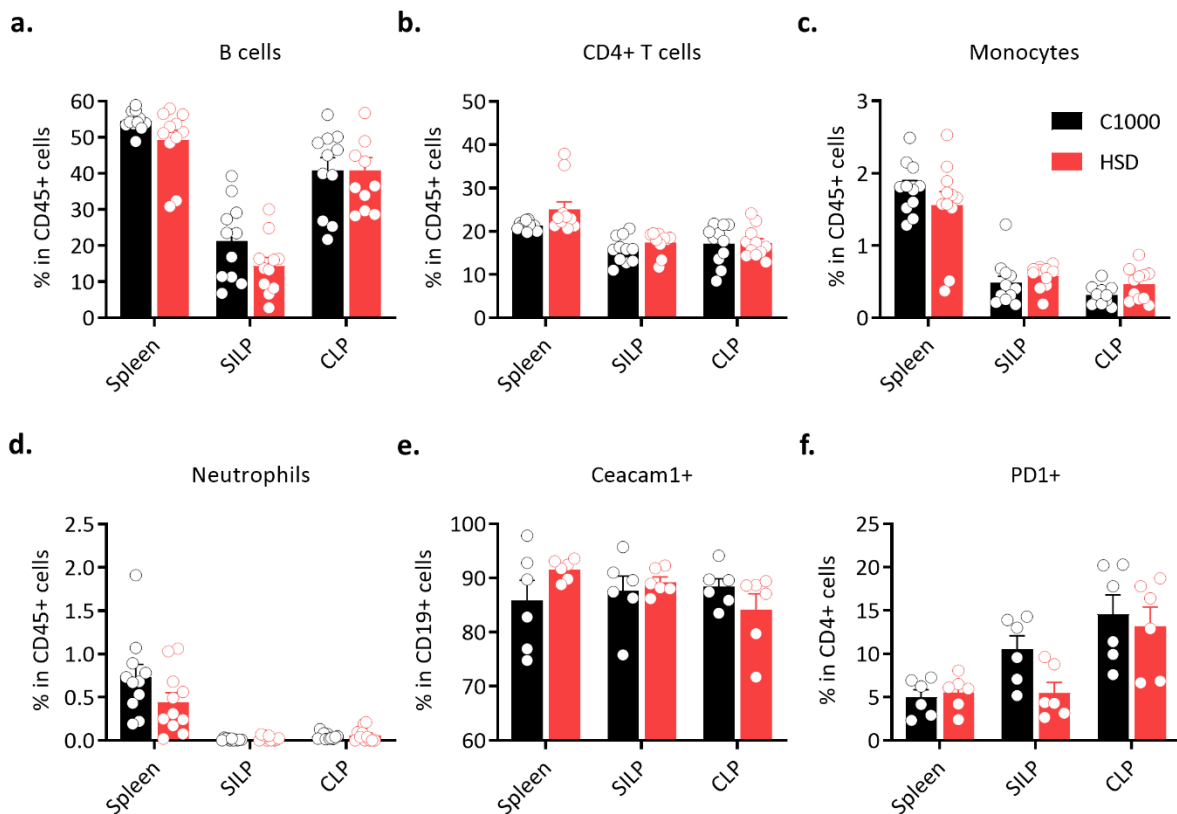


Figure 3.14. HSD does not alter overall immune cell frequencies in WT mice. a-d. Frequencies of B cells (a), CD4+ T cells (b) Monocytes (CD11b+ Ly6C+) (c) and Neutrophils (CD11b+ Ly6G+) (d) in the spleen, Small intestine lamina propria (SILP) and Colon lamina propria (CLP) of WT mice 3-4 weeks after diet switch (C1000 n=11, HSD n=11). Data from 3 separate experiments are pooled. Each circle represents an individual mouse. **e.** Frequencies of Ceacam1+ B cells in the spleen, SILP, and CLP of WT mice 3-4 weeks after diet switch (C1000 n=6, HSD n=6). Each circle represents an individual mouse. **f.** Frequencies of PD1+ CD4+ T cells in the spleen, SILP, and CLP of WT mice 3-4 weeks after diet switch (C1000 n=6, HSD n=6). Each circle represents an individual mouse. All data represented as mean \pm s.e.m.

CD4+ T cell subpopulations in the spleen, SILP, and CLP were next characterized, with a specific focus on the key effector cell subsets - IL-17+ and IFN γ + cells, and the regulatory subset - FoxP3+ cells. Consistent with prior reports, FACS analysis showed that HSD-fed mice had increased frequencies of IL-17+ T_H17 cells in the SILP (**Fig.3.15. a**), with no difference observed in the spleen and CLP. The frequencies of IFN γ + T_H1 cells and IL-17+ IFN γ + T cells were not significantly different (**Fig.3.15. b, c**). In addition, FoxP3+ T_{reg} cell frequencies were found to be increased in the CLP under HSD, and unaltered in the spleen and SILP (**Fig.3.15. d**).

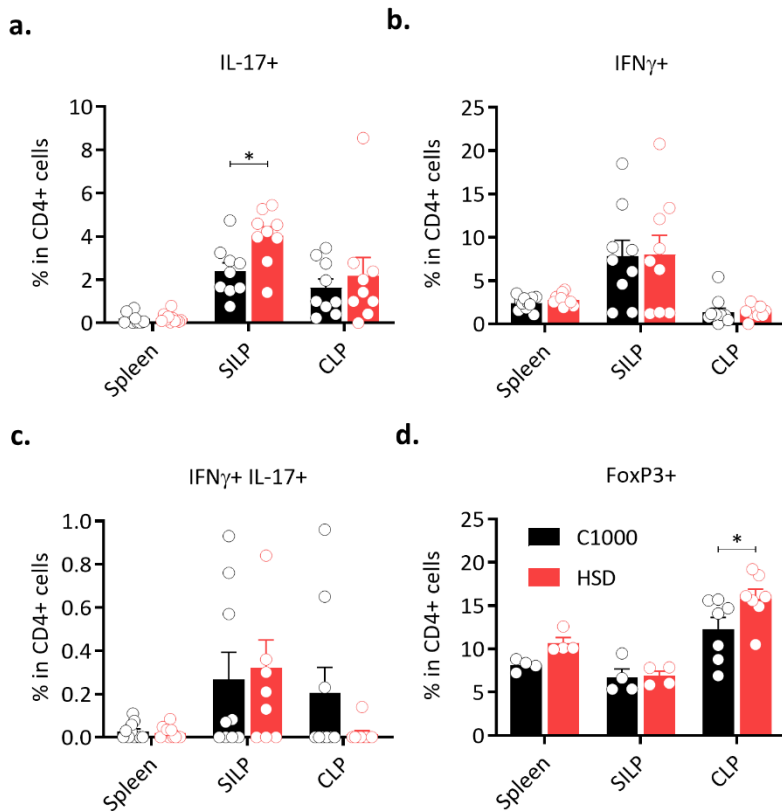


Figure 3.15. HSD alters CD4+ T cell subset frequencies in WT mice. a-c. Frequencies of IL-17+ (T_H17) (a), IFN γ + (T_H1) (b) and IFN γ + IL-17+ T cells (c) in the spleen, SILP and CLP of WT mice 3-4 weeks after diet switch (C1000 n=9, HSD n=9). *P = 0.0315 (Mann Whitney's U test). Data from 3 separate experiments are pooled. Each circle represents an individual mouse. **d.** Frequencies of FoxP3+ (T_{reg}) cells in the spleen, SILP, and CLP of WT mice 3-4 weeks after diet switch (C1000 n=4-7, HSD n=4-7). *P = 0.0291 (Mann Whitney's U test). Each circle represents an individual mouse. All data represented as mean \pm s.e.m.

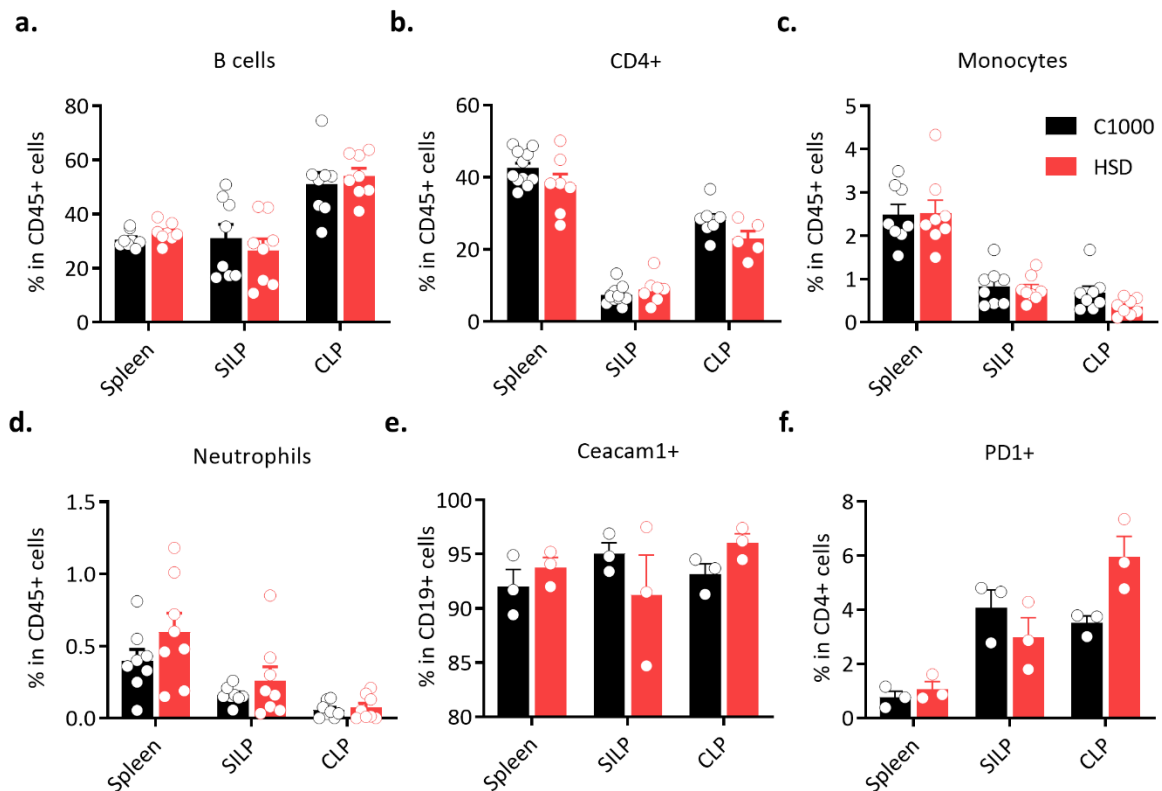


Figure 3.16. HSD does not alter overall immune cell frequencies in OSE mice. a-d. Frequencies of B cells (a), CD4+ T cells (b) Monocytes (c) and Neutrophils (d) in the spleen, Small intestine lamina propria (SILP), and Colon lamina propria (CLP) of OSE mice 3-4 weeks after diet switch (C1000 n=11, HSD n=11). Data from 2 separate experiments are pooled. Each circle represents an individual mouse. **e.** Frequencies of Ceacam1+ B cells in the spleen, SILP, and CLP of OSE mice 3-4 weeks after diet switch (C1000 n=3, HSD

n=3). Each circle represents an individual mouse. **f.** Frequencies of PD1+ CD4+ T cells in the spleen, SILP, and CLP of WT mice 3-4 weeks after diet switch (C1000 n=3, HSD n=3). Each circle represents an individual mouse. All data represented as mean \pm s.e.m.

It was next essential to validate these observations in OSE mice. First, the overall frequencies of CD4+ T cells, B cells, neutrophils, and monocytes in the spleen, SILP, and CLP in OSE mice were quantified 3-4 weeks after switch to C1000 or HSD. FACS analysis showed that frequencies of all these populations were comparable under both diets (**Fig.3.16. a-d**). Further analyses to quantify frequencies of Ceacam1+ B cells and PD1+ T cells showed that both populations were unaltered under HSD (**Fig.3.16. e, f**).

Subsequently, the frequencies of CD4+ T cell subsets in the spleen, SILP, and CLP were analyzed 3-4 weeks after the diet switch. FACS analysis showed that similar to the observation in WT mice, HSD-fed OSE mice had increased frequencies of IL-17+ cells in the SILP, with marginal difference in the spleen and no difference observed in the CLP (**Fig.3.17. a**). The levels of IFN γ + cells and IL-17+ IFN γ + T cells were not altered (**Fig.3.17. b, c, e**). However, unlike in WT mice, FoxP3+ cell levels in the CLP were not altered in OSE mice (**Fig.3.17. e, f**). It was also observed that OSE mice had an overall higher frequency of IL-17+ cells in the SILP (8-15%) in comparison to WT mice (2-6%).

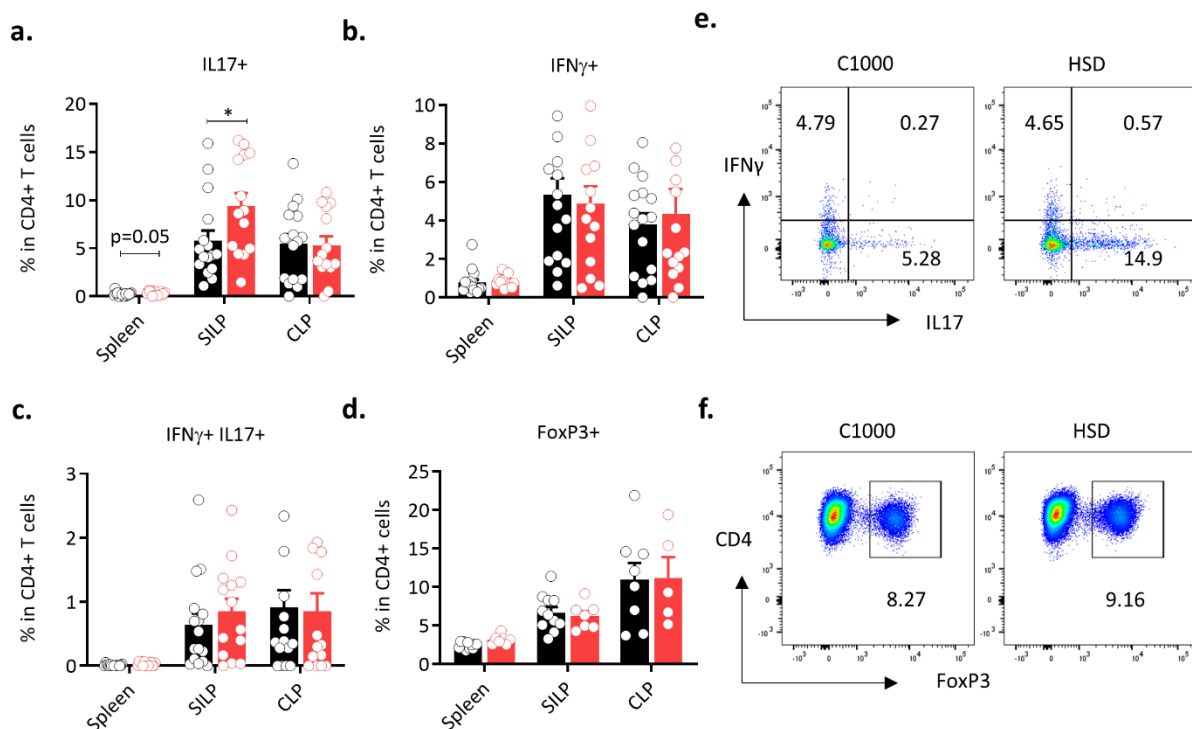


Figure 3.17. HSD alters CD4+ T cell subset frequencies in OSE mice. a-c. Frequencies of IL-17+ (T_H17) (a), IFN γ + (T_H1) (b) and IFN γ + IL-17+ T cells (c) in the spleen, SILP and CLP of OSE mice 3-4 weeks after diet switch (C1000 n=16, HSD n=14). *P = 0.0275 (Mann Whitney's U test). Data from 3 separate experiments are pooled. Each circle represents an individual mouse. **d.** Frequencies of FoxP3+ (T_{reg}) cells in the spleen, SILP, and CLP of OSE mice 3-4 weeks after diet switch (C1000 n=7-11, HSD n=5-7). Each circle represents an individual mouse for spleen and SILP, and a pool of 2 mice for the CLP. All data represented as mean \pm

s.e.m. **e.** Representative FACS plots of cytokine staining, gated on CD4+ cells. **f.** Representative FACS plots of FoxP3 staining, gated on CD4+ cells.

Taken together, while no difference was observed in overall immune cell frequencies, FoxP3+ T cell frequencies under HSD were higher in WT mice, and IL-17+ T cells were increased in frequencies under HSD in both WT and OSE mice. Therefore, the next step was to identify if the observed increase in T_H17 and T_{reg} cell frequencies was a direct effect of NaCl or an indirect effect through NaCl-modified metabolites.

This was explored through in vitro differentiation of CD4+ T cells to T_H17 and T_{reg} cells. The addition of NaCl during differentiation of CD4+ T cells to T_H17 cells (as described in methods) showed that T_H17 cell levels were significantly increased due to NaCl, as evidenced by the higher frequency of IL-17+ cells observed through FACS analysis, and the increased production of IL-17 quantified by ELISA (**Fig.3.18. a, b**). On the other hand, T_{reg} cells differentiation was not affected by NaCl (**Fig.3.18. c**). Subsequently, the differentiation of CD4+ T cells to T_H17 and T_{reg} cells was performed in the presence of caecal extracts (in methanol) from C1000 and HSD-fed mice to identify if an indirect effect of HSD via metabolites could contribute to altered T cell differentiation. Neither T_H17 nor T_{reg} cell differentiation was affected by treatment with caecal methanol extracts from HSD-fed mice (**Fig.3.18. e, f**).

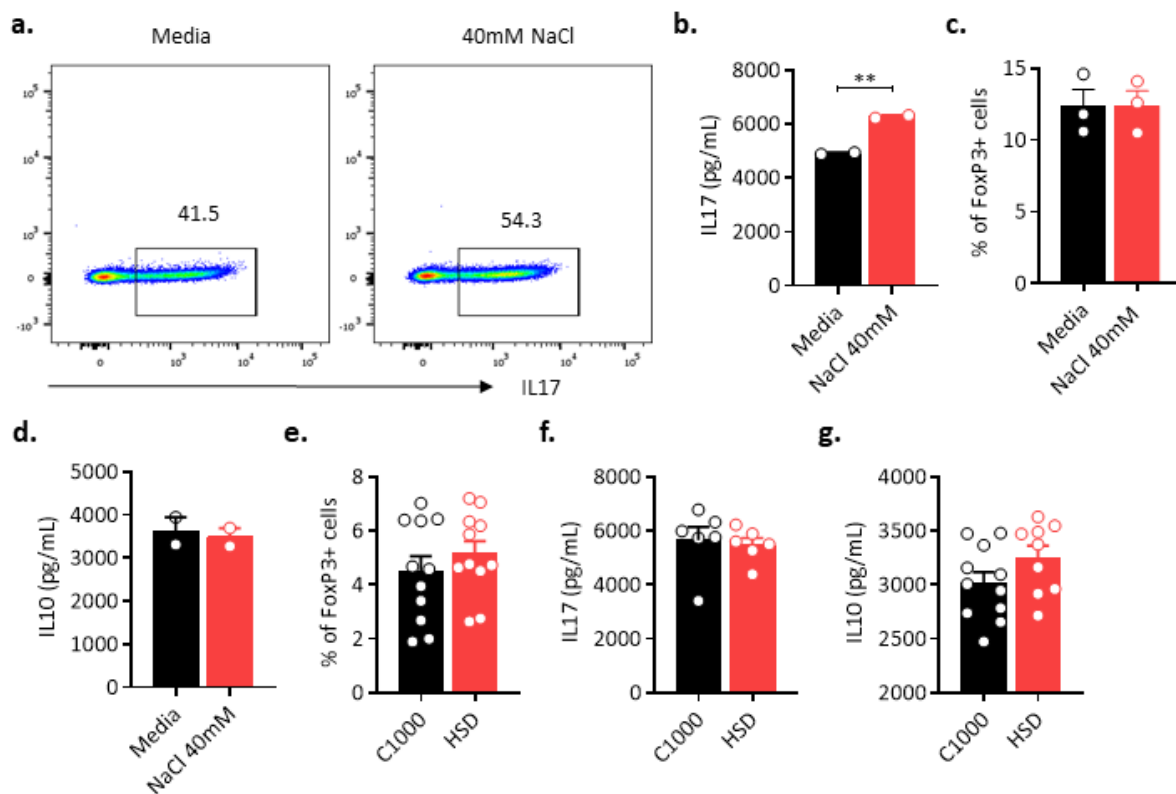


Figure 3.18. NaCl affects T cell differentiation in vitro. **a-g.** Naïve CD4+ T cells were cultured in vitro with anti-CD3 and anti-CD28, with or without cytokine stimulus to induce differentiation of specific T cell subsets. **a.** Production of IL-17 by Naïve T cells stimulated with TGFβ + IL-6 to induce T_H17 cell differentiation, with and without treatment with 40mM NaCl. One representative assay out of 3 is shown. **P = 0.0019 (Unpaired t test, two tailed). **b.** Representative FACS plots of IL-17+ cell frequencies when

Naïve T cells were stimulated with TGF β + IL-6 to induce T_H17 cell differentiation, with and without treatment with 40mM NaCl. Plots from one representative experiment out of 3 are shown. **c.** Frequencies of FoxP3+ (T_{reg}) cells with and without treatment with 40mM NaCl. Naïve T cells were stimulated with TGF β to induce T_{reg} cell differentiation. One representative assay out of 3 is shown. **d.** Production of IL10 by T cells, with and without treatment with 40mM NaCl. **e.** Frequencies of FoxP3+ (T_{reg}) cells on treatment with caecal extracts from C1000 and HSD-fed mice. Naïve T cells were stimulated with TGF β to induce T_{reg} cell differentiation. Each circle represents an individual mouse. **f.** Production of IL-17 by Naïve T cells stimulated with TGF β + IL-6 to induce T_H17 cell differentiation, on treatment with caecal extracts from C1000 and HSD-fed mice. Each circle represents an individual mouse. **g.** Production of IL10 by T cells, on treatment with caecal extracts from C1000 and HSD-fed mice. Each circle represents an individual mouse. All data represented as mean \pm s.e.m.

Various T cell subsets including T_H17 and T_{reg} cells have been shown to produce the anti-inflammatory cytokine IL-10 which regulates neuroinflammation [312]. Hence, we measured through ELISA, the production of IL-10 by CD4+ T cells stimulated with anti-CD3 and anti-CD28 in the presence of salt or salt-modified metabolites. Neither the addition of NaCl nor treatment with caecal extracts from HSD-fed mice resulted in increased IL-10 production by CD4+ T cells (**Fig.3.18. d, g**).

Having ascertained the effect of NaCl and HSD-derived metabolites on T cells, it was also essential to assess the likelihood of the previously observed microbial alterations – notably the increase in *Enterococci sp.*, contributing to the changes in T_H17 and T_{reg} cells under HSD. It has been well established that the commensal microbiota plays a vital role in the development and function of T_H17 and T_{reg} cells in the gut, and changes in the microbiota can potentially contribute to alterations in T_H17 and T_{reg} cell frequencies or functions.

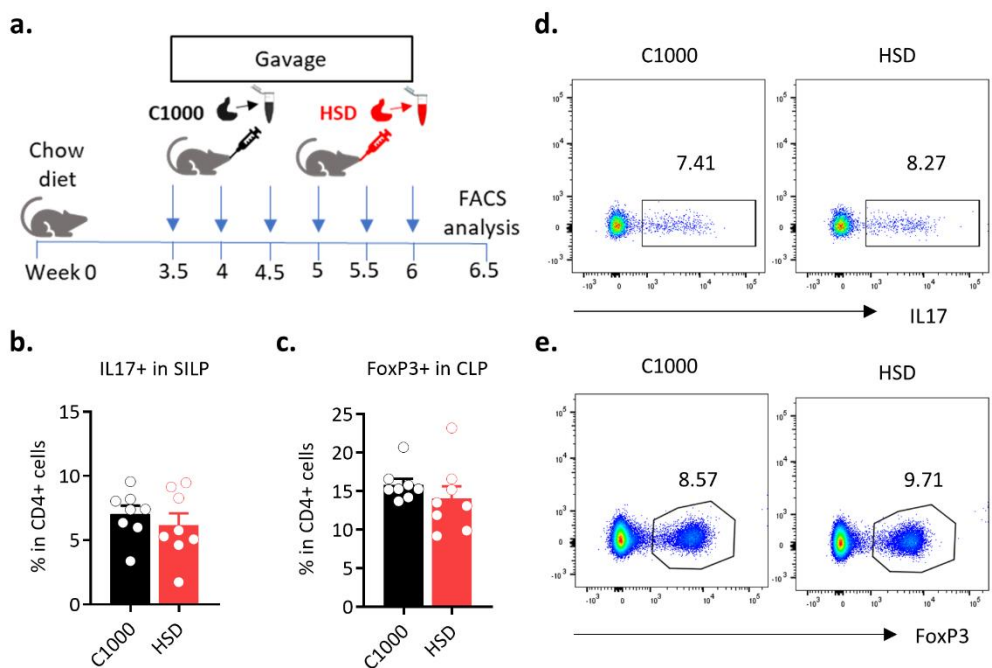


Figure 3.19. Caecal content from HSD-fed mice do not alter CD4+ T cell subset frequencies. a. Experimental plan for caecal content gavage to WT mice. **b.** Frequencies of IL-17+ T cells in the Small intestine lamina propria (SILP) of chow fed WT mice receiving caecal contents from C1000 (n=8) or HSD

(n=8) fed mice. One representative experiment out of 3 experiments performed is shown. Each circle represents an individual mouse. **c.** Frequencies of FoxP3+ (T_{reg}) cells in the Colon lamina propria (CLP) of chow fed WT mice receiving caecal contents from C1000 (n=8) or HSD (n=8) fed mice. One representative experiment out of 3 experiments performed is shown. Each circle represents an individual mouse. **d.** Representative FACS plots of IL-17 staining, gated on CD4+ cells. **e.** Representative FACS plots of FoxP3 staining, gated on CD4+ cells. All data represented as mean \pm s.e.m.

To validate this, caecal contents from C1000 and HSD-fed mice were gavaged to WT mice fed a regular chow diet. Frequencies of T_H17 cells in the SILP and T_{reg} cells in the CLP were analyzed by FACS and interestingly, no difference was observed (**Fig.3.19. a-e**). This indicated that the microbial alterations do not contribute to the increase in the T cell subsets observed under HSD. Summarily, while T_H17 cell differentiation is enhanced as a direct effect of NaCl, T_{reg} cell differentiation is unaffected. Also, HSD-modified metabolites and microbiota may not contribute to alterations in T_H17 or T_{reg} cell differentiation.

Moving on, the T cell compartment was explored further to characterize potential immune regulatory phenotype which would be in line with the observed protection from EAE. We specifically focused on the SILP T_{reg} compartment, as the SILP T_{reg} cells are known to express CD103 and ROR γ T, both of which have been shown to enhance T_{reg} cell mediated suppression of effector cell response [313]. Interestingly, FACS analysis of T_{reg} cells in C1000 and HSD-fed OSE mice showed higher levels of CD103+ ROR γ T+ T_{reg} cells in the SILP without any difference in the spleen (**Fig.3.20. a, e**). Additional markers that are known to affect T_{reg} cell expansion and functionality, like KLRG1, Ki67, and Helios were also analyzed in the SILP and spleen and showed no difference (**Fig.3.20. b-d**).

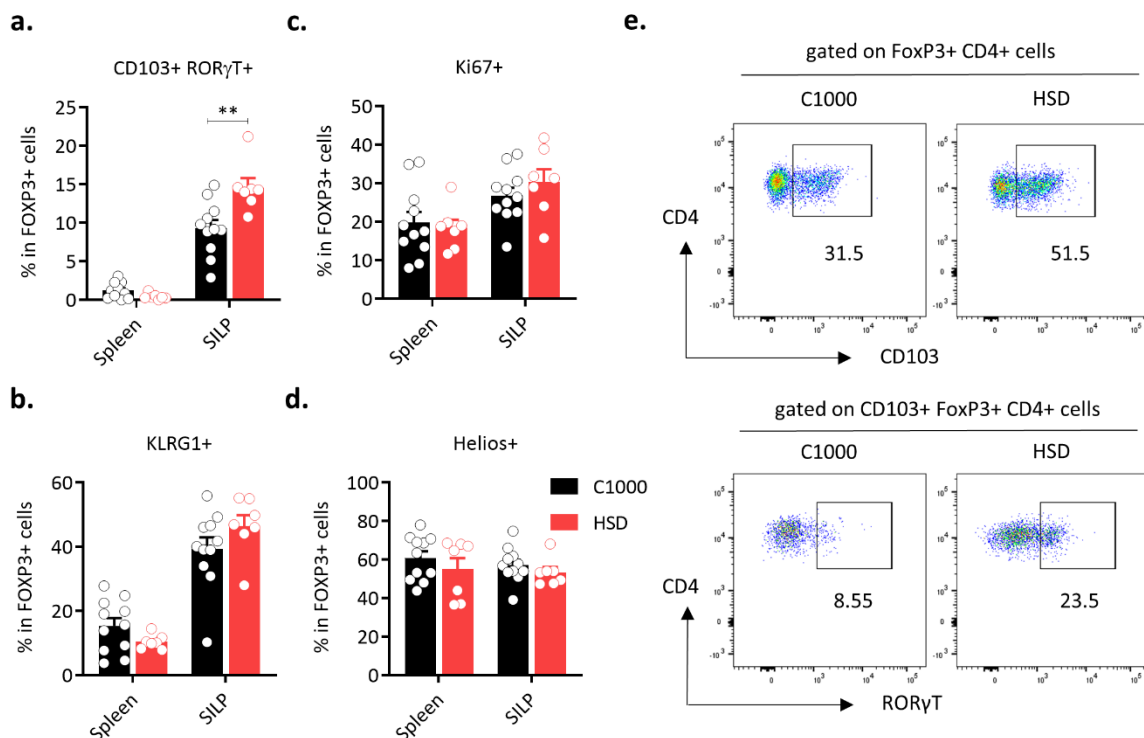


Figure 3.20. T_{reg} cell subsets are altered in HSD-fed OSE mice. **a.** Frequencies of CD103+ ROR γ T+ T_{reg} cells in the Spleen and Small intestine lamina propria (SILP) of OSE mice 3-4 weeks after diet switch (C1000 n=11,

HSD n=7). **P = 0.0059 (Mann Whitney's U test). Data from 2 separate experiments are pooled. Each circle represents an individual mouse. **b-d**. Frequencies of KLRG1+ (**b**), Ki67+ (**c**), and Helios+ (**d**) T_{reg} cells in the Spleen and SILP of OSE mice 3-4 weeks after diet switch (C1000 n=11, HSD n=7). Data from 2 separate experiments are pooled. Each circle represents an individual mouse. **e**. Representative FACS plot of CD103 gated on CD4+ FoxP3+ cells (top), and RORγT staining gated on CD103+ FoxP3+ CD4+ cells (bottom) respectively. All data represented as mean ± s.e.m.

Since alterations in the T_{reg} compartment indicated a potentially enhanced regulatory phenotype, our further investigation was on IL-10 production by T_{reg} cells, which is crucial for T_{reg} mediated regulation of effector T cell responses [54]. Since the overall T_{reg} cell frequencies were observed to be much higher in WT mice than in OSE mice (**Fig.3.15. d** and **Fig 3.17. d**), T_{reg} cells from the cervical lymph nodes (cLN) and SILP of C1000 and HSD-fed WT mice were sorted and cultured with anti-CD3 and anti-CD28. The production of IL-10 was quantified by ELISA after 60 h and found to be significantly increased in T_{reg} cells from cLN of mice fed HSD, but not in the SILP (**Fig.3.21**).

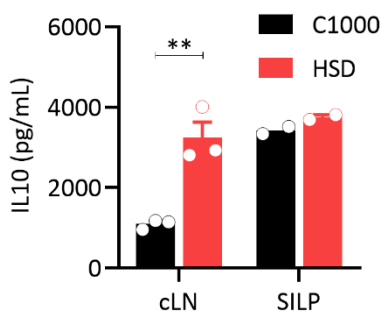


Figure 3.21. HSD enhances IL-10 production by peripheral T_{reg} cells. IL-10 levels in T_{reg} cells isolated from WT mice 3-4 weeks after diet switch and cultured in the presence of anti-CD3 and anti-CD28. CD4+ CD25+ cells were sorted from cervical lymph nodes (cLN) or small intestine lamina propria (SILP) of C1000 and HSD-fed mice. Each circle represents a pool of 2 mice (C1000 n=2-3, HSD n= 2-3). One representative experiment out of 2 experiments performed is shown.

In summary, HSD causes alterations in the T_{reg} compartment, resulting in increased frequencies of CD103+ RORγT+ T_{reg} cells in the gut and enhanced IL-10 production by peripheral T_{regs}. Resultantly, we wanted to ascertain if these alterations had any functional relevance in HSD-mediated protection from EAE. This was achieved through depletion and neutralization experiments.

3.9. T_{REG} CELL DEPLETION HAS NO EFFECT ON DISEASE SUSCEPTIBILITY

First, T_{reg} cells were depleted in HSD-fed OSE mice using an anti-CD25 antibody and the disease incidence was monitored. This depletion did not increase disease incidence (**Fig.3.22. a-c**). Subsequently, HSD-fed OSE mice were treated with anti-IL-10 antibodies to neutralize IL-10, to assess whether the enhanced IL-10 levels under HSD impacts disease protection. This treatment also failed to reverse protection from EAE (**Fig.3.22. a, d**). This indicated that these alterations in the T_{reg} compartment do not play a significant role in HSD-mediated disease protection.

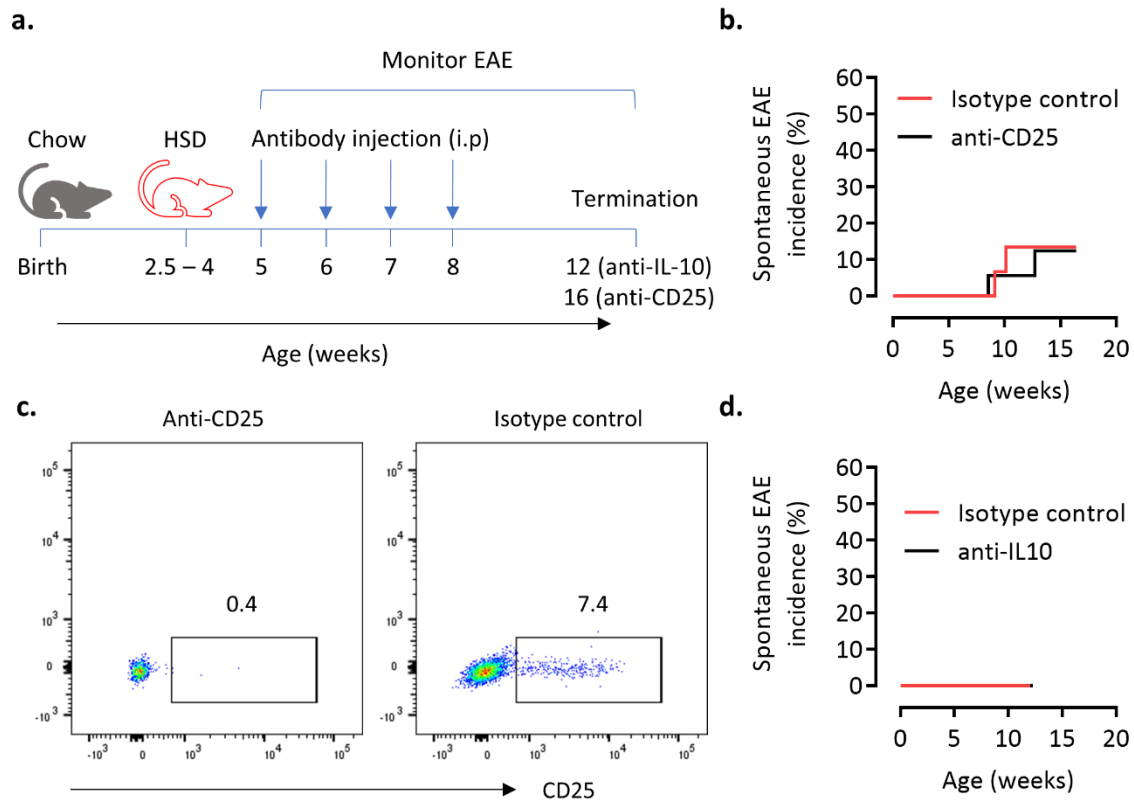


Figure 3.22. T_{reg} cell depletion in OSE mice does not reverse protection from EAE. **a.** Experimental plan of anti-CD25 and anti-IL-10 treatment in HSD-fed OSE mice. The experiment was terminated at 12 weeks for anti-IL-10 treatment and 16 weeks for anti-CD25 treatment. **b.** Incidence of spontaneous EAE in HSD-fed OSE mice after anti-CD25 treatment (Isotype control n=16, anti-CD25 n=18). **c.** Representative FACS plots showing depletion of CD25+ cells in vivo after treatment with anti-CD25 antibody. **d.** Incidence of spontaneous EAE in HSD-fed OSE mice after anti-IL-10 treatment (Isotype control n=7, anti-IL-10 n=9).

3.10. B CELL FUNCTIONALITY IS UNALTERED UNDER HSD

Consequent to ascertaining that alterations in the T cells do not contribute to disease protection, our focus was on characterizing the B cell compartment. Initially, the frequencies of GL7+ B cells and PD-L1+ B cells were analyzed. GL7 is a B cell activation and germinal center marker, and PD-L1 is a marker for regulatory B cells whose expression on B cells has been shown to enhance the ability of B cells to regulate autoimmunity [314]. Frequencies of both GL7+ and PD-L1+ B cells, analyzed in the spleen, cervical and mesenteric lymph nodes (cLN and mLN) of OSE mice by FACS were found to be similar under C1000 and HSD (**Fig.3.23. a, b**).

We subsequently quantified the titers of both total and MOG-specific antibodies in the sera, as autoantibodies are also key factors in the progression of EAE [315]. To this end, firstly the serum titers of total IgG and IgE in C1000 and HSD-fed mice were measured and found to be comparable (**Fig.3.23. d, e**). Subsequently, the autoantibody production was measured. OSE mice have been shown to have high serum titers of anti-MOG antibodies [34] the relative levels of which could be quantified by ELISA. To this end, a direct comparison of OD at 450nm of MOG-specific IgG1 (IgG1^a), IgG2 (IgG2^a), and IgM (IgM^a) in the serum was done and this

showed that the serum autoantibody titers are unaltered under HSD (**Fig.3.23. f**). Coupled with the earlier observation that proliferation of B cells and their antigen presenting capability is not diminished, this thus indicates an unaltered B cell functionality due to HSD.

Consequently, it was also necessary to validate this in vivo. We hypothesized that if altered B cell functionality due to HSD can potentially contribute to protection from EAE, then the introduction of Th B cells previously unexposed to HSD, into OSE mice fed HSD, would restore functional B cells in the mice and thus reverse disease protection. Hence, Th iGB cells taken from chow fed mice and expanded in vitro were injected i.p. to HSD-fed OSE mice. Mice were monitored for EAE for 4 weeks after cell transfer. It was observed that the injection of Th iGB cells did not reverse disease protection due to HSD (**Fig.3.23. c**). This further validated that B cell functionality is unaltered under HSD.

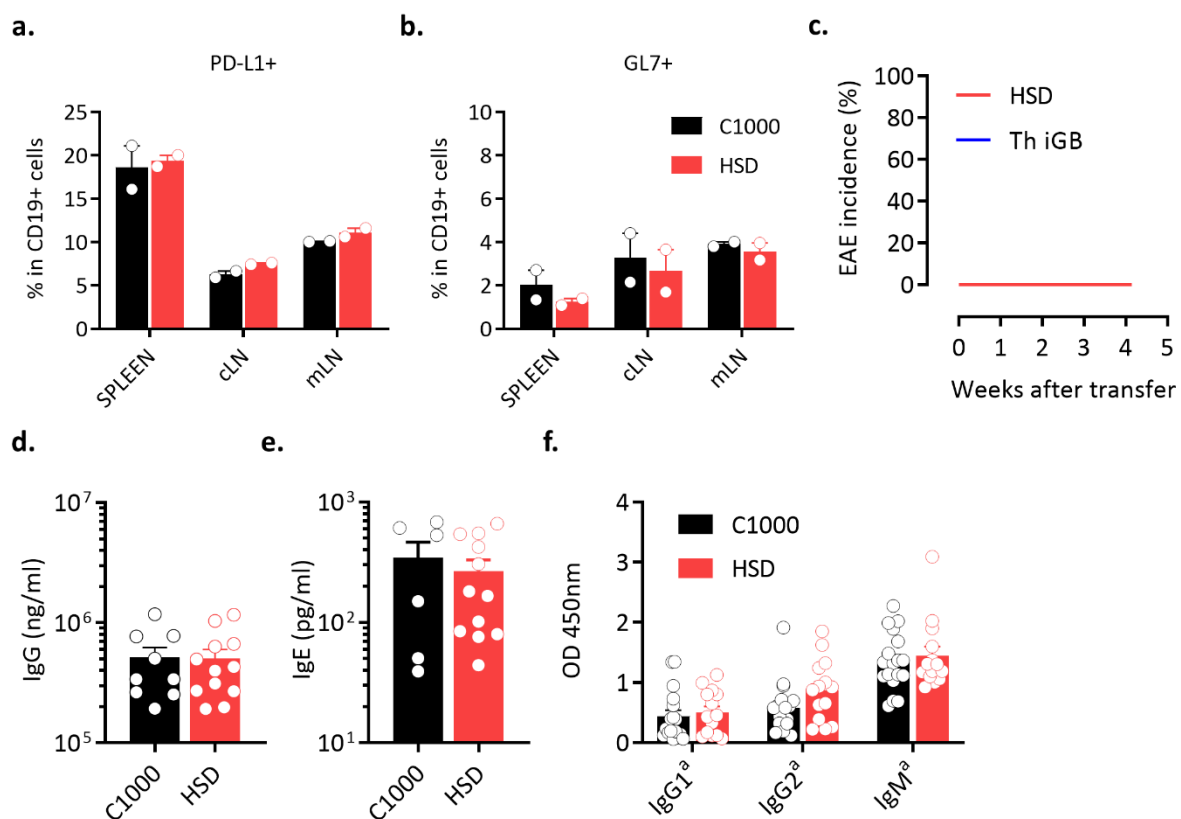


Figure 3.23. Serum autoantibody levels are unaltered under HSD. **a.** Total serum IgE, quantified by ELISA with sera from OSE mice fed for 3-4 weeks (C1000 n=9, HSD n=12). Each circle represents an individual mouse. **b.** Total serum IgG, quantified by ELISA with sera from OSE mice fed for 3-4 weeks (C1000 n=6, HSD n=12). Each circle represents an individual mouse. **c.** Incidence of spontaneous EAE in HSD-fed OSE mice after injection of Th iGB cells i.p. (HSD (control) n=5, Th iGB n=6). **d-f.** MOG specific antibodies - IgG1^a (**c**), IgG2^a (**d**), and IgM^a (**e**), quantified by ELISA with sera from OSE mice fed for 3-4 weeks (C1000 n=18, HSD n=14). OD at 450nm was measured and directly compared. Each circle represents an individual mouse. All data represented as mean \pm s.e.m.

3.11. HSD DOES NOT AFFECT INTEGRINS ASSOCIATED WITH IMMUNE CELL MIGRATION

Having seen that alterations in the immune cell subsets did not contribute to disease protection, yet another critical factor in EAE – the markers associated with immune cell migration to the CNS – was investigated. The integrins $\alpha_4\beta_1$ (VLA-4) and $\alpha_L\beta_2$ (LFA-1) in particular are involved in T_H1 and T_H17 cell migration and their subsequent attachment to the CNS endothelia during EAE [114]. Therefore, the levels of integrins β_1 , α_4 , CD18 (β_2), and CD11a (α_L) in the SILP CD4⁺ T cells of OSE mice were analyzed by FACS 3-4 weeks after diet switch. Integrin expression in both IL-17⁺ and IFN γ ⁺ CD4⁺ T cells was analyzed and found to remain unaltered due to HSD (**Fig.3.24. a-d**).

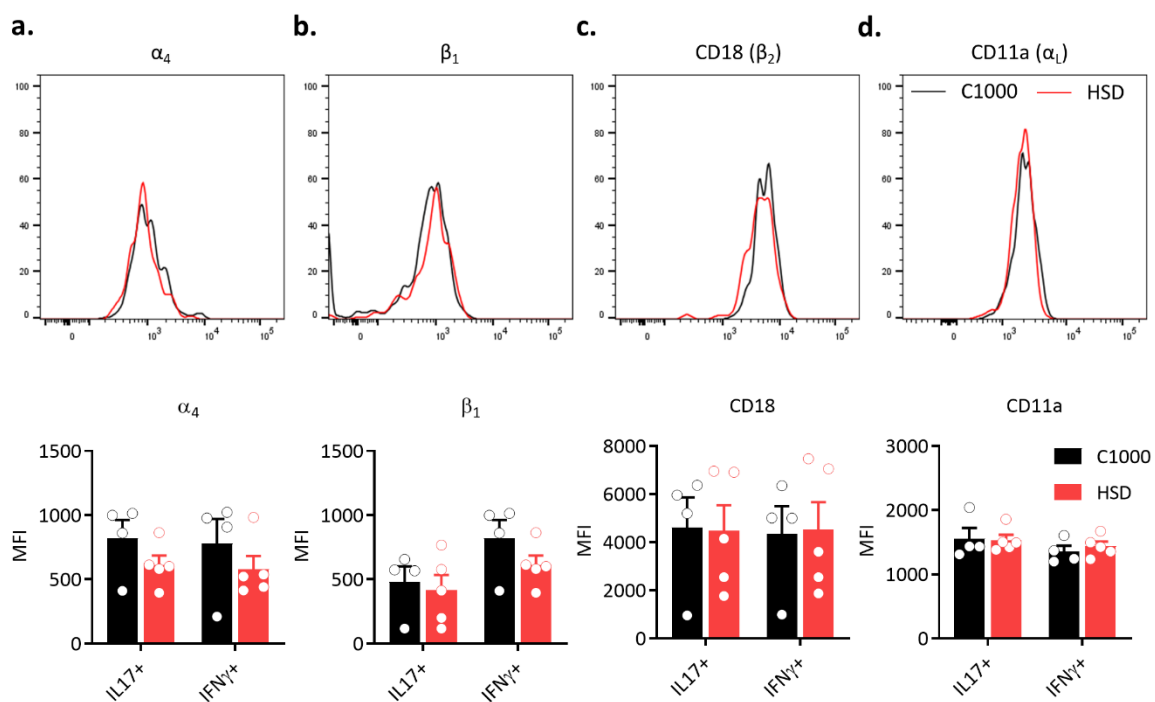


Figure 3.24. Expression of integrins on CD4⁺ T cells is unaffected under HSD. Representative FACS plots (top) and mean fluorescence intensity (MFI) (bottom) of α_4 (a), β_1 (b), CD18 (β_2) (c) and CD11a (α_L) (d) in IL-17⁺ and IFN γ ⁺ CD4⁺ T cells in the small intestine lamina propria (SILP) of OSE mice 3-4 weeks after diet switch (C1000 n=4, HSD n=5). Each circle represents an individual mouse. All data represented as mean \pm s.e.m.

Taken together, all of these results conclusively indicated that any HSD-mediated alterations in the immune cells did not hold any functional relevance in disease protection. To validate this even further, active EAE experiments were performed in OSE mice.

3.12. HSD-FED OSE MICE ARE NOT PROTECTED FROM ACTIVE EAE

OSE mice were weaned onto C1000 and HSD. Active EAE was induced only in mice that remained healthy up to 12 weeks of age (**Fig.3.25. a**). More than 80% of the mice developed EAE under both C1000 and HSD. Moreover, there was no difference in EAE incidence or severity between mice under both diets (**Fig.3.25. b, c**). Subsequently, EAE induction with a 10-fold lower dose of CFA was also performed. Unlike in WT mice, the EAE severity in OSE

mice was still very high even with the lower CFA dose. But there was no difference in EAE incidence or severity between both dietary conditions (**Fig.3.25. d, e**).

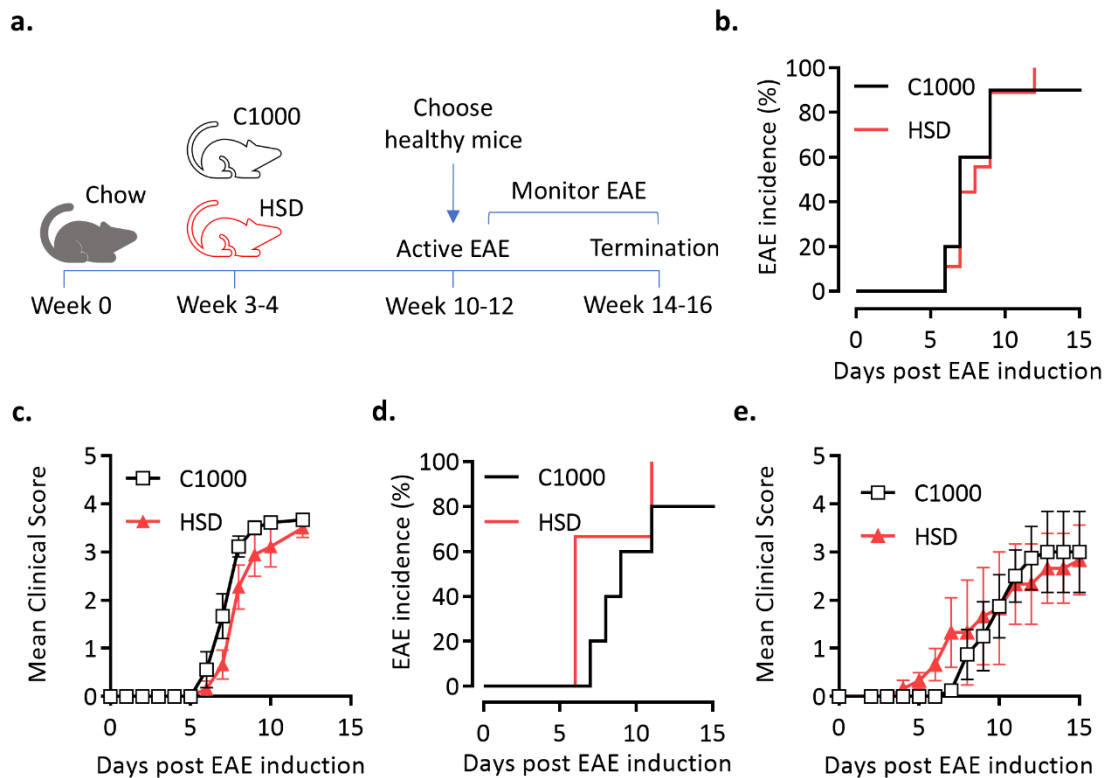


Figure 3.25. HSD does not affect active EAE in OSE mice. **a.** Experimental plan of active EAE induction in OSE mice. **b, c.** Disease incidence (**b**) and Mean clinical score (**c**) after active EAE induction with 100µg MOG 35-55 in CFA with 500µg MTB (C1000 n=10, HSD n=9). **d, e.** Disease incidence (**d**) and Mean clinical score (**e**) after active EAE induction with 100µg MOG 35-55 in CFA with 50µg MTB (C1000 n=5, HSD n=3). For plotting mean clinical scores (**c, e**), only mice that developed EAE were taken into consideration.

This indicated that the immune cells in HSD-fed mice were still capable of inducing disease when they are stimulated – thus showing that they are functionally fully capable. Therefore, it is likely that factors other than immune cells may play a role in HSD-mediated protection from spontaneous EAE.

3.13. NO EFFECT OF HSD ON ADHESION MOLECULES

Our resultant focus was hence on the BBB, as it is the regulator of immune cell entry into the CNS. As described in (**Fig.1.2**), the first step in immune cell infiltration is their attachment to the BBB, which depends on the expression of cell adhesion molecules on the endothelia. The key cell adhesion molecules involved in immune cell attachment are ICAM-1 and ICAM-2. Hypothesizing that a reduced expression of these molecules could contribute to lesser immune cell infiltration, the levels of both these molecules in the brain and spinal cord endothelial cells were determined by FACS in WT mice fed C1000 or HSD for 3-4 weeks. Both ICAM-1 and ICAM-2 were expressed in low levels and remained comparable under C1000 and HSD (**Fig.3.26. a-d**).

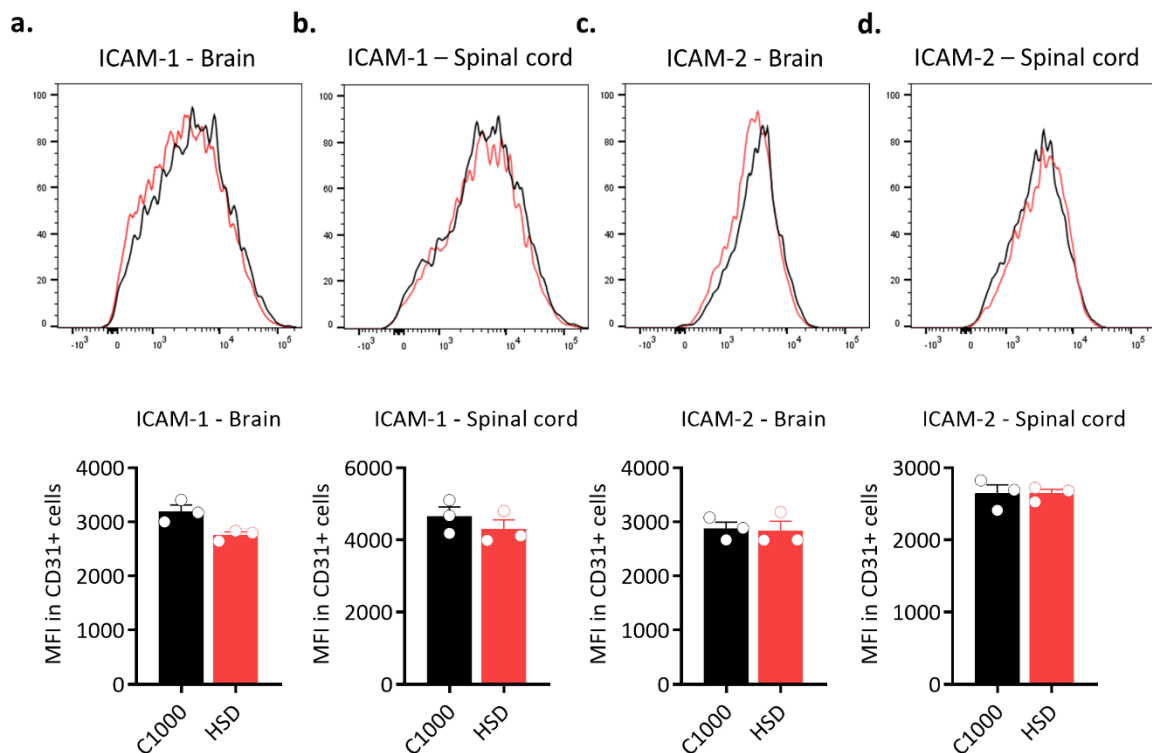


Figure 3.26. Expression of Adhesion molecules on CNS endothelial cells unaffected. Representative FACS plots (top) and Mean fluorescence intensity (bottom) of ICAM-1 in the brain (a), ICAM-1 in the spinal cord (b), ICAM-2 in the brain (c), and ICAM-2 in the spinal cord (d) of CD31+ endothelial cells of WT mice 3-4 weeks after diet switch (C1000 n=3, HSD n=3). One representative experiment out of 2 is shown. Each circle represents an individual mouse. All data represented as mean \pm s.e.m.

3.14. HSD ALTERS BLOOD BRAIN BARRIER PERMEABILITY IN VIVO

The loss of integrity of the BBB during EAE has been well documented in previous studies [128]. A rescue of BBB integrity has also been shown to protect from EAE [131]. The barrier integrity is regulated by tight junction proteins like ZO-1, JAM-2, Claudins, and Occludin. In this regard, the expression of the tight junction proteins ZO-1 and Claudin-5 was investigated. Brain endothelial were isolated from OSE mice fed C1000 or HSD for 3-4 weeks. Western blot was used to quantify the expression of both junction proteins. The expression of both ZO-1 and Claudin-5 relative to β -actin were quantified, and both showed significantly increased expression under HSD (Fig.3.27. a-c).

Furthermore, a direct in vivo quantification of BBB permeability using WT mice showed that HSD-fed mice had decreased permeability of the BBB, as evidenced by the decreased levels of FITC in the brain after intravenous injection of FITC-dextran (Fig.3.27. d). This indicated that there is an alteration in the BBB integrity towards a 'tightening' of the barrier. While here we observed an increase in ZO-1 and Claudin-5 consistent with decreased in-vivo BBB permeability, the contributions of other junction proteins which were not analyzed in this study – like JAM-2 and Occludins may also play an additional role in regulating BBB integrity.

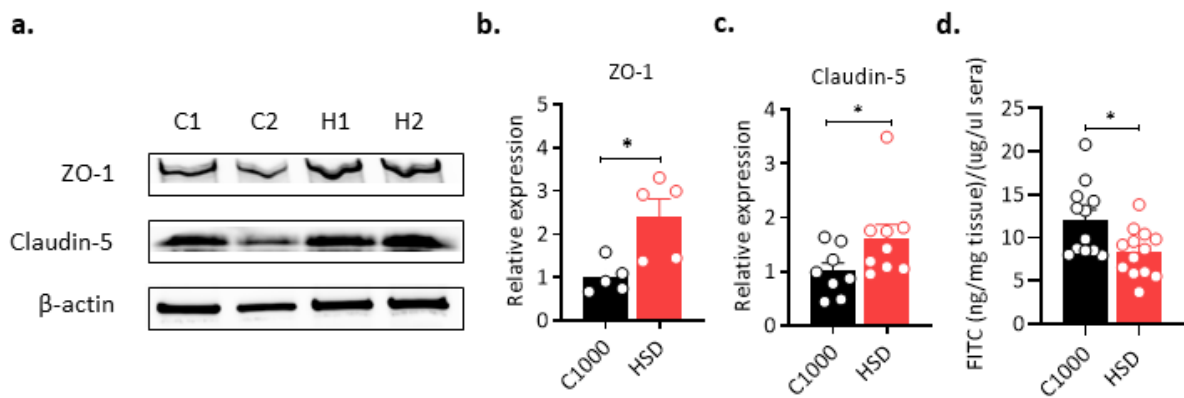


Figure 3.27. HSD alters BBB permeability in vivo. **a.** Representative Western blot images of ZO-1 (top) and Claudin-5 (middle) expression relative to β -actin (bottom) in brain endothelia isolated from OSE mice 3-4 weeks after diet switch. **b, c.** Relative expression of ZO-1 (**b**) and Claudin-5 (**c**) in the brain endothelia of OSE mice 3-4 weeks after diet switch (C1000 $n=5$, HSD $n=5$), normalized to β -actin. Each circle represents a pool of cells from 2 mice. **d.** BBB permeability in vivo, quantified by i.v. injection of FITC-Dextran 4kDa and measurement of FITC fluorescence in the Brain tissue of WT mice 3-4 weeks after diet switch. FITC levels in the brain are normalized first to tissue weight and then to serum FITC levels. Data pooled from 3 experiments is shown (C1000 $n=12$, HSD $n=13$). Each circle represents an individual mouse. All data represented as mean \pm s.e.m.

3.15. HSD-MEDIATED DISEASE PROTECTION IS REVERSED BY PERTUSSIS TOXIN

Our subsequent focus was on trying to reverse HSD-mediated disease protection by targeting the BBB, to validate that HSD-mediated protection was due to a “tightening” of the BBB. Pertussis toxin used in active EAE has the role of disrupting the BBB. It was thus investigated whether alteration in the BBB integrity by Pertussis toxin without external stimulation of the immune cells would be sufficient to make HSD-fed mice susceptible to EAE.

Pertussis toxin was injected i.p. once per week to OSE mice fed HSD. 80% of the mice treated with Pertussis toxin developed EAE (**Fig.3.28. a-c**). Additionally, luxol fast blue staining was performed on spinal cord sections from both PBS and Pertussis toxin treated mice, and demyelination was seen only in Pertussis toxin treated mice, corroborating the observed EAE incidence in vivo. This indicated that changes to BBB integrity early after diet switch can reverse HSD-mediated disease protection, thus establishing that alterations to BBB integrity are responsible for disease protection by HSD.

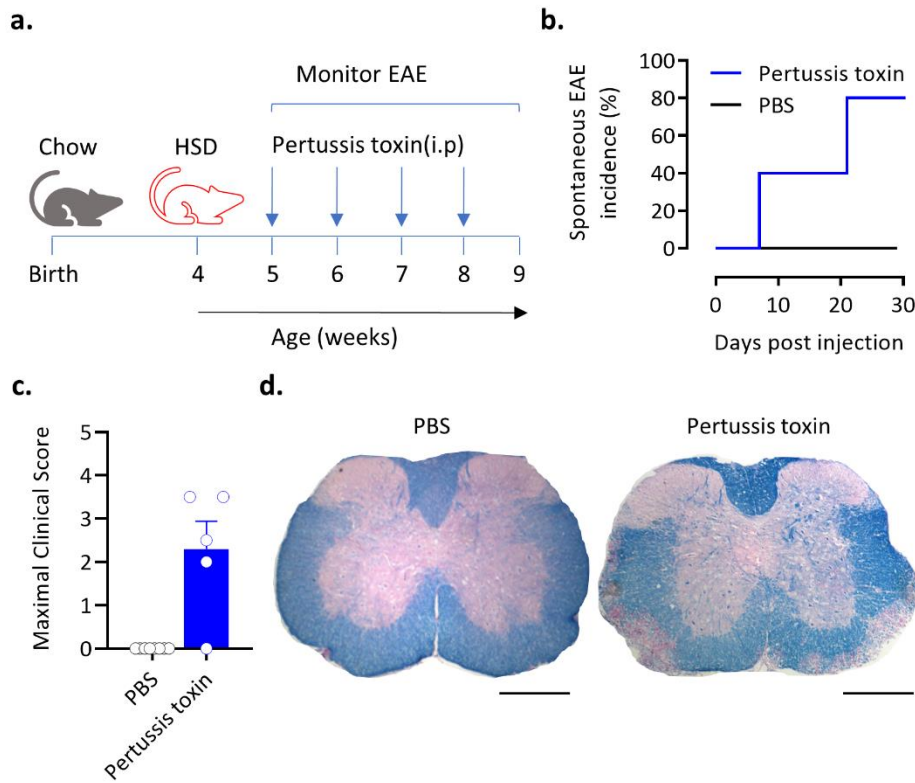


Figure 3.28. Pertussis toxin reverses HSD-mediated disease protection. a-d. Experimental plan (a), EAE incidence (b), maximal clinical score (c), and representative images of spinal cord sections stained with luxol fast blue (d) in OSE mice after treatment with PBS or 400ng Pertussis toxin i.p. (PBS n=8, Pertussis toxin n=5). For (b) and (c) One representative experiment out of 2 is shown. Scale bar, 500 μ m

4. DISCUSSION

The objective of this study was to characterize the role of the High Salt Diet (HSD) in spontaneous CNS autoimmunity. The role of HSD in autoimmunity has been addressed by several studies in the past using induced autoimmunity models for colitis, EAE, and SLE among others, with HSD being shown to have an exacerbating effect on autoimmunity [225, 290, 304, 305, 316]. Induced autoimmunity models are very good tools to understand disease pathogenesis. They are also useful in studies involving the characterization of therapeutic compounds. Yet, their caveat is that the disease induction is largely artificial - with the use of adjuvants in EAE or chemicals like Dextran sodium sulfate in colitis. In the context of EAE, actively induced EAE involves immunization of mice with the cognate antigen coupled with a strong adjuvant (CFA) and Pertussis toxin. The resulting disease is influenced by immune cell activation and expansion due to CFA, and blood-brain-barrier disruption by Pertussis toxin. Hence, unlike earlier studies that have employed an actively induced EAE model [290, 291] to characterize the role of HSD, this study employs a mouse model that spontaneously develops EAE (OSE) [34].

The use of the spontaneous model eliminates the necessity of using adjuvants and enables a study of disease under relatively less artificial settings. This also makes the results better translatable to human MS. These mice can be useful to study mechanisms that trigger EAE. Still, this system also has its caveats. First, the OSE model is not completely representative of the natural setting i.e., the mice are transgenic and their T and B cell repertoires are tailored to be specific to MOG. Next, the disease incidence starts very early in adult life, soon after weaning (**Fig 3.3**). This makes the time window for experiments aimed at prevention or some form of intervention like microbiota transplantation, very short. On the other hand, while a significant proportion of the mice develop EAE within 4 weeks after weaning, the disease course can also extend over 8-10 weeks, making it less ideal for therapeutic studies. Further, as noted previously the immune repertoire is skewed towards effector T_H1 and T_H17 cell populations, and T_{reg} cells are reduced in numbers. Also, $CD8^+$ T cells are lacking in the model. Thus, their contributions to the disease process cannot be understood with this system.

Yet, despite its caveats, this system would serve as a good tool to understand the role of HSD in EAE under less artificial settings. When OSE mice were fed HSD and monitored for EAE, HSD was observed to confer protection from EAE, something that had not been reported previously and is in contrast to reports on induced EAE. This conflicting result has to be interpreted carefully given the prior ones.

To begin with, the diet regimen implemented in the present study used C1000 as a control diet instead of a regular chow diet. While the overall crude fiber and nutrient composition in chow and HSD are not hugely different, there are marginal differences between them. While the HSD is less moisture rich, chow diet has more moisture content, but lesser vitamins, fatty acid and amino acid concentrations compared to HSD. chow diet also has lower disaccharide and polysaccharide content. This is likely because chow is crudely derived from wheat and

soy fibers, which would be a mix of several components in addition to carbohydrates. HSD on the other hand derives fiber from cellulose, a purified source. Thus, the C1000 diet, which is identical to HSD in fiber sources, macronutrients, and vitamin concentrations, made for a more appropriate control diet. The original observations on exacerbation of active EAE by HSD reported by Wu et al. and Kleinewietfeld et al. had been performed using regular chow fed mice as control [289, 291]. Wilck et al. on the other hand, had used a compositionally identical control diet corresponding to HSD and also found, similar to the other reports, an exacerbation in EAE [290]. Yet in our system, HSD had protective effects in the spontaneous EAE model.

The diet regimen used here also differs in another regard from protocols used in the previous EAE studies. In the prior studies, animals were fed 4% NaCl supplemented food pellets augmented with 1% NaCl in drinking water [289, 291]. On the one hand, chronic and excessive salt feeding can have adverse effects on the animal's health. This is crucial to note in our system, as the OSE model requires the diet regimen to be maintained until 3-4 months of age to complete observation of the disease course. On the other hand, some previous studies on HSD's role in colitis and hypertension have also used NaCl only in food pellets [317, 318]. Nevertheless, our lab has also shown that in contrast to the prior reports, usage of 4% NaCl supplemented food pellets augmented with 1% NaCl in drinking water does not exacerbate active EAE [319]. Because of this, in this study, the salt was only administered (at 4% concentration) with diet and not in water. This also makes the results more relevant to be translatable to human MS.

Under this diet regimen, body weight changes under HSD were comparable to that of mice fed a C1000 diet. This negated the likelihood of HSD-fed mice having significantly reduced food intake due to the presence of salt. The leptin levels in the serum were also comparable under both C1000 and HSD. Leptin is a hormone produced by adipocytes and is involved in the regulation of hunger, food intake, and energy homeostasis. Leptin levels are altered due to fasting or changes in calorie intake [320]. Thus, the unaltered level of leptin was further indication that HSD-fed mice did not have altered food intake compared to their C1000 counterparts. Interestingly, HSD has previously been shown to contribute to leptin resistance, leading to obesity, evidenced by rapid weight gain [321]. This was also not observed with our HSD regimen. Thus, it can be concluded that this diet regimen was well tolerated by the mice.

Our key observation was that HSD confers protection from spontaneous EAE. But, though the incidence of EAE was lower under HSD, around 20% of the mice do develop EAE, and disease severity in these mice did not differ from that of sick mice under C1000. One can thus conclude that once the animal developed the disease, HSD had no further impact.

It is of essence to translate and understand these results in the clinical setting. The disease protection observed in OSE mice indicates that the consumption of a salt-rich diet from an early age can help reduce the risk of MS, particularly in predisposed individuals. Also, early dietary intervention on a larger scale can help reduce the prevalence of MS. On the other

hand, in MS patients, starting the consumption of a salt-rich diet after diagnosis will likely not have any impact on the disease course. This is because HSD has no impact after EAE incidence in OSE mice, and MS diagnosis at present relies largely on the occurrence of symptoms, which is already indicative of damage in the CNS i.e., the disease has manifested.

Our next observation on active EAE experiment in WT mice under our diet regimen showed no exacerbation under HSD, as opposed to prior reports [289, 291]. While there were differences in the diet regimen concerning the quantum of salt given, the duration of feeding before EAE induction, and the EAE induction protocol were similar to the prior reports. At first glance, the difference in results might be attributed to the exclusion of 1% NaCl in drinking water from this diet regimen. But our lab has recently shown that even after the inclusion of 1% NaCl in drinking water, there is no exacerbation in EAE due to HSD [319].

Another factor this may be attributed to is a difference in the gut microbiota composition across mice housed in different facilities. The microbiota can have a significant impact on the immune system and autoimmunity [322-324]. A difference in the gut microbial composition may thus lead to different immune cell profiles and hence differences in EAE course. But, as the microbiota are a dynamically changing parameter and microbiota within the same facility over different periods may already be different, exploring this avenue would not be feasible.

In addition, a third factor may be that the aforementioned active EAE studies [290, 291] had recorded a low EAE severity (score 2) in the animals under control diet and hence an exacerbation under HSD was observable. But in our animals, the severity under control condition was already high (score > 3). Hypothesizing that marginal increases in disease severity can be discerned only if there was less severe disease under control conditions, the CFA concentration was lowered by 10-fold during EAE induction. This resulted in EAE with lower severity (score~2) in control animals. Yet, here too HSD did not exacerbate EAE. While no exacerbation was noted in active EAE, unlike spontaneous EAE, HSD-fed mice were not protected from active EAE. This further reinforces that in clinical settings, a salt-rich diet would not help if consumed after the disease has manifested.

The present study subsequently focused on alterations due to HSD and their relevance in protection from spontaneous EAE. Metabolic, systemic, and immune system alterations were all characterized. First to be probed were systemic alterations, the focus being the gut microbiota. Diet has been shown to rapidly and reversibly alter the microbiota [217]. HSD has, in particular, been shown to bring about a reduction in *Lactobacillus* in the gut [223, 225, 290]. But in this study, based on the observed increase in the abundance of *Enterococci* under HSD in a prior 16s rRNA sequencing data (unpublished) comparing chow and HSD-fed mice, *Enterococci* was investigated in detail. qPCR on fecal samples and fecal microbiota culture in Bile-Esculin agar followed by sequencing of the colonies had both showed higher *Enterococci* levels under HSD. The sequencing of colonies from Bile-Esculin agar plates showed *Enterococci hirae*, in particular, to be dominant under HSD. While normally *Enterococci hirae* is a very scarcely abundant commensal in the mouse gut, its increased abundance under HSD

is as expected, since *Enterococci hirae* is known to be salt tolerant and this was also verified here through in vitro culture in the presence of salt.

On subsequent investigation comparing *Enterococci* abundance in C1000 and HSD-fed mice, it was interesting that C1000 fed mice already had substantially higher *Enterococci* levels than chow fed mice. As elucidated before, chow and C1000 differ in their fiber sources. The difference in *Enterococci* levels between chow and C1000 can be explained in view of a previous report by our lab that showed that a diet high in cellulose caused an increase in *Enterococci hirae* in the gut [234]. Nevertheless, C1000 fed mice had significantly lesser *Enterococci* levels than HSD-fed mice. Also, the results from 16s rRNA sequencing comparing the microbiota in C1000 and HSD-fed mice showed that indeed, *Enterococci* levels were increased under HSD, in addition to the differential abundance of other genera including *Lactobacillus*, *Blautia*, and *Akkermansia*.

These microbial alterations were accompanied by alterations in the fecal metabolome. The most differentially abundant compounds were amino acid derivatives, bile acids as well as long and short chain fatty acids. Metabolites influence autoimmunity predominantly through their action on immune cell subsets in the gut, via receptors like Ahr. Ahr has been well characterized and implicated in CNS autoimmunity, primarily through the mediation of T cell differentiation [224, 290]. Resultantly, caecal metabolites from C1000 and HSD were assessed using EROD assay for their capability to activate Ahr, and this was found to be unaltered due to HSD. While this showed that Ahr was not differentially activated due to HSD-modified metabolome, it does not preclude the possibility of differential activation of other receptors like those for bile acids or GPCRs activated by fatty acids. Thus, while HSD resulted in a modified metabolome, the functional effects of these changes were not ascertained.

However, the consequent characterization of other parameters conventionally associated with microbiota alterations – namely fecal albumin and IgA – showed no alterations under HSD. This indicated that alterations in the microbiota did not result in a corresponding alteration to the intestinal barrier integrity or the mucosal humoral immune response. Microbiota alterations have been previously shown to alter intestinal barrier permeability [299]. An altered gut barrier integrity would result in the movement of big molecules like albumin from the serum into the interstitial fluid and subsequently into the gut, and then excretion via the feces. The measurement of fecal albumin is hence taken as a proxy indicator for intestinal barrier permeability.

But all microbial alterations need not necessarily affect gut barrier integrity. One cause for barrier integrity changes along with microbial alterations is the altered metabolism of various dietary components, which generates an altered metabolome pool that affects barrier permeability by differentially regulating signal transduction pathways involved in tight junction protein production. Another factor regulating barrier integrity is the cytokine milieu in the gut, which in turn is influenced by the activation of gut immune cell populations in response to microbial antigens [327]. Therefore, the lack of alterations in the barrier integrity

may be because neither the change in the metabolome nor the cytokine milieu in the gut under HSD affects the regulation of tight junction proteins.

Fecal IgA levels are used as a measure of alterations in the mucosal humoral immune response due to an alteration in the microbiota. Like with barrier integrity, microbial alterations need not always affect IgA responses in the gut. As IgA production is influenced by microbial antigens, different microbial species may elicit the production of IgA in very similar levels if their antigenicities are comparable. In conclusion, HSD altered the gut microbiota and the metabolome without accompanying functional alterations in the intestinal barrier and mucosal IgA responses.

The observed alteration in the microbiome brings about the question of its relevance in disease protection due to HSD. While this can be addressed by establishing the desired microbial species in the gut and monitoring EAE, there are limitations with regard to our model. Under SPF conditions, establishing desired microbiota in the gut requires daily gavages throughout the disease course. Previous studies that have performed microbial colonization experiments have used daily gavages of the desired bacterium to establish it in the gut [290]. But OSE mice have to be monitored for spontaneous EAE at least up to 3-4 months of age. Daily gavages would therefore not be feasible and would contribute to increased stress for the animals. So, in lieu of establishing definitively the role of the microbiota, the focus subsequently moved towards investigating the mechanism by which HSD directly or via the microbiome may influence spontaneous EAE.

Going ahead, the presentation of antigen by peripheral APCs to T cells – a key requirement for the activation of T cells and their subsequent infiltration into the CNS, was first analyzed. B cells play the dominant role in antigen presentation in OSE mice. T cell proliferation depends on efficient antigen presentation by B cells, alterations in which would lead to reduced T cell proliferation. Antigen presenting capability of B cells, subsequent T and B cell activation and proliferation were all compared using both antigen-specific and non-specific stimuli. When splenocytes from C1000 and HSD-fed OSE mice were cultured with recombinant MOG protein, MOG 35-55 peptide, or with anti-CD3 as stimuli, both B and T cells proliferated at comparable rates. This indicated that B cells had presented antigen to the T cells equally efficiently in both diet conditions. This was also supported by the comparable frequencies of activated T and B cells (CD69+ CD25+) under both diets. In addition, under both dietary conditions, splenocytes produced comparable levels of the conventionally 'proinflammatory' cytokines IFN γ and IL-17, both of which play key roles in EAE. The levels of the anti-inflammatory cytokine IL-10 were also measured and found to be comparable. Altogether, HSD-exposed lymphocytes are not deficient in antigen presentation, activation, proliferation, or cytokine production on exposure to cognate antigen.

This result necessitated the exploration of other alterations in the immune system. As most dietary components are enriched primarily in the gut, they predominantly affect the GALT, which is directly exposed to them. Pursuant to our investigation of changes in various immune

cell frequencies in the GALT, IL-17+ CD4+ T cells in the SILP were found to be higher in frequencies in both WT and OSE mice, with no changes in IFN γ + cells or IL-17+ IFN γ + cells. This result is in line with many previous reports [290, 293, 305, 317]. But these reports associate the increase in the GALT T_H17 cells with a pro-inflammatory phenotype. Thus, the observed increase in T_H17 cells in the present study may seem paradoxical and functionally inconsistent with protection from spontaneous EAE, due to the well documented role of T_H17 cells in generating a pro-inflammatory phenotype [328-330]. But recent research has highlighted the plasticity of the various T cell subsets and shown that depending on the environment the cells are exposed to, the surrounding cytokine milieu, or the presence of microbial metabolites, IL-17+ T cells can also exhibit an anti-inflammatory phenotype [312, 331-333].

In continuing to characterize the alterations in GALT, it was seen that WT mice had increased FoxP3+ T_{reg} cell frequencies in the CLP under HSD. Yet, OSE mice did not show this difference. It was also interesting to note that the overall frequencies of T_{reg} cells were much lower in OSE mice – less than 5% in the OSE spleen compared to around 8-15% in WT spleen (**Fig 3.16, Fig 3.18**). Nevertheless, an increase in the T_{reg} frequencies would suggest the possibility of a regulatory phenotype under HSD. Various preceding reports have addressed this and the majority of them have shown that HSD promotes a pro-inflammatory phenotype. NaCl was shown to skew the T_{reg}/T_H17 balance towards T_H17 cells, via regulation of SGK1 [334, 335]. NaCl was also shown to inhibit the suppressive function of T_{reg} cells [336]. However, Luo et al. reported that NaCl reduced the functionality of only thymic T_{reg} cells and had no effect on TGF β induced T_{reg} cells [337]. On the other hand, Matthias et al. have recently shown that NaCl induces an anti-inflammatory phenotype in T_H17 cells by inducing upregulation of FoxP3, whose expression can be stably maintained even after NaCl is removed. They also showed that NaCl amplifies the pathogenicity of T_H17 cells only in a pro-inflammatory microenvironment [338]. This suggests that NaCl has a milieu dependent bipartite role in T cell differentiation.

Subsequently, it was essential to correlate the increased frequencies of T_H17 and T_{reg} cells to a direct effect of NaCl or an indirect result of microbial or metabolite changes. While in vitro T cell differentiation in the presence of NaCl was shown to enhance T_H17 cell differentiation, it had no impact on T_{reg} cell differentiation. Also, caecal metabolites from HSD-fed mice failed to enhance the differentiation of both T_H17 and T_{reg} cells in vitro. Consequently, the role of HSD modified microbiota in altering T_{reg} cell frequencies was investigated, by gavage of caecal content from C1000 or HSD-fed WT mice into chow fed WT mice and subsequent FACS analysis of immune cells in the GALT. Mice gavaged with caecal content from HSD-fed mice did not show any difference in either T_H17 or T_{reg} cell frequencies in the GALT. The caveat of this setup was that while it can be definitively concluded that metabolites from mice fed HSD do not differentially modulate the GALT immune cells, the role of the microbiota cannot be ruled out entirely. This is because the establishment of the HSD-modified microbiota in the gut was not validated.

Subsequently continuing the analysis of GALT in OSE mice, T_{reg} cells were investigated in greater depth. The SILP in HSD-fed mice had an increase in CD103⁺ ROR γ T⁺ FoxP3⁺ T_{reg} cells, while other markers like Helios and KLRG-1 were unaltered. This is also consistent with a regulatory phenotype under HSD. With mounting evidence on the plasticity of both T_H17 and T_{reg} cells, it has already been shown that T_{reg} cells can also produce ROR γ T and function in regulatory capacity [339]. These cells have even been shown to have enhanced suppression capacity [313]. CD103 has also been identified as a marker for increased potency of regulatory T cells [340, 341]. Both CD103⁺ and ROR γ T⁺ T_{reg} cells produce IL-10 which plays a key role in their immunoregulatory phenotype. This necessitated our quantification of the production of IL-10 specifically in T_{reg} cells isolated from both the periphery (cervical lymph node) and SILP. While it was previously observed that antigen-stimulated splenocytes from HSD-fed mice do not produce more IL-10, peripheral T_{reg} cells from HSD-fed mice showed significantly increased production of IL-10. In summary, the T_{reg} compartment was seen to have alterations due to HSD, both in the frequencies of CD103⁺ ROR γ T⁺ T_{reg} subset and their production of IL-10 in the periphery.

We next proceeded to assess whether these alterations held any functional relevance in HSD-mediated disease protection. This was done by the use of 2 in vivo depletion systems - T_{reg} cell depletion using anti-CD25 antibody, and IL-10 blocking using anti-IL-10 antibody - in HSD-fed OSE mice. Having observed that neither T_{reg} cell depletion nor IL-10 blocking could reverse protection and bring back EAE, it was concluded that while these changes were significant, they were not the key players in disease protection under HSD. In further validation of this, our group had also observed that the suppressive capacity of T_{reg} cells was unaltered due to HSD [319].

The resultant focus, therefore, shifted to an analysis of alterations in the B cells. B cells are the primary APCs in the OSE model. But as elucidated previously, HSD did not functionally alter their APC capacity, activation, or proliferation. But in addition to serving as APCs, B cells also act as regulators of effector T cell responses, and this regulatory phenotype is associated with elevated expression of PD-L1 [314], whose characterization using FACS showed no difference due to HSD. Further, dietary and microbial antigens are known to regulate the expression of the germinal center marker GL7. GL7^{high} B cells have been shown to have higher functional activity for producing antibodies and presenting antigens [342]. This marker too was hence characterized using FACS and showed no difference due to HSD.

B cells in OSE mice produce significant quantities of MOG-specific IgM which undergo class switch to IgG [34]. These antibodies may diffuse into the CNS along with activated T cells and augment disease progression. Our subsequent comparison of total IgG, total IgE, and MOG-specific IgG1^a, IgG2^a, and IgM^a in the serum from C1000 and HSD-fed mice showed no changes. B cells from HSD-fed mice are thus still capable of efficient antibody production. Finally, transfer of Th iGB cells from chow fed mice into HSD-fed OSE mice failed to reverse disease protection, establishing that under HSD, B cells retain their full functionality and do not play a role in HSD-mediated disease protection.

Having established that T and B cells are not functionally different under HSD, it was hypothesized that immune cell migration from the periphery to the CNS could be impaired under HSD. T_H1 and T_H17 cells express the integrins LFA-1 and VLA-4, which are crucial for their migration from the gut to the CNS [114, 115]. Characterization of LFA-1 and VLA-4 expression in both IL-17⁺ and IFN γ ⁺ cells in the GALT of OSE mice showed no difference. Furthermore, our lab has also recently shown that splenocytes transferred from both C1000 and HSD-fed mice to RAG ^{-/-} recipient mice are equally capable of inducing EAE [319]. Taken together, this establishes that the immune cells from HSD-fed mice are not limited by an inability to migrate to the CNS.

In further validation of our observations, an investigation of active EAE progression in OSE mice under HSD that remained healthy until 12 weeks of age showed no exacerbation under HSD, yet the OSE mice were not protected from EAE either. Interestingly, compared to WT mice, OSE mice irrespective of diet showed accelerated disease courses during active EAE. This can be attributed to expeditious activation of the pre-existing MOG specific T and B cells. The presence of autoantibodies in the sera of healthy OSE mice could also contribute to the accelerated disease progression. Taken together, it was evident that while frequencies of some T cell subsets are altered due to HSD, immune cell functionality in terms of T and B cell proliferation, cytokine production, antigen presentation by B cells, autoantibody production, the regulatory function of the T_{reg} cells and ability to migrate to the CNS are unaffected by HSD. Further, HSD-fed mice do develop active EAE. This was additional evidence that the immune system is still functionally competent under HSD.

As a result, we hypothesized that other non-immune parameters might potentially play a role in disease protection. Having previously ascertained that intestinal barrier integrity was not altered, the other major non-immune factor was the BBB, whose integrity is a crucial mediator of immune cell infiltration into the CNS [128]. Effects on the BBB could be either directed towards a reduced immune cell attachment to the BBB, or reduced extravasation into CNS through the BBB. To characterize effects on immune cell attachment, we analyzed the expression of the cell adhesion molecules (CAMs) ICAM-1 and ICAM-2 on brain and spinal cord endothelial cells. These CAMs bind LFA-1 and VLA-4 on the immune cell surface to facilitate their attachment to BBB endothelia and movement along the BBB until their extravasation into the CNS. FACS analysis showed that the expression of ICAM-1 and ICAM-2 was not different. This indicated that the immune cell attachment mediated by these CAMs along the BBB is less likely to be affected under HSD.

We then investigated the possibility of reduced extravasation of immune cells into the CNS. Under normal conditions, very few immune cells extravasate through the BBB, but previous studies show that there is a large-scale dysregulation of the junction protein expression during EAE, resulting in a compromised BBB, the rescue of which results in alleviation of EAE [128]. Hence our subsequent focus was on investigating alterations in the BBB permeability under HSD. The common method for investigating barrier alterations is the injection of fluorescent tracers tagged to dextran by i.v. and subsequent fluorescence quantification in

the CNS. Here, the injection of FITC-dextran by i.v. and its subsequent quantification in the brain showed that indeed, HSD-fed mice had reduced FITC-dextran levels in the brain, indicating a change in the BBB permeability in vivo due to HSD. The reduced levels of FITC-dextran suggested that the barrier was 'tightened' following HSD, and this could thus translate to reduced immune cell infiltration into the CNS.

As explained in **Fig. 1.2**, the permeability of the BBB is regulated by the expression and localization of several tight junction proteins on the BBB endothelia, and their increased expression reduces barrier permeability by restricting the movement of cells or solutes across the endothelial layer. Hence, we characterized the expression of the tight junction proteins ZO-1 and Claudin-5, by the isolation of brain endothelial cells via gradient centrifugation using percoll, followed by sorting and subsequent western blot analysis. Indeed, there was a significant increase in the expression levels of both junction proteins under HSD, thus corroborating the observed decrease in the BBB permeability in vivo. But while this study has shown alterations in ZO-1 and Claudin-5 due to HSD, the contribution of the other tight junction proteins like JAM, Occludin, and Cadherins would also be interesting to explore.

In conclusion, HSD altered the BBB permeability, resulting in a tightened barrier restricting the entry of immune cells into the CNS. But the relevance of this alteration to HSD-mediated disease protection needed to be characterized. Hence, Pertussis toxin, a known disrupter of the BBB integrity, was injected into OSE mice, beginning early – 1-1.5 weeks post diet switch. This treatment indeed resulted in EAE, reversing HSD-mediated disease protection. This showed that the BBB permeability alteration was indeed important to HSD-mediated disease protection.

The present study has thus shown that HSD has a protective effect on spontaneous EAE, resulting from alterations in the BBB integrity. Translated to a clinical setting, this would not only mean that HSD can potentially prevent MS development, but also that the BBB can be explored as a therapeutic target, and BBB modulators can be identified and potentially used in therapy for MS. It has been observed that both primary and secondary progressive MS tissues have an abnormal distribution of both ZO-1 and JAM proteins, and also that in EAE, the disruption of the BBB and alterations in junction proteins, especially ZO-1 occurs before the onset of clinical disease [128].

Having identified that BBB integrity is crucial in HSD-mediated disease protection, further analyses would have to be performed to characterize the potential roles of HSD-modified microbiota or metabolites in altering the barrier integrity. As we observed in this study, HSD acts as a preventive from EAE and does not act therapeutically. While compounds like resveratrol and idazoxan have been shown to ameliorate EAE by modulating JAM-1, Occludin, Claudin-5, and ZO-1 in the CNS endothelia, the only therapeutic drug used in MS targeting the BBB is Laquinimod [131, 343, 344]. In this regard, if further studies reveal associations between HSD-modified metabolites or microbiota and BBB alterations, these microbial species/metabolites can be explored therapeutically.

REFERENCES:

1. Lassmann, H., W. Brück, and C.F. Lucchinetti, *The Immunopathology of Multiple Sclerosis: An Overview*. 2007. **17**(2): p. 210-218.
2. Walton, C., et al., *Rising prevalence of multiple sclerosis worldwide: Insights from the Atlas of MS, third edition*. 2020. **26**(14): p. 1816-1821.
3. Tsang, B.K. and R. Macdonell, *Multiple sclerosis- diagnosis, management and prognosis*. Aust Fam Physician, 2011. **40**(12): p. 948-55.
4. Polman, C.H., et al., *Diagnostic criteria for multiple sclerosis: 2005 revisions to the "McDonald Criteria"*. 2005. **58**(6): p. 840-846.
5. Baranzini, S.E., *Revealing the genetic basis of multiple sclerosis: are we there yet?* Current Opinion in Genetics & Development, 2011. **21**(3): p. 317-324.
6. Milo, R. and E. Kahana, *Multiple sclerosis: Geoeidemiology, genetics and the environment*. Autoimmunity Reviews, 2010. **9**(5): p. A387-A394.
7. Ascherio, A. and K.L. Munger, *Environmental risk factors for multiple sclerosis. Part I: The role of infection*. 2007. **61**(4): p. 288-299.
8. Compston, A. and A. Coles, *Multiple sclerosis*. The Lancet, 2008. **372**(9648): p. 1502-1517.
9. Loma, I. and R. Heyman, *Multiple sclerosis: pathogenesis and treatment*. Current neuropharmacology, 2011. **9**(3): p. 409-416.
10. Jacobs, L.D., et al., *Intramuscular interferon beta-1a for disease progression in relapsing multiple sclerosis. The Multiple Sclerosis Collaborative Research Group (MSCRG)*. Ann Neurol, 1996. **39**(3): p. 285-94.
11. Procaccini, C., et al., *Animal models of Multiple Sclerosis*. European journal of pharmacology, 2015. **759**: p. 182-191.
12. Handel, A.E., M.R. Lincoln, and S.V. Ramagopalan, *Of mice and men: experimental autoimmune encephalitis and multiple sclerosis*. 2011. **41**(11): p. 1254-1258.
13. Rivers, T.M., D.H. Sprunt, and G.P. Berry, *OBSERVATIONS ON ATTEMPTS TO PRODUCE ACUTE DISSEMINATED ENCEPHALOMYELITIS IN MONKEYS*. The Journal of experimental medicine, 1933. **58**(1): p. 39-53.
14. Kabat, E.A., A. Wolf, and A.E. Bezer, *THE RAPID PRODUCTION OF ACUTE DISSEMINATED ENCEPHALOMYELITIS IN RHESUS MONKEYS BY INJECTION OF HETEROLOGOUS AND HOMOLOGOUS BRAIN TISSUE WITH ADJUVANTS*. The Journal of experimental medicine, 1947. **85**(1): p. 117-130.
15. Lipton, M.M. and J. Freund, *Encephalomyelitis in the rat following intracutaneous injection of central nervous system tissue with adjuvant*. Proc Soc Exp Biol Med, 1952. **81**(1): p. 260-1.
16. Olitsky, P.K. and R.H. Yager, *Experimental disseminated encephalomyelitis in white mice*. J Exp Med, 1949. **90**(3): p. 213-24.
17. Tuohy, V.K., et al., *Identification of an encephalitogenic determinant of myelin proteolipid protein for SJL mice*. J Immunol, 1989. **142**(5): p. 1523-7.
18. McRae, B.L., et al., *Induction of active and adoptive relapsing experimental autoimmune encephalomyelitis (EAE) using an encephalitogenic epitope of proteolipid protein*. J Neuroimmunol, 1992. **38**(3): p. 229-40.
19. Mendel, I., N. Kerlero de Rosbo, and A. Ben-Nun, *A myelin oligodendrocyte glycoprotein peptide induces typical chronic experimental autoimmune encephalomyelitis in H-2b mice: fine specificity and T cell receptor V beta expression of encephalitogenic T cells*. Eur J Immunol, 1995. **25**(7): p. 1951-9.
20. Gandhi, R., A. Laroni, and H.L. Weiner, *Role of the innate immune system in the pathogenesis of multiple sclerosis*. Journal of neuroimmunology, 2010. **221**(1-2): p. 7-14.
21. Goverman, J., *Autoimmune T cell responses in the central nervous system*. Nature Reviews Immunology, 2009. **9**(6): p. 393-407.

22. McFarland, H.F. and R. Martin, *Multiple sclerosis: a complicated picture of autoimmunity*. Nat Immunol, 2007. **8**(9): p. 913-9.
23. Hemmer, B., M. Kerschensteiner, and T. Korn, *Role of the innate and adaptive immune responses in the course of multiple sclerosis*. The Lancet Neurology, 2015. **14**(4): p. 406-419.
24. McMurray, R.W., *Adhesion molecules in autoimmune disease*. Semin Arthritis Rheum, 1996. **25**(4): p. 215-33.
25. Constantinescu, C.S., et al., *Experimental autoimmune encephalomyelitis (EAE) as a model for multiple sclerosis (MS)*. British journal of pharmacology, 2011. **164**(4): p. 1079-1106.
26. Zamvil, S., et al., *T-cell clones specific for myelin basic protein induce chronic relapsing paralysis and demyelination*. Nature, 1985. **317**(6035): p. 355-358.
27. Mathey, E.K., et al., *Neurofascin as a novel target for autoantibody-mediated axonal injury*. J Exp Med, 2007. **204**(10): p. 2363-72.
28. Krishnamoorthy, G., et al., *Myelin-specific T cells also recognize neuronal autoantigen in a transgenic mouse model of multiple sclerosis*. Nat Med, 2009. **15**(6): p. 626-32.
29. Derfuss, T., et al., *Contactin-2/TAG-1-directed autoimmunity is identified in multiple sclerosis patients and mediates gray matter pathology in animals*. Proc Natl Acad Sci U S A, 2009. **106**(20): p. 8302-7.
30. Goverman, J., et al., *Transgenic mice that express a myelin basic protein-specific T cell receptor develop spontaneous autoimmunity*. Cell, 1993. **72**(4): p. 551-560.
31. Adlard, K., et al., *Immunoregulation of encephalitogenic MBP-NAC1-11-reactive T cells by CD4+ TCR-specific T cells involves IL-4, IL-10 and IFN-gamma*. Autoimmunity, 1999. **31**(4): p. 237-248.
32. Bettelli, E., et al., *Myelin oligodendrocyte glycoprotein-specific T cell receptor transgenic mice develop spontaneous autoimmune optic neuritis*. J Exp Med, 2003. **197**(9): p. 1073-81.
33. Litzenburger, T., et al., *B lymphocytes producing demyelinating autoantibodies: development and function in gene-targeted transgenic mice*. J Exp Med, 1998. **188**(1): p. 169-80.
34. Krishnamoorthy, G., et al., *Spontaneous optico-spinal encephalomyelitis in a double-transgenic mouse model of autoimmune T cell/B cell cooperation* Journal of Clinical Investigation, 2006. **116**(9): p. 2385-2392.
35. Pöllinger, B., et al., *Spontaneous relapsing-remitting EAE in the SJL/J mouse: MOG-reactive transgenic T cells recruit endogenous MOG-specific B cells*. Journal of Experimental Medicine, 2009. **206**(6): p. 1303-1316.
36. Mosmann, T.R., et al., *Two types of murine helper T cell clone. I. Definition according to profiles of lymphokine activities and secreted proteins*. J Immunol, 1986. **136**(7): p. 2348-57.
37. Fletcher, J.M., et al., *T cells in multiple sclerosis and experimental autoimmune encephalomyelitis*. Clinical and Experimental Immunology, 2010. **162**(1): p. 1-11.
38. Panitch, H.S., et al., *Exacerbations of multiple sclerosis in patients treated with gamma interferon*. Lancet, 1987. **1**(8538): p. 893-895.
39. Bettelli, E., et al., *Loss of T-bet, but not STAT1, prevents the development of experimental autoimmune encephalomyelitis*. J Exp Med, 2004. **200**(1): p. 79-87.
40. Ferber, I.A., et al., *Mice with a disrupted IFN-gamma gene are susceptible to the induction of experimental autoimmune encephalomyelitis (EAE)*. J Immunol, 1996. **156**(1): p. 5-7.
41. Cua, D.J., et al., *Interleukin-23 rather than interleukin-12 is the critical cytokine for autoimmune inflammation of the brain*. Nature, 2003. **421**(6924): p. 744-8.
42. Langrish, C.L., et al., *IL-23 drives a pathogenic T cell population that induces autoimmune inflammation*. J Exp Med, 2005. **201**(2): p. 233-40.
43. Ruan, Q., et al., *The Th17 immune response is controlled by the Rel-RORγ-RORγT transcriptional axis*. The Journal of experimental medicine, 2011. **208**(11): p. 2321-2333.
44. Komiyama, Y., et al., *IL-17 plays an important role in the development of experimental autoimmune encephalomyelitis*. J Immunol, 2006. **177**(1): p. 566-73.

45. Hofstetter, H.H., et al., *Therapeutic efficacy of IL-17 neutralization in murine experimental autoimmune encephalomyelitis*. Cell Immunol, 2005. **237**(2): p. 123-30.
46. Grifka-Walk, H.M., D.A. Giles, and B.M. Segal, *IL-12-polarized Th1 cells produce GM-CSF and induce EAE independent of IL-23*. European journal of immunology, 2015. **45**(10): p. 2780-2786.
47. O'Connor, R.A., et al., *Cutting edge: Th1 cells facilitate the entry of Th17 cells to the central nervous system during experimental autoimmune encephalomyelitis*. J Immunol, 2008. **181**(6): p. 3750-4.
48. Lees, J.R., Y. Iwakura, and J.H. Russell, *Host T cells are the main producers of IL-17 within the central nervous system during initiation of experimental autoimmune encephalomyelitis induced by adoptive transfer of Th1 cell lines*. J Immunol, 2008. **180**(12): p. 8066-72.
49. Kroenke, M.A., et al., *IL-12- and IL-23-modulated T cells induce distinct types of EAE based on histology, CNS chemokine profile, and response to cytokine inhibition*. J Exp Med, 2008. **205**(7): p. 1535-41.
50. Abromson-Leeman, S., R.T. Bronson, and M.E. Dorf, *Encephalitogenic T cells that stably express both T-bet and ROR gamma t consistently produce IFN γ but have a spectrum of IL-17 profiles*. J Neuroimmunol, 2009. **215**(1-2): p. 10-24.
51. Gocke, A.R., et al., *T-bet regulates the fate of Th1 and Th17 lymphocytes in autoimmunity*. J Immunol, 2007. **178**(3): p. 1341-8.
52. Haas, J., et al., *Reduced suppressive effect of CD4⁺CD25^{high} regulatory T cells on the T cell immune response against myelin oligodendrocyte glycoprotein in patients with multiple sclerosis*. Eur J Immunol, 2005. **35**(11): p. 3343-52.
53. Kohm, A.P., et al., *Cutting edge: CD4⁺CD25⁺ regulatory T cells suppress antigen-specific autoreactive immune responses and central nervous system inflammation during active experimental autoimmune encephalomyelitis*. J Immunol, 2002. **169**(9): p. 4712-6.
54. Zhang, X., et al., *IL-10 is involved in the suppression of experimental autoimmune encephalomyelitis by CD25⁺CD4⁺ regulatory T cells*. Int Immunol, 2004. **16**(2): p. 249-56.
55. Reddy, J., et al., *Myelin proteolipid protein-specific CD4⁺CD25⁺ regulatory cells mediate genetic resistance to experimental autoimmune encephalomyelitis*. Proc Natl Acad Sci U S A, 2004. **101**(43): p. 15434-9.
56. McGeachy, M.J., L.A. Stephens, and S.M. Anderson, *Natural recovery and protection from autoimmune encephalomyelitis: contribution of CD4⁺CD25⁺ regulatory cells within the central nervous system*. J Immunol, 2005. **175**(5): p. 3025-32.
57. Korn, T., et al., *Myelin-specific regulatory T cells accumulate in the CNS but fail to control autoimmune inflammation*. Nat Med, 2007. **13**(4): p. 423-31.
58. Fletcher, J.M., et al., *CD39⁺Foxp3⁺ regulatory T Cells suppress pathogenic Th17 cells and are impaired in multiple sclerosis*. J Immunol, 2009. **183**(11): p. 7602-10.
59. Zang, Y.C., et al., *Increased CD8⁺ cytotoxic T cell responses to myelin basic protein in multiple sclerosis*. J Immunol, 2004. **172**(8): p. 5120-7.
60. Tsuchida, T., et al., *Autoreactive CD8⁺ T-cell responses to human myelin protein-derived peptides*. Proceedings of the National Academy of Sciences of the United States of America, 1994. **91**(23): p. 10859-10863.
61. Healy, B.C., et al., *HLA B*44: protective effects in MS susceptibility and MRI outcome measures*. Neurology, 2010. **75**(7): p. 634-40.
62. Huseby, E.S., et al., *A pathogenic role for myelin-specific CD8⁺ T cells in a model for multiple sclerosis*. The Journal of experimental medicine, 2001. **194**(5): p. 669-676.
63. Sun, D., et al., *Myelin Antigen-Specific CD8⁺ T Cells Are Encephalitogenic and Produce Severe Disease in C57BL/6 Mice*. 2001. **166**(12): p. 7579-7587.
64. Ford, M.L. and B.D. Evavold, *Specificity, magnitude, and kinetics of MOG-specific CD8⁺ T cell responses during experimental autoimmune encephalomyelitis*. Eur J Immunol, 2005. **35**(1): p. 76-85.

65. Sasaki, K., et al., *Relapsing-remitting central nervous system autoimmunity mediated by GFAP-specific CD8 T cells*. Journal of immunology (Baltimore, Md. : 1950), 2014. **192**(7): p. 3029-3042.
66. Huber, M., et al., *IL-17A secretion by CD8+ T cells supports Th17-mediated autoimmune encephalomyelitis*. The Journal of clinical investigation, 2013. **123**(1): p. 247-260.
67. Mars, L.T., et al., *CD8 T Cell Responses to Myelin Oligodendrocyte Glycoprotein-Derived Peptides in Humanized HLA-A*0201-Transgenic Mice*. 2007. **179**(8): p. 5090-5098.
68. Brisebois, M., et al., *A Pathogenic Role for CD8+ T Cells in a Spontaneous Model of Demyelinating Disease*. 2006. **177**(4): p. 2403-2411.
69. Na, S.-Y., et al., *Naïve CD8 T-cells initiate spontaneous autoimmunity to a sequestered model antigen of the central nervous system*. Brain, 2008. **131**(9): p. 2353-2365.
70. Wagner, C.A., et al., *Myelin-specific CD8+ T cells exacerbate brain inflammation in CNS autoimmunity*. The Journal of Clinical Investigation, 2020. **130**(1): p. 203-213.
71. Koh, D.-R., et al., *Less Mortality but More Relapses in Experimental Allergic Encephalomyelitis in CD8^{-/-} Mice*. 1992. **256**(5060): p. 1210-1213.
72. Friese, M.A., et al., *Opposing effects of HLA class I molecules in tuning autoreactive CD8+ T cells in multiple sclerosis*. Nature Medicine, 2008. **14**(11): p. 1227-1235.
73. Boyden, A., et al., *CNS-specific autoregulatory CD8 T cells rely on IFN γ signaling for optimal suppression of pathogenic CD4 T cell responses during inhibition of demyelinating disease*. 2019. **202**(1 Supplement): p. 115.9-115.9.
74. York, N.R., et al., *Immune regulatory CNS-reactive CD8+T cells in experimental autoimmune encephalomyelitis*. Journal of autoimmunity, 2010. **35**(1): p. 33-44.
75. Jiang, H., et al., *CD8+ T cells control the TH phenotype of MBP-reactive CD4+ T cells in EAE mice*. Proceedings of the National Academy of Sciences of the United States of America, 2001. **98**(11): p. 6301-6306.
76. Tyler, A.F., et al., *CD8(+) T Cells Are Required For Glatiramer Acetate Therapy in Autoimmune Demyelinating Disease*. PloS one, 2013. **8**(6): p. e66772-e66772.
77. Willenborg, D.O. and S.J. Prowse, *Immunoglobulin-deficient rats fail to develop experimental allergic encephalomyelitis*. J Neuroimmunol, 1983. **5**(2): p. 99-109.
78. Willenborg, D.O., P. Sjollem, and G. Danta, *Immunoglobulin deficient rats as donors and recipients of effector cells of allergic encephalomyelitis*. J Neuroimmunol, 1986. **11**(2): p. 93-103.
79. Schluesener, H.J., et al., *A monoclonal antibody against a myelin oligodendrocyte glycoprotein induces relapses and demyelination in central nervous system autoimmune disease*. J Immunol, 1987. **139**(12): p. 4016-21.
80. Monson, N.L., et al., *Rituximab therapy reduces organ-specific T cell responses and ameliorates experimental autoimmune encephalomyelitis*. PLoS One, 2011. **6**(2): p. e17103.
81. Fillatreau, S., et al., *B cells regulate autoimmunity by provision of IL-10*. Nat Immunol, 2002. **3**(10): p. 944-50.
82. Harris, D.P., et al., *Reciprocal regulation of polarized cytokine production by effector B and T cells*. Nat Immunol, 2000. **1**(6): p. 475-82.
83. Mann, M.K., et al., *B cell regulation of CD4+CD25+ T regulatory cells and IL-10 via B7 is essential for recovery from experimental autoimmune encephalomyelitis*. J Immunol, 2007. **178**(6): p. 3447-56.
84. Ray, A., et al., *A novel IL-10-independent regulatory role for B cells in suppressing autoimmunity by maintenance of regulatory T cells via GITR ligand*. Journal of immunology (Baltimore, Md. : 1950), 2012. **188**(7): p. 3188-3198.
85. Schubert, R.D., et al., *IFN- β Treatment Requires B Cells for Efficacy in Neuroautoimmunity*. 2015. **194**(5): p. 2110-2116.
86. Matsushita, T., et al., *Regulatory B cells inhibit EAE initiation in mice while other B cells promote disease progression*. J Clin Invest, 2008. **118**(10): p. 3420-30.

87. Lisak, R.P., et al., *B cells from patients with multiple sclerosis induce cell death via apoptosis in neurons in vitro*. Journal of Neuroimmunology, 2017. **309**: p. 88-99.
88. Lisak, R.P., et al., *Secretory products of multiple sclerosis B cells are cytotoxic to oligodendroglia in vitro*. Journal of Neuroimmunology, 2012. **246**(1): p. 85-95.
89. Wang, J., et al., *Targeting Microglia and Macrophages: A Potential Treatment Strategy for Multiple Sclerosis*. 2019. **10**(286).
90. Yamasaki, R., et al., *Differential roles of microglia and monocytes in the inflamed central nervous system*. Journal of Experimental Medicine, 2014. **211**(8): p. 1533-1549.
91. Trebst, C., et al., *CCR1+/CCR5+ Mononuclear Phagocytes Accumulate in the Central Nervous System of Patients with Multiple Sclerosis*. The American Journal of Pathology, 2001. **159**(5): p. 1701-1710.
92. Valentin-Torres, A., et al., *Sustained TNF production by central nervous system infiltrating macrophages promotes progressive autoimmune encephalomyelitis*. Journal of Neuroinflammation, 2016. **13**(1): p. 46.
93. Tsutsui, M., et al., *TRPM2 Exacerbates Central Nervous System Inflammation in Experimental Autoimmune Encephalomyelitis by Increasing Production of CXCL2 Chemokines*. 2018. **38**(39): p. 8484-8495.
94. Terrazas, C., et al., *Helminth-induced Ly6Chi monocyte-derived alternatively activated macrophages suppress experimental autoimmune encephalomyelitis*. Scientific Reports, 2017. **7**(1): p. 40814.
95. Denney, L., et al., *Activation of Invariant NKT Cells in Early Phase of Experimental Autoimmune Encephalomyelitis Results in Differentiation of Ly6C^{hi} Inflammatory Monocyte to M2 Macrophages and Improved Outcome*. 2012. **189**(2): p. 551-557.
96. Yang, Q., et al., *Spermidine alleviates experimental autoimmune encephalomyelitis through inducing inhibitory macrophages*. Cell Death & Differentiation, 2016. **23**(11): p. 1850-1861.
97. Weng, Q., et al., *Lenalidomide regulates CNS autoimmunity by promoting M2 macrophages polarization*. Cell Death & Disease, 2018. **9**(2): p. 251.
98. Naegele, M., et al., *Neutrophils in multiple sclerosis are characterized by a primed phenotype*. J Neuroimmunol, 2012. **242**(1-2): p. 60-71.
99. Demirci, S., et al., *The clinical significance of the neutrophil-to-lymphocyte ratio in multiple sclerosis*. International Journal of Neuroscience, 2016. **126**(8): p. 700-706.
100. Steinbach, K., et al., *Neutrophils Amplify Autoimmune Central Nervous System Infiltrates by Maturing Local APCs*. 2013. **191**(9): p. 4531-4539.
101. Pierson, E.R., C.A. Wagner, and J.M. Goverman, *The contribution of neutrophils to CNS autoimmunity*. Clinical immunology (Orlando, Fla.), 2018. **189**: p. 23-28.
102. Aubé, B., et al., *Neutrophils mediate blood-spinal cord barrier disruption in demyelinating neuroinflammatory diseases*. J Immunol, 2014. **193**(5): p. 2438-54.
103. McColl, S.R., et al., *Treatment with anti-granulocyte antibodies inhibits the effector phase of experimental autoimmune encephalomyelitis*. J Immunol, 1998. **161**(11): p. 6421-6.
104. Greter, M., et al., *Dendritic cells permit immune invasion of the CNS in an animal model of multiple sclerosis*. Nature Medicine, 2005. **11**(3): p. 328-334.
105. Wu, G.F., et al., *Limited sufficiency of antigen presentation by dendritic cells in models of central nervous system autoimmunity*. J Autoimmun, 2011. **36**(1): p. 56-64.
106. Isaksson, M., et al., *Plasmacytoid DC promote priming of autoimmune Th17 cells and EAE*. 2009. **39**(10): p. 2925-2935.
107. Zozulya, A.L., et al., *The role of dendritic cells in CNS autoimmunity*. Journal of molecular medicine (Berlin, Germany), 2010. **88**(6): p. 535-544.
108. Clarkson, B.D., et al., *Innate-adaptive crosstalk: how dendritic cells shape immune responses in the CNS*. Advances in experimental medicine and biology, 2012. **946**: p. 309-333.
109. Yogev, N., et al., *Dendritic Cells Ameliorate Autoimmunity in the CNS by Controlling the Homeostasis of PD-1 Receptor+ Regulatory T Cells*. Immunity, 2012. **37**(2): p. 264-275.

110. Kashi, V., S. Ortega, and N. Karandikar, *Neuroantigen-Specific Autoregulatory CD8+T Cells Inhibit Autoimmune Demyelination through Modulation of Dendritic Cell Function*. PloS one, 2014. **9**: p. e105763.
111. Wei, H.-J., et al., *A unique tolerizing dendritic cell phenotype induced by the synthetic triterpenoid CDDO-DFPA (RTA-408) is protective against EAE*. Scientific Reports, 2017. **7**(1): p. 9886.
112. Quintana, F.J., A. Yeste, and I.D. Manciasfroni, *Role and therapeutic value of dendritic cells in central nervous system autoimmunity*. Cell Death & Differentiation, 2015. **22**(2): p. 215-224.
113. Dopp, J.M., S.M. Breneman, and J.A. Olschowka, *Expression of ICAM-1, VCAM-1, L-selectin, and leukosialin in the mouse central nervous system during the induction and remission stages of experimental allergic encephalomyelitis*. J Neuroimmunol, 1994. **54**(1-2): p. 129-44.
114. Glatigny, S., et al., *Cutting Edge: Loss of $\alpha 4$ Integrin Expression Differentially Affects the Homing of Th1 and Th17 Cells*. 2011. **187**(12): p. 6176-6179.
115. Rothhammer, V., et al., *Th17 lymphocytes traffic to the central nervous system independently of $\alpha 4$ integrin expression during EAE*. Journal of Experimental Medicine, 2011. **208**(12): p. 2465-2476.
116. Kuwahara, H., K. Nishina, and T. Yokota, *Blood-brain barrier: A novel therapeutic target in multiple sclerosis*. 2015. **6**(2): p. 129-138.
117. Krumbholz, M., et al., *Chemokines in multiple sclerosis: CXCL12 and CXCL13 up-regulation is differentially linked to CNS immune cell recruitment*. Brain, 2005. **129**(1): p. 200-211.
118. Holman, D.W., R.S. Klein, and R.M. Ransohoff, *The blood-brain barrier, chemokines and multiple sclerosis*. Biochim Biophys Acta, 2011. **1812**(2): p. 220-30.
119. Karpus, W.J., *Cytokines and Chemokines in the Pathogenesis of Experimental Autoimmune Encephalomyelitis*. 2020. **204**(2): p. 316-326.
120. Mony, J.T., R. Khoroshi, and T. Owens, *Chemokine receptor expression by inflammatory T cells in EAE*. Front Cell Neurosci, 2014. **8**: p. 187.
121. Reboldi, A., et al., *C-C chemokine receptor 6-regulated entry of TH-17 cells into the CNS through the choroid plexus is required for the initiation of EAE*. Nat Immunol, 2009. **10**(5): p. 514-23.
122. Piccio, L., et al., *Molecular mechanisms involved in lymphocyte recruitment in inflamed brain microvessels: critical roles for P-selectin glycoprotein ligand-1 and heterotrimeric G(i)-linked receptors*. J Immunol, 2002. **168**(4): p. 1940-9.
123. Kerfoot, S.M., et al., *Reevaluation of P-Selectin and $\alpha 4$ Integrin as Targets for the Treatment of Experimental Autoimmune Encephalomyelitis*. 2006. **176**(10): p. 6225-6234.
124. Lyck, R. and B. Engelhardt, *Going against the tide--how encephalitogenic T cells breach the blood-brain barrier*. J Vasc Res, 2012. **49**(6): p. 497-509.
125. Muller, W.A., *Leukocyte-endothelial-cell interactions in leukocyte transmigration and the inflammatory response*. Trends Immunol, 2003. **24**(6): p. 327-34.
126. Lutz, S.E., et al., *Caveolin1 Is Required for Th1 Cell Infiltration, but Not Tight Junction Remodeling, at the Blood-Brain Barrier in Autoimmune Neuroinflammation*. Cell Reports, 2017. **21**(8): p. 2104-2117.
127. Gao, J., et al., *Impact of the Gut Microbiota on Intestinal Immunity Mediated by Tryptophan Metabolism*. Front Cell Infect Microbiol, 2018. **8**: p. 13.
128. Bennett, J., et al., *Blood-brain barrier disruption and enhanced vascular permeability in the multiple sclerosis model EAE*. J Neuroimmunol, 2010. **229**(1-2): p. 180-91.
129. Kebir, H., et al., *Human TH17 lymphocytes promote blood-brain barrier disruption and central nervous system inflammation*. Nature medicine, 2007. **13**(10): p. 1173-1175.
130. Kügler, S., et al., *Pertussis toxin transiently affects barrier integrity, organelle organization and transmigration of monocytes in a human brain microvascular endothelial cell barrier model*. Cell Microbiol, 2007. **9**(3): p. 619-32.

131. Wang, D., et al., *Resveratrol defends blood-brain barrier integrity in experimental autoimmune encephalomyelitis mice*. Journal of neurophysiology, 2016. **116**(5): p. 2173-2179.
132. van Horssen, J., et al., *Clusters of activated microglia in normal-appearing white matter show signs of innate immune activation*. Journal of Neuroinflammation, 2012. **9**(1): p. 156.
133. Singh, S., et al., *Microglial nodules in early multiple sclerosis white matter are associated with degenerating axons*. Acta Neuropathologica, 2013. **125**(4): p. 595-608.
134. Jordão, M.J.C., et al., *Single-cell profiling identifies myeloid cell subsets with distinct fates during neuroinflammation*. 2019. **363**(6425): p. eaat7554.
135. Murphy, Á.C., et al., *Infiltration of Th1 and Th17 cells and activation of microglia in the CNS during the course of experimental autoimmune encephalomyelitis*. Brain, Behavior, and Immunity, 2010. **24**(4): p. 641-651.
136. Sanchis, P., et al., *Interleukin-6 Derived from the Central Nervous System May Influence the Pathogenesis of Experimental Autoimmune Encephalomyelitis in a Cell-Dependent Manner*. 2020. **9**(2): p. 330.
137. Farez, M.F., et al., *Toll-like receptor 2 and poly(ADP-ribose) polymerase 1 promote central nervous system neuroinflammation in progressive EAE*. Nature Immunology, 2009. **10**(9): p. 958-964.
138. Musella, A., et al., *Central Modulation of Selective Sphingosine-1-Phosphate Receptor 1 Ameliorates Experimental Multiple Sclerosis*. 2020. **9**(5): p. 1290.
139. Plastini, M.J., H.L. Desu, and R. Brambilla, *Dynamic Responses of Microglia in Animal Models of Multiple Sclerosis*. 2020. **14**(269).
140. Ding, X., et al., *Silencing IFN- γ Binding/Signaling in Astrocytes versus Microglia Leads to Opposite Effects on Central Nervous System Autoimmunity*. 2015. **194**(9): p. 4251-4264.
141. Kocur, M., et al., *IFN β secreted by microglia mediates clearance of myelin debris in CNS autoimmunity*. Acta Neuropathologica Communications, 2015. **3**(1): p. 20.
142. Khorooshi, R., et al., *Induction of endogenous Type I interferon within the central nervous system plays a protective role in experimental autoimmune encephalomyelitis*. Acta Neuropathologica, 2015. **130**(1): p. 107-118.
143. Rothhammer, V., et al., *Microglial control of astrocytes in response to microbial metabolites*. Nature, 2018. **557**(7707): p. 724-728.
144. Włodarczyk, A., et al., *CSF1R Stimulation Promotes Increased Neuroprotection by CD11c+ Microglia in EAE*. 2019. **12**(523).
145. Pham, H., et al., *The astrocytic response in early experimental autoimmune encephalomyelitis occurs across both the grey and white matter compartments*. J Neuroimmunol, 2009. **208**(1-2): p. 30-9.
146. Luo, J., et al., *Bioluminescence in vivo imaging of autoimmune encephalomyelitis predicts disease*. J Neuroinflammation, 2008. **5**: p. 6.
147. D'Amelio, F.E., M.E. Smith, and L.F. Eng, *Sequence of tissue responses in the early stages of experimental allergic encephalomyelitis (EAE): immunohistochemical, light microscopic, and ultrastructural observations in the spinal cord*. Glia, 1990. **3**(4): p. 229-40.
148. Mayo, L., et al., *Regulation of astrocyte activation by glycolipids drives chronic CNS inflammation*. Nat Med, 2014. **20**(10): p. 1147-56.
149. Toft-Hansen, H., L. Füchtbauer, and T. Owens, *Inhibition of reactive astrocytosis in established experimental autoimmune encephalomyelitis favors infiltration by myeloid cells over T cells and enhances severity of disease*. Glia, 2011. **59**(1): p. 166-76.
150. Tran, E.H., et al., *Astrocytes and microglia express inducible nitric oxide synthase in mice with experimental allergic encephalomyelitis*. J Neuroimmunol, 1997. **74**(1-2): p. 121-9.
151. Agrawal, S., et al., *Dystroglycan is selectively cleaved at the parenchymal basement membrane at sites of leukocyte extravasation in experimental autoimmune encephalomyelitis*. J Exp Med, 2006. **203**(4): p. 1007-19.

152. Alvarez, J.I., et al., *The Hedgehog pathway promotes blood-brain barrier integrity and CNS immune quiescence*. Science, 2011. **334**(6063): p. 1727-31.
153. Rothhammer, V., et al., *Sphingosine 1-phosphate receptor modulation suppresses pathogenic astrocyte activation and chronic progressive CNS inflammation*. Proc Natl Acad Sci U S A, 2017. **114**(8): p. 2012-2017.
154. Choi, J.W., et al., *FTY720 (fingolimod) efficacy in an animal model of multiple sclerosis requires astrocyte sphingosine 1-phosphate receptor 1 (S1P1) modulation*. Proc Natl Acad Sci U S A, 2011. **108**(2): p. 751-6.
155. Rothhammer, V., et al., *Type I interferons and microbial metabolites of tryptophan modulate astrocyte activity and central nervous system inflammation via the aryl hydrocarbon receptor*. Nat Med, 2016. **22**(6): p. 586-97.
156. Willer, C.J., et al., *Twin concordance and sibling recurrence rates in multiple sclerosis*. 2003. **100**(22): p. 12877-12882.
157. Handel, A.E., et al., *Environmental factors and their timing in adult-onset multiple sclerosis*. Nature Reviews Neurology, 2010. **6**(3): p. 156-166.
158. Fleming, J. and Z. Fabry, *The hygiene hypothesis and multiple sclerosis*. Annals of Neurology, 2007. **61**(2): p. 85-89.
159. Rook, G.W., *Hygiene Hypothesis and Autoimmune Diseases*. Clinical Reviews in Allergy & Immunology, 2012. **42**(1): p. 5-15.
160. Scudellari, M., *News Feature: Cleaning up the hygiene hypothesis*. Proceedings of the National Academy of Sciences, 2017. **114**(7): p. 1433-1436.
161. Bach, J.F., *The hygiene hypothesis in autoimmunity: the role of pathogens and commensals*. Nat Rev Immunol, 2018. **18**(2): p. 105-120.
162. Bloomfield, S.F., et al., *Time to abandon the hygiene hypothesis: new perspectives on allergic disease, the human microbiome, infectious disease prevention and the role of targeted hygiene*. Perspectives in Public Health, 2016. **136**(4): p. 213-224.
163. Okada, H., et al., *The 'hygiene hypothesis' for autoimmune and allergic diseases: an update*. Clinical and Experimental Immunology, 2010. **160**(1): p. 1-9.
164. Kuo, C.-H., et al., *Early life exposure to antibiotics and the risk of childhood allergic diseases: An update from the perspective of the hygiene hypothesis*. Journal of Microbiology, Immunology and Infection, 2013. **46**(5): p. 320-329.
165. Bloomfield, S.F., et al., *Too clean, or not too clean: the hygiene hypothesis and home hygiene*. Clinical and experimental allergy : journal of the British Society for Allergy and Clinical Immunology, 2006. **36**(4): p. 402-425.
166. Clemente, J.C., et al., *The impact of the gut microbiota on human health: An integrative view*. Cell, 2012. **148**(6): p. 1258-1270.
167. Human Microbiome Project, C., *Structure, function and diversity of the healthy human microbiome*. Nature, 2012. **486**(7402): p. 207-14.
168. Shreiner, A.B., J.Y. Kao, and V.B. Young, *The gut microbiome in health and in disease*. Current opinion in gastroenterology, 2015. **31**(1): p. 69-75.
169. Dominguez-Bello, M.G., et al., *Delivery mode shapes the acquisition and structure of the initial microbiota across multiple body habitats in newborns*. 2010. **107**(26): p. 11971-11975.
170. Yoshioka, H., K. Iseki, and K. Fujita, *Development and differences of intestinal flora in the neonatal period in breast-fed and bottle-fed infants*. Pediatrics, 1983. **72**(3): p. 317-21.
171. Tamburini, S., et al., *The microbiome in early life: implications for health outcomes*. Nature Medicine, 2016. **22**(7): p. 713-722.
172. Larsbrink, J., et al., *A discrete genetic locus confers xyloglucan metabolism in select human gut Bacteroidetes*. Nature, 2014. **506**(7489): p. 498-502.
173. Xu, J., et al., *A Genomic View of the Human-Bacteroides thetaiotaomicron Symbiosis*. 2003. **299**(5615): p. 2074-2076.

174. Koh, A., et al., *From Dietary Fiber to Host Physiology: Short-Chain Fatty Acids as Key Bacterial Metabolites*. Cell, 2016. **165**(6): p. 1332-1345.
175. Portune, K.J., et al., *Gut microbiota role in dietary protein metabolism and health-related outcomes: The two sides of the coin*. Trends in Food Science & Technology, 2016. **57**: p. 213-232.
176. Pugin, B., et al., *A wide diversity of bacteria from the human gut produces and degrades biogenic amines*. Microb Ecol Health Dis, 2017. **28**(1): p. 1353881.
177. Li, G. and K.D. Young, *Indole production by the tryptophanase TnaA in Escherichia coli is determined by the amount of exogenous tryptophan*. 2013. **159**(Pt_2): p. 402-410.
178. Martens, J.H., et al., *Microbial production of vitamin B12*. Applied Microbiology and Biotechnology, 2002. **58**(3): p. 275-285.
179. LeBlanc, J.G., et al., *Bacteria as vitamin suppliers to their host: a gut microbiota perspective*. Current Opinion in Biotechnology, 2013. **24**(2): p. 160-168.
180. Hill, M.J., *Intestinal flora and endogenous vitamin synthesis*. Eur J Cancer Prev, 1997. **6 Suppl 1**: p. S43-5.
181. Dao, M.C., et al., *Akkermansia muciniphila and improved metabolic health during a dietary intervention in obesity: relationship with gut microbiome richness and ecology*. Gut, 2016. **65**(3): p. 426-36.
182. Visconti, A., et al., *Interplay between the human gut microbiome and host metabolism*. Nature Communications, 2019. **10**(1): p. 4505.
183. Rey, F.E., et al., *Metabolic niche of a prominent sulfate-reducing human gut bacterium*. Proc Natl Acad Sci U S A, 2013. **110**(33): p. 13582-7.
184. Takeno, S. and T. Sakai, *Involvement of the intestinal microflora in nitrazepam-induced teratogenicity in rats and its relationship to nitroreduction*. Teratology, 1991. **44**(2): p. 209-14.
185. Elmer, G.W. and R.P. Remmel, *Role of the intestinal microflora in clonazepam metabolism in the rat*. Xenobiotica, 1984. **14**(11): p. 829-40.
186. Basit, A.W. and L.F. Lacey, *Colonic metabolism of ranitidine: implications for its delivery and absorption*. Int J Pharm, 2001. **227**(1-2): p. 157-65.
187. Koch, R.L., et al., *Acetamide--a metabolite of metronidazole formed by the intestinal flora*. Biochem Pharmacol, 1979. **28**(24): p. 3611-5.
188. Goldin, B.R., M.A. Peppercorn, and P. Goldman, *Contributions of host and intestinal microflora in the metabolism of L-dopa by the rat*. J Pharmacol Exp Ther, 1973. **186**(1): p. 160-6.
189. Holt, R., *The bacterial degradation of chloramphenicol*. Lancet, 1967. **1**(7502): p. 1259-60.
190. Lindenbaum, J., et al., *Inactivation of digoxin by the gut flora: reversal by antibiotic therapy*. N Engl J Med, 1981. **305**(14): p. 789-94.
191. Zheng, D., T. Liwinski, and E. Elinav, *Interaction between microbiota and immunity in health and disease*. Cell Research, 2020. **30**(6): p. 492-506.
192. Wu, H.-J. and E. Wu, *The role of gut microbiota in immune homeostasis and autoimmunity*. Gut microbes, 2012. **3**(1): p. 4-14.
193. Round, J.L. and S.K. Mazmanian, *The gut microbiota shapes intestinal immune responses during health and disease*. Nature Reviews Immunology, 2009. **9**(5): p. 313-323.
194. Rachmilewitz, D., et al., *Toll-like receptor 9 signaling mediates the anti-inflammatory effects of probiotics in murine experimental colitis*. Gastroenterology, 2004. **126**(2): p. 520-8.
195. Rakoff-Nahoum, S., et al., *Recognition of Commensal Microflora by Toll-Like Receptors Is Required for Intestinal Homeostasis*. Cell, 2004. **118**(2): p. 229-241.
196. Abreu, M.T., *Toll-like receptor signalling in the intestinal epithelium: how bacterial recognition shapes intestinal function*. Nature Reviews Immunology, 2010. **10**(2): p. 131-144.
197. Bachem, A., et al., *Microbiota-Derived Short-Chain Fatty Acids Promote the Memory Potential of Antigen-Activated CD8+ T Cells*. Immunity, 2019. **51**(2): p. 285-297.e5.
198. Teng, F., et al., *Gut Microbiota Drive Autoimmune Arthritis by Promoting Differentiation and Migration of Peyer's Patch T Follicular Helper Cells*. Immunity, 2016. **44**(4): p. 875-888.

199. Rosser, E.C., et al., *Regulatory B cells are induced by gut microbiota–driven interleukin-18 and interleukin-6 production*. *Nature Medicine*, 2014. **20**(11): p. 1334-1339.
200. Sommer, F. and F. Bäckhed, *The gut microbiota — masters of host development and physiology*. *Nature Reviews Microbiology*, 2013. **11**(4): p. 227-238.
201. Schmidt, B., et al., *Establishment of Normal Gut Microbiota Is Compromised under Excessive Hygiene Conditions*. *PLOS ONE*, 2011. **6**(12): p. e28284.
202. Turnbaugh, P.J., et al., *A core gut microbiome in obese and lean twins*. *Nature*, 2009. **457**(7228): p. 480-484.
203. Goodrich, Julia K., et al., *Human Genetics Shape the Gut Microbiome*. *Cell*, 2014. **159**(4): p. 789-799.
204. Goodrich, Julia K., et al., *Genetic Determinants of the Gut Microbiome in UK Twins*. *Cell Host & Microbe*, 2016. **19**(5): p. 731-743.
205. Spor, A., O. Koren, and R. Ley, *Unravelling the effects of the environment and host genotype on the gut microbiome*. *Nature Reviews Microbiology*, 2011. **9**(4): p. 279-290.
206. Willmann, M., et al., *Distinct impact of antibiotics on the gut microbiome and resistome: a longitudinal multicenter cohort study*. *BMC Biology*, 2019. **17**(1): p. 76.
207. Elvers, K.T., et al., *Antibiotic-induced changes in the human gut microbiota for the most commonly prescribed antibiotics in primary care in the UK: a systematic review*. 2020. **10**(9): p. e035677.
208. Brismar, B., C. Edlund, and C.E. Nord, *Impact of cefpodoxime proxetil and amoxicillin on the normal oral and intestinal microflora*. *Eur J Clin Microbiol Infect Dis*, 1993. **12**(9): p. 714-9.
209. Edlund, C., et al., *Comparative effects of moxifloxacin and clarithromycin on the normal intestinal microflora*. *Scand J Infect Dis*, 2000. **32**(1): p. 81-5.
210. Mangin, I., et al., *Long-term changes in human colonic Bifidobacterium populations induced by a 5-day oral amoxicillin-clavulanic acid treatment*. *PLoS One*, 2012. **7**(11): p. e50257.
211. Vich Vila, A., et al., *Impact of commonly used drugs on the composition and metabolic function of the gut microbiota*. *Nature Communications*, 2020. **11**(1): p. 362.
212. Freedberg, D.E., et al., *Proton Pump Inhibitors Alter Specific Taxa in the Human Gastrointestinal Microbiome: A Crossover Trial*. *Gastroenterology*, 2015. **149**(4): p. 883-885.e9.
213. Imhann, F., et al., *Proton pump inhibitors affect the gut microbiome*. 2016. **65**(5): p. 740-748.
214. Forslund, K., et al., *Disentangling type 2 diabetes and metformin treatment signatures in the human gut microbiota*. *Nature*, 2015. **528**(7581): p. 262-266.
215. Carmody, Rachel N., et al., *Diet Dominates Host Genotype in Shaping the Murine Gut Microbiota*. *Cell Host & Microbe*, 2015. **17**(1): p. 72-84.
216. Wu, G.D., et al., *Linking Long-Term Dietary Patterns with Gut Microbial Enterotypes*. 2011. **334**(6052): p. 105-108.
217. David, L.A., et al., *Diet rapidly and reproducibly alters the human gut microbiome*. *Nature*, 2014. **505**(7484): p. 559-563.
218. Muegge, B.D., et al., *Diet Drives Convergence in Gut Microbiome Functions Across Mammalian Phylogeny and Within Humans*. 2011. **332**(6032): p. 970-974.
219. Smits, S.A., et al., *Seasonal cycling in the gut microbiome of the Hadza hunter-gatherers of Tanzania*. *Science (New York, N.Y.)*, 2017. **357**(6353): p. 802-806.
220. Kolodziejczyk, A.A., D. Zheng, and E. Elinav, *Diet–microbiota interactions and personalized nutrition*. *Nature Reviews Microbiology*, 2019. **17**(12): p. 742-753.
221. Zinöcker, M.K. and I.A. Lindseth, *The Western Diet-Microbiome-Host Interaction and Its Role in Metabolic Disease*. *Nutrients*, 2018. **10**(3).
222. Noble, E.E., T.M. Hsu, and S.E. Kanoski, *Gut to Brain Dysbiosis: Mechanisms Linking Western Diet Consumption, the Microbiome, and Cognitive Impairment*. 2017. **11**(9).
223. Bier, A., et al., *A High Salt Diet Modulates the Gut Microbiota and Short Chain Fatty Acids Production in a Salt-Sensitive Hypertension Rat Model*. *Nutrients*, 2018. **10**(9): p. 1154.

224. Zelante, T., et al., *Tryptophan Catabolites from Microbiota Engage Aryl Hydrocarbon Receptor and Balance Mucosal Reactivity via Interleukin-22*. *Immunity*, 2013. **39**(2): p. 372-385.
225. Miranda, P.M., et al., *High salt diet exacerbates colitis in mice by decreasing Lactobacillus levels and butyrate production*. *Microbiome*, 2018. **6**(1): p. 57.
226. Parks, B.W., et al., *Genetic control of obesity and gut microbiota composition in response to high-fat, high-sucrose diet in mice*. *Cell Metab*, 2013. **17**(1): p. 141-52.
227. Wolters, M., et al., *Dietary fat, the gut microbiota, and metabolic health - A systematic review conducted within the MyNewGut project*. *Clin Nutr*, 2019. **38**(6): p. 2504-2520.
228. Laursen, M.F., et al., *Infant Gut Microbiota Development Is Driven by Transition to Family Foods Independent of Maternal Obesity*. *mSphere*, 2016. **1**(1).
229. Wan, Y., et al., *Effects of dietary fat on gut microbiota and faecal metabolites, and their relationship with cardiometabolic risk factors: a 6-month randomised controlled-feeding trial*. *Gut*, 2019. **68**(8): p. 1417-1429.
230. Watson, H., et al., *A randomised trial of the effect of omega-3 polyunsaturated fatty acid supplements on the human intestinal microbiota*. *Gut*, 2018. **67**(11): p. 1974-1983.
231. Zhu, Y., et al., *Meat, dairy and plant proteins alter bacterial composition of rat gut bacteria*. *Sci Rep*, 2015. **5**: p. 15220.
232. Świątecka, D., et al., *The study on the impact of glycated pea proteins on human intestinal bacteria*. *Int J Food Microbiol*, 2011. **145**(1): p. 267-72.
233. Rivière, A., et al., *The ability of bifidobacteria to degrade arabinoxylan oligosaccharide constituents and derived oligosaccharides is strain dependent*. *Applied and environmental microbiology*, 2014. **80**(1): p. 204-217.
234. Berer, K., et al., *Dietary non-fermentable fiber prevents autoimmune neurological disease by changing gut metabolic and immune status*. *Scientific Reports*, 2018. **8**(1): p. 10431.
235. Townsend, G.E., 2nd, et al., *Dietary sugar silences a colonization factor in a mammalian gut symbiont*. *Proc Natl Acad Sci U S A*, 2019. **116**(1): p. 233-238.
236. Png, C.W., et al., *Mucolytic bacteria with increased prevalence in IBD mucosa augment in vitro utilization of mucin by other bacteria*. *Am J Gastroenterol*, 2010. **105**(11): p. 2420-8.
237. Desai, M.S., et al., *A Dietary Fiber-Deprived Gut Microbiota Degrades the Colonic Mucus Barrier and Enhances Pathogen Susceptibility*. *Cell*, 2016. **167**(5): p. 1339-1353.e21.
238. Chassaing, B., et al., *Dietary emulsifiers impact the mouse gut microbiota promoting colitis and metabolic syndrome*. *Nature*, 2015. **519**(7541): p. 92-6.
239. Ruiz-Ojeda, F.J., et al., *Effects of Sweeteners on the Gut Microbiota: A Review of Experimental Studies and Clinical Trials*. *Adv Nutr*, 2019. **10**(suppl_1): p. S31-s48.
240. Bray, G.A. and B.M. Popkin, *Dietary fat intake does affect obesity!* *The American Journal of Clinical Nutrition*, 1998. **68**(6): p. 1157-1173.
241. Ridaura, V.K., et al., *Gut Microbiota from Twins Discordant for Obesity Modulate Metabolism in Mice*. 2013. **341**(6150): p. 1241214.
242. De Vadder, F., et al., *Microbiota-Generated Metabolites Promote Metabolic Benefits via Gut-Brain Neural Circuits*. *Cell*, 2014. **156**(1): p. 84-96.
243. Haraszthy, V.I., et al., *Identification of Periodontal Pathogens in Atheromatous Plaques*. 2000. **71**(10): p. 1554-1560.
244. Ha, S.K., *Dietary salt intake and hypertension*. *Electrolyte & blood pressure : E & BP*, 2014. **12**(1): p. 7-18.
245. Adnan, S., et al., *Alterations in the gut microbiota can elicit hypertension in rats*. 2017. **49**(2): p. 96-104.
246. Mell, B., et al., *Evidence for a link between gut microbiota and hypertension in the Dahl rat*. 2015. **47**(6): p. 187-197.
247. Manzel, A., et al., *Role of "Western Diet" in Inflammatory Autoimmune Diseases*. *Current Allergy and Asthma Reports*, 2013. **14**(1): p. 404.

248. Hou, J.K., B. Abraham, and H. El-Serag, *Dietary Intake and Risk of Developing Inflammatory Bowel Disease: A Systematic Review of the Literature*. 2011. **106**(4): p. 563-573.
249. Frank, D.N., et al., *Molecular-phylogenetic characterization of microbial community imbalances in human inflammatory bowel diseases*. 2007. **104**(34): p. 13780-13785.
250. Li, J., et al., *Functional Impacts of the Intestinal Microbiome in the Pathogenesis of Inflammatory Bowel Disease*. *Inflammatory Bowel Diseases*, 2014. **21**(1): p. 139-153.
251. Lepage, P., et al., *Twin Study Indicates Loss of Interaction Between Microbiota and Mucosa of Patients With Ulcerative Colitis*. *Gastroenterology*, 2011. **141**(1): p. 227-236.
252. Albenberg, L.G., J.D. Lewis, and G.D. Wu, *Food and the gut microbiota in inflammatory bowel diseases: a critical connection*. *Current opinion in gastroenterology*, 2012. **28**(4): p. 314-320.
253. Wu, H.-J., et al., *Gut-residing segmented filamentous bacteria drive autoimmune arthritis via T helper 17 cells*. *Immunity*, 2010. **32**(6): p. 815-827.
254. Cha, H.R., et al., *Downregulation of Th17 cells in the small intestine by disruption of gut flora in the absence of retinoic acid*. *J Immunol*, 2010. **184**(12): p. 6799-806.
255. Mu, Q., H. Zhang, and X.M. Luo, *SLE: Another Autoimmune Disorder Influenced by Microbes and Diet?* *Front Immunol*, 2015. **6**: p. 608.
256. Llewellyn, S.R., et al., *Interactions Between Diet and the Intestinal Microbiota Alter Intestinal Permeability and Colitis Severity in Mice*. *Gastroenterology*, 2018. **154**(4): p. 1037-1046.e2.
257. Berer, K., et al., *Commensal microbiota and myelin autoantigen cooperate to trigger autoimmune demyelination*. *Nature*, 2011. **479**(7374): p. 538-541.
258. Ochoa-Repáraz, J., et al., *Role of Gut Commensal Microflora in the Development of Experimental Autoimmune Encephalomyelitis*. 2009. **183**(10): p. 6041-6050.
259. Jangi, S., et al., *Alterations of the human gut microbiome in multiple sclerosis*. *Nature Communications*, 2016. **7**(1): p. 12015.
260. Chen, J., et al., *Multiple sclerosis patients have a distinct gut microbiota compared to healthy controls*. *Scientific Reports*, 2016. **6**(1): p. 28484.
261. Berer, K., et al., *Gut microbiota from multiple sclerosis patients enables spontaneous autoimmune encephalomyelitis in mice*. 2017. **114**(40): p. 10719-10724.
262. Ivanov, I.I., et al., *Induction of intestinal Th17 cells by segmented filamentous bacteria*. *Cell*, 2009. **139**(3): p. 485-98.
263. Wang, Y., et al., *Induction of Intestinal Th17 Cells by Flagellins From Segmented Filamentous Bacteria*. *Frontiers in immunology*, 2019. **10**: p. 2750-2750.
264. Cekanaviciute, E., et al., *Gut bacteria from multiple sclerosis patients modulate human T cells and exacerbate symptoms in mouse models*. 2017. **114**(40): p. 10713-10718.
265. Ochoa-Repáraz, J., et al., *Central Nervous System Demyelinating Disease Protection by the Human Commensal *Bacteroides fragilis* Depends on Polysaccharide A Expression*. 2010. **185**(7): p. 4101-4108.
266. Atarashi, K., et al., *Induction of colonic regulatory T cells by indigenous *Clostridium* species*. *Science*, 2011. **331**(6015): p. 337-41.
267. Coombes, J.L., et al., *A functionally specialized population of mucosal CD103⁺ DCs induces Foxp3⁺ regulatory T cells via a TGF-beta and retinoic acid-dependent mechanism*. *J Exp Med*, 2007. **204**(8): p. 1757-64.
268. Pröbstel, A.K., et al., *Gut microbiota-specific IgA(+) B cells traffic to the CNS in active multiple sclerosis*. *Sci Immunol*, 2020. **5**(53).
269. Rojas, O.L., et al., *Recirculating Intestinal IgA-Producing Cells Regulate Neuroinflammation via IL-10*. *Cell*, 2019. **176**(3): p. 610-624.e18.
270. Erny, D., et al., *Host microbiota constantly control maturation and function of microglia in the CNS*. *Nat Neurosci*, 2015. **18**(7): p. 965-77.
271. Braniste, V., et al., *The gut microbiota influences blood-brain barrier permeability in mice*. *Sci Transl Med*, 2014. **6**(263): p. 263ra158.

272. Secher, T., et al., *Oral Administration of the Probiotic Strain Escherichia coli Nissle 1917 Reduces Susceptibility to Neuroinflammation and Repairs Experimental Autoimmune Encephalomyelitis-Induced Intestinal Barrier Dysfunction*. 2017. **8**(1096).
273. Mangalam, A., et al., *Human Gut-Derived Commensal Bacteria Suppress CNS Inflammatory and Demyelinating Disease*. *Cell Rep*, 2017. **20**(6): p. 1269-1277.
274. Mueller, P.S., et al., *PREVENTION OF EXPERIMENTAL ALLERGIC ENCEPHALOMYELITIS (EAE) BY VITAMIN C DEPRIVATION*. *Journal of Experimental Medicine*, 1962. **115**(2): p. 329-338.
275. Harbige, L.S. and M.K. Sharief, *Polyunsaturated fatty acids in the pathogenesis and treatment of multiple sclerosis*. *Br J Nutr*, 2007. **98 Suppl 1**: p. S46-53.
276. Hadgkiss, E.J., et al., *The association of diet with quality of life, disability, and relapse rate in an international sample of people with multiple sclerosis*. *Nutritional neuroscience*, 2015. **18**(3): p. 125-136.
277. Farez, M.F., et al., *Sodium intake is associated with increased disease activity in multiple sclerosis*. *J Neurol Neurosurg Psychiatry*, 2015. **86**(1): p. 26-31.
278. Cortese, M., et al., *No association between dietary sodium intake and the risk of multiple sclerosis*. *Neurology*, 2017. **89**(13): p. 1322-1329.
279. Choi, I.Y., et al., *A Diet Mimicking Fasting Promotes Regeneration and Reduces Autoimmunity and Multiple Sclerosis Symptoms*. *Cell reports*, 2016. **15**(10): p. 2136-2146.
280. Haghikia, A., et al., *Dietary Fatty Acids Directly Impact Central Nervous System Autoimmunity via the Small Intestine*. *Immunity*, 2015. **43**(4): p. 817-829.
281. Kong, W., J.-H. Yen, and D. Ganea, *Docosahexaenoic acid prevents dendritic cell maturation, inhibits antigen-specific Th1/Th17 differentiation and suppresses experimental autoimmune encephalomyelitis*. *Brain, behavior, and immunity*, 2011. **25**(5): p. 872-882.
282. Harbige, L.S., et al., *The protective effects of omega-6 fatty acids in experimental autoimmune encephalomyelitis (EAE) in relation to transforming growth factor-beta 1 (TGF-beta1) up-regulation and increased prostaglandin E2 (PGE2) production*. *Clinical and Experimental Immunology*, 2000. **122**(3): p. 445-452.
283. Erny, D., et al., *Host microbiota constantly control maturation and function of microglia in the CNS*. *Nature neuroscience*, 2015. **18**(7): p. 965-977.
284. Quintana, F.J., et al., *Control of Treg and TH17 cell differentiation by the aryl hydrocarbon receptor*. *Nature*, 2008. **453**(7191): p. 65-71.
285. Gutiérrez-Vázquez, C. and F.J. Quintana, *Regulation of the Immune Response by the Aryl Hydrocarbon Receptor*. *Immunity*, 2018. **48**(1): p. 19-33.
286. Mezrich, J.D., et al., *An interaction between kynurenine and the aryl hydrocarbon receptor can generate regulatory T cells*. *J Immunol*, 2010. **185**(6): p. 3190-8.
287. Matteoli, G., et al., *Gut CD103+ dendritic cells express indoleamine 2,3-dioxygenase which influences T regulatory/T effector cell balance and oral tolerance induction*. *Gut*, 2010. **59**(5): p. 595-604.
288. Rothhammer, V., et al., *Type I interferons and microbial metabolites of tryptophan modulate astrocyte activity and central nervous system inflammation via the aryl hydrocarbon receptor*. *Nature medicine*, 2016. **22**(6): p. 586-597.
289. Wu, C., et al., *Induction of pathogenic TH17 cells by inducible salt-sensing kinase SGK1*. *Nature*, 2013. **496**(7446): p. 513-7.
290. Wilck, N., et al., *Salt-responsive gut commensal modulates TH17 axis and disease*. *Nature*, 2017. **551**(7682): p. 585-589.
291. Kleinewietfeld, M., et al., *Sodium chloride drives autoimmune disease by the induction of pathogenic TH17 cells*. *Nature*, 2013. **496**(7446): p. 518-22.
292. Haase, S., et al., *Sodium chloride triggers Th17 mediated autoimmunity*. *J Neuroimmunol*, 2019. **329**: p. 9-13.
293. Faraco, G., et al., *Dietary salt promotes neurovascular and cognitive dysfunction through a gut-initiated TH17 response*. *Nat Neurosci*, 2018. **21**(2): p. 240-249.

294. Mucida, D., et al., *Reciprocal T_H17 and Regulatory T Cell Differentiation Mediated by Retinoic Acid*. 2007. **317**(5835): p. 256-260.
295. Iwata, M., et al., *Retinoic acid imprints gut-homing specificity on T cells*. *Immunity*, 2004. **21**(4): p. 527-38.
296. Lemire, J.M. and D.C. Archer, *1,25-dihydroxyvitamin D3 prevents the in vivo induction of murine experimental autoimmune encephalomyelitis*. *The Journal of clinical investigation*, 1991. **87**(3): p. 1103-1107.
297. Spach, K.M., et al., *IL-10 signaling is essential for 1,25-dihydroxyvitamin D3-mediated inhibition of experimental autoimmune encephalomyelitis*. *J Immunol*, 2006. **177**(9): p. 6030-7.
298. Clark, A. and N. Mach, *Role of Vitamin D in the Hygiene Hypothesis: The Interplay between Vitamin D, Vitamin D Receptors, Gut Microbiota, and Immune Response*. *Front Immunol*, 2016. **7**: p. 627.
299. Chakaroun, R.M., L. Massier, and P. Kovacs, *Gut Microbiome, Intestinal Permeability, and Tissue Bacteria in Metabolic Disease: Perpetrators or Bystanders?* *Nutrients*, 2020. **12**(4): p. 1082.
300. De Santis, S., et al., *Nutritional Keys for Intestinal Barrier Modulation*. *Frontiers in immunology*, 2015. **6**: p. 612-612.
301. Lerner, A. and T. Matthias, *Changes in intestinal tight junction permeability associated with industrial food additives explain the rising incidence of autoimmune disease*. *Autoimmunity Reviews*, 2015. **14**(6): p. 479-489.
302. Cignarella, F., et al., *Intermittent Fasting Confers Protection in CNS Autoimmunity by Altering the Gut Microbiota*. *Cell Metab*, 2018. **27**(6): p. 1222-1235.e6.
303. Piccio, L., J.L. Stark, and A.H. Cross, *Chronic calorie restriction attenuates experimental autoimmune encephalomyelitis*. *Journal of leukocyte biology*, 2008. **84**(4): p. 940-948.
304. Tubbs, A.L., et al., *Dietary Salt Exacerbates Experimental Colitis*. *The Journal of Immunology*, 2017.
305. Wei, Y., et al., *High salt diet stimulates gut Th17 response and exacerbates TNBS-induced colitis in mice*. *Oncotarget*, 2017. **8**(1): p. 70-82.
306. Wu, H., et al., *High salt promotes autoimmunity by TET2-induced DNA demethylation and driving the differentiation of Tfh cells*. *Scientific Reports*, 2016. **6**: p. 28065.
307. Hubbard, T.D., I.A. Murray, and G.H. Perdew, *Indole and Tryptophan Metabolism: Endogenous and Dietary Routes to Ah Receptor Activation*. *Drug metabolism and disposition: the biological fate of chemicals*, 2015. **43**(10): p. 1522-1535.
308. Rojas, O.L., et al., *Recirculating Intestinal IgA-Producing Cells Regulate Neuroinflammation via IL-10*. *Cell*, 2019. **176**(3): p. 610-624 e18.
309. Khairnar, V., et al., *CEACAM1 induces B-cell survival and is essential for protective antiviral antibody production*. *Nature Communications*, 2015. **6**(1): p. 6217.
310. Rovituso, D.M., et al., *CEACAM1 mediates B cell aggregation in central nervous system autoimmunity*. *Sci Rep*, 2016. **6**: p. 29847.
311. Sharpe, A.H. and K.E. Pauken, *The diverse functions of the PD1 inhibitory pathway*. *Nature Reviews Immunology*, 2018. **18**(3): p. 153-167.
312. Guo, B., *IL-10 Modulates Th17 Pathogenicity during Autoimmune Diseases*. *Journal of clinical & cellular immunology*, 2016. **7**(2): p. 400.
313. Yang, B.H., et al., *Foxp3(+) T cells expressing RORyt represent a stable regulatory T-cell effector lineage with enhanced suppressive capacity during intestinal inflammation*. *Mucosal Immunol*, 2016. **9**(2): p. 444-57.
314. Khan, A.R., et al., *PD-L1hi B cells are critical regulators of humoral immunity*. *Nature Communications*, 2015. **6**(1): p. 5997.

315. Lyons, J.A., M.J. Ramsbottom, and A.H. Cross, *Critical role of antigen-specific antibody in experimental autoimmune encephalomyelitis induced by recombinant myelin oligodendrocyte glycoprotein*. Eur J Immunol, 2002. **32**(7): p. 1905-13.
316. Xiao, Z.X., et al., *High salt diet accelerates the progression of murine lupus through dendritic cells via the p38 MAPK and STAT1 signaling pathways*. Signal Transduction and Targeted Therapy, 2020. **5**(1): p. 34.
317. Aguiar, S.L.F., et al., *High-Salt Diet Induces IL-17-Dependent Gut Inflammation and Exacerbates Colitis in Mice*. 2018. **8**(1969).
318. Guo, C.-p., et al., *High salt induced hypertension leads to cognitive defect*. Oncotarget, 2017. **8**.
319. Na, S.-Y., et al., *High-salt diet suppresses autoimmune demyelination by regulating the blood-brain barrier permeability*. 2021. **118**(12): p. e2025944118.
320. Varkaneh Kord, H., et al., *The influence of fasting and energy-restricted diets on leptin and adiponectin levels in humans: A systematic review and meta-analysis*. Clinical Nutrition, 2020.
321. Lanaspá, M.A., et al., *High salt intake causes leptin resistance and obesity in mice by stimulating endogenous fructose production and metabolism*. Proceedings of the National Academy of Sciences of the United States of America, 2018. **115**(12): p. 3138-3143.
322. Vogelzang, A., et al., *Microbiota - an amplifier of autoimmunity*. Current Opinion in Immunology, 2018. **55**: p. 15-21.
323. Chervonsky, A.V., *Microbiota and autoimmunity*. Cold Spring Harbor Perspectives in Biology, 2013. **5**(3).
324. Belkaid, Y. and Timothy W. Hand, *Role of the Microbiota in Immunity and Inflammation*. Cell, 2014. **157**(1): p. 121-141.
325. Takeda, Y., et al., *Effects of high sodium intake on cardiovascular aldosterone synthesis in stroke-prone spontaneously hypertensive rats*. J Hypertens, 2001. **19**(3 Pt 2): p. 635-9.
326. Herrada, A.A., et al., *Aldosterone Promotes Autoimmune Damage by Enhancing Th17-Mediated Immunity*. 2010. **184**(1): p. 191-202.
327. Chelakkot, C., J. Ghim, and S.H. Ryu, *Mechanisms regulating intestinal barrier integrity and its pathological implications*. Experimental & Molecular Medicine, 2018. **50**(8): p. 1-9.
328. Atarashi, K., et al., *ATP drives lamina propria TH17 cell differentiation*. Nature, 2008. **455**: p. 808-812.
329. Aranami, T. and T. Yamamura, *Th17 Cells and autoimmune encephalomyelitis (EAE/MS)*. Allergol.Int., 2008. **57**(2): p. 115-120.
330. Korn, T., et al., *Th17 cells: Effector T cells with inflammatory properties*. Seminars in Immunology, 2007. **19**(6): p. 362-371.
331. Lee, K., et al., *Bacillus-derived poly-γ-glutamic acid reciprocally regulates the differentiation of T helper 17 and regulatory T cells and attenuates experimental autoimmune encephalomyelitis*. Clinical and Experimental Immunology, 2012. **170**(1): p. 66-76.
332. Wu, X., J. Tian, and S. Wang, *Insight Into Non-Pathogenic Th17 Cells in Autoimmune Diseases*. Frontiers in Immunology, 2018. **9**(1112).
333. Noster, R., et al., *Two types of human Th17 cells with pro- and anti-inflammatory properties and distinct roles in autoinflammation*. Pediatric Rheumatology Online Journal, 2015. **13**(Suppl 1): p. O49-O49.
334. Dar, H.Y., et al., *High dietary salt intake correlates with modulated Th17-Treg cell balance resulting in enhanced bone loss and impaired bone-microarchitecture in male mice*. Sci Rep, 2018. **8**(1): p. 2503.
335. Wu, C., et al., *SGK1 Governs the Reciprocal Development of Th17 and Regulatory T Cells*. Cell Reports, 2018. **22**(3): p. 653-665.
336. Hernandez, A.L., et al., *Sodium chloride inhibits the suppressive function of FOXP3+ regulatory T cells*. The Journal of Clinical Investigation, 2015. **125**(11): p. 4212-4222.

337. Luo, Y., et al., *Negligible Effect of Sodium Chloride on the Development and Function of TGF- β -Induced CD4+ Foxp3+ Regulatory T Cells*. Cell Reports, 2019. **26**(7): p. 1869-1879.e3.
338. Matthias, J., et al., *Salt generates antiinflammatory Th17 cells but amplifies pathogenicity in proinflammatory cytokine microenvironments*. The Journal of Clinical Investigation, 2020. **130**(9): p. 4587-4600.
339. Lochner, M., et al., *In vivo equilibrium of proinflammatory IL-17+ and regulatory IL-10+ Foxp3+ RORgamma t+ T cells*. J Exp Med, 2008. **205**(6): p. 1381-93.
340. Zhao, D., et al., *In vivo-activated CD103+CD4+ regulatory T cells ameliorate ongoing chronic graft-versus-host disease*. Blood, 2008. **112**(5): p. 2129-38.
341. Lehmann, J., et al., *Expression of the integrin alpha Ebeta 7 identifies unique subsets of CD25+ as well as CD25- regulatory T cells*. Proc Natl Acad Sci U S A, 2002. **99**(20): p. 13031-6.
342. Cervenak, L., et al., *Differential expression of GL7 activation antigen on bone marrow B cell subpopulations and peripheral B cells*. Immunol Lett, 2001. **78**(2): p. 89-96.
343. Lühder, F., et al., *Laquinimod enhances central nervous system barrier functions*. Neurobiol Dis, 2017. **102**: p. 60-69.
344. Wang, X.S., et al., *Idazoxan reduces blood-brain barrier damage during experimental autoimmune encephalomyelitis in mouse*. Eur J Pharmacol, 2014. **736**: p. 70-6.

ABBREVIATIONS

| | |
|--|--|
| Ahr – Aryl hydrocarbon receptor | GALT – Gut associated lymphoid tissue |
| APC – Antigen presenting cells | GF – Germ free |
| BBB – Blood brain barrier | GFAP – Glial fibrillary acidic protein |
| BHI – Brain heart infusion | GITRL – Glucocorticoid induced TNF ligand |
| BP – Blood pressure | GM-CSF – Granulocyte monocyte – colony stimulating factor |
| BSA – Bovine serum albumin | GPCR – G protein coupled receptor |
| CAM – Cell adhesion molecule | HBSS - Hank's Balanced Salt Solution |
| CDs – Cluster of differentiations | HLA – Human leukocyte antigen |
| CD – Crohn's disease | HSD – High salt diet |
| CFA – Complete Freund's adjuvant | IAA – Indole acetic acid |
| CFU – Colony forming unit | IBD – Inflammatory bowel disease |
| CIS – Clinically isolated syndrome | ICAM – Intercellular adhesion molecule |
| CLP – Colon lamina propria | IEL – Intra-epithelial lymphocytes |
| CNS – Central nervous system | IFA – Incomplete Freund's adjuvant |
| CSF – Cerebro-spinal fluid | IFNγ – Interferon γ |
| CTLA4 – Cytotoxic T lymphocyte associated protein 4 | Ig – Immunoglobulin |
| DC – Dendritic cells | iGB – in vitro derived Germinal center B cells |
| DHA – Docosahexaenoic acid | IL – Interleukin |
| DMEM – Dulbecco's modified eagles' medium | IMDM – Iscove's modified Dulbecco's medium |
| EAE – Experimental autoimmune encephalomyelitis | JAM – Junctional adhesion molecule |
| EBV – Epstein barr virus | LacCer – Lactosylceramide |
| EROD – Ethoxyresorufin-O-deethylase | LC/MS – Liquid chromatography/ Mass spectrometry |
| FACS – Fluorescence associated cell sorting | LCFA – Long chain fatty acid |
| FBS – Fetal bovine serum | LFA-1 – Lymphocyte function-associated antigen 1 |
| FMD – Fasting mimicking diet | MACS – Magnetic activated cell sorting |
| FoxP3 – Forkhead box P3 | |

MBP – Myelin basic protein

MHC – Major histocompatibility complex

MOG – Myelin oligodendrocyte glycoprotein

MS – Multiple sclerosis

MTB – Mycobacterium tuberculosis

NFM – Neurofilament M

NO – Nitric oxide

OSE – Opticospinal encephalomyelitis

OTU – Operational taxonomic unit

PBMC – Peripheral blood mononuclear cells

PBS – Phosphate buffered saline

PCR – Polymerase chain reaction

PD1 – Programmed cell death protein 1

PD-L – Programmed death ligand

PECAM-1 – Platelet/endothelial cell adhesion molecule 1

PFA – Paraformaldehyde

PLP – Proteolipid protein

PMA – Phorbol myristate acetate

PPI – Proton pump inhibitor

PPMS – Primary progressive multiple sclerosis

PUFA – Poly-unsaturated fatty acids

RA – Retinoic acid

RAG – Recombination activation gene

RIPA - Radioimmunoprecipitation assay

ROR γ T – Retinoid related Orphan receptor γ

RPMI – Roswell park memorial institute

RR – Relapsing-remitting

RRMS – Relapsing-remitting multiple sclerosis

RT – Room temperature

SCFA – Short chain fatty acid

SDS – Sodium dodecyl sulphate

SFB – Segmented filamentous bacteria

SILP – Small intestine lamina propria

SPF – Specific pathogen free

SPMS – Secondary progressive multiple sclerosis

T2D – Type 2 Diabetes

TAG-1 – Transient axonal glycoprotein 1

TBS – Tris buffered saline

TCR – T cell receptor

TCR β – T cell receptor β

TE – Tris EDTA

Tfh – T follicular helper

TGF β – Transforming growth factor β

T_H – T helper

TJP – Tight junction protein

TLR – Toll like receptors

TMB – Tetramethylbenzidine

TNF α – Tumor necrosis formula α

T_{reg} – T regulatory cell

UC – Ulcerative colitis

VCAM – Vascular cell adhesion molecule

VLA-4 – Very late antigen 4

WT – Wild type

ACKNOWLEDGEMENT

Firstly, I would like to express my thanks to my supervisor Dr. Gurumoorthy Krishnamoorthy, for granting me the opportunity to pursue my PhD studies under his mentorship and his constant support and encouragement throughout these 4 years. Guru was always available to discuss and advise me on my experiments, and steadily tutored me in animal handling and other techniques/tools during my initial year. I am grateful for all the time and effort he invested in me which has enabled me to become a better researcher.

I am particularly thankful to my colleague Dr. Shin-Young Na, for her valuable inputs at various stages of the project, help with my experiments and for being readily available for any discussions about the project. I would also like to thank my colleagues Birgit Kunkel, Dr. Jeeva Varadarajulu and Dr. Alexei Leliavski who have all helped me with learning several experimental techniques which were necessary for the project and have given valuable suggestions during group meetings. It has been a rewarding experience working with my colleagues, being in a supportive environment and having learnt a lot from all of them.

I would further like to thank the members of my thesis advisory committee – Dr. Naoto Kawakami and Dr. Peter Murray, for their valuable inputs into my project. I also thank the MPI for Biochemistry, Dr. Reinhard Fassler and all my co-workers at MPI. The department seminars were very helpful giving me comments and feedback on the progress of my work. In addition, the career development workshop and the training courses in programming offered by MPI proved incredibly helpful.

I offer thanks to Dr. Chris Turk at the MPI of Psychiatry for his help with the metabolomics analysis. I also acknowledge my colleague Jakob Reber at the MPI for Biochemistry for helping me with translation of portions of the thesis in Deutsch. Finally, special thanks to my family for their unconditional support and motivation throughout.

RESOURCES

16s rRNA sequencing for ceecal samples was performed by Novogene Co. LC/MS for fecal metabolome was performed by Chris Turk from the MPI for Psychiatry. Isolation of brain endothelial cells and the subsequent western blot were done together by me and Dr. Shin-Young Na.



LUDWIG-
MAXIMILIANS-
UNIVERSITÄT
MÜNCHEN

Promotionsbüro
Medizinische Fakultät



Eidesstattliche Versicherung

Name, Vorname

Ich erkläre hiermit an Eides statt,
dass ich die vorliegende Dissertation mit dem Titel

selbständig verfasst, mich außer der angegebenen keiner weiteren Hilfsmittel bedient und alle Erkenntnisse, die aus dem Schrifttum ganz oder annähernd übernommen sind, als solche kenntlich gemacht und nach ihrer Herkunft unter Bezeichnung der Fundstelle einzeln nachgewiesen habe.

Ich erkläre des Weiteren, dass die hier vorgelegte Dissertation nicht in gleicher oder in ähnlicher Form bei einer anderen Stelle zur Erlangung eines akademischen Grades eingereicht wurde.

Ort, Datum

Mathangi Janakiraman

Unterschrift Doktorandin bzw. Doktorand



LUDWIG-
MAXIMILIANS-
UNIVERSITÄT
MÜNCHEN

Promotionsbüro
Medizinische Fakultät



Erklärung zur Übereinstimmung der gebundenen Ausgabe der Dissertation mit der elektronischen Fassung

Name, Vorname

Straße, Hausnummer

PLZ, Ort

Hiermit erkläre ich, dass die elektronische Version der eingereichten Dissertation mit dem Titel

in Inhalt und Formatierung mit den gedruckten und gebundenen Exemplaren übereinstimmt.

Ort, Datum

Mathangi Janakiraman

Unterschrift Doktorandin bzw. Doktorand